Alma Mater Studiorum - **Università di Bologna**
Facoltà di Medicina Veterinaria

Dipartimento di Morfofisiologia Veterinaria e Produzioni Animali

Sezione di Anatomia

Dottorato di Ricerca in

Applicazioni Biotecnologiche in Neuromorfofisiologia

XIX ciclo

NERVE GROWTH FACTOR in modelli di patologie sperimentali e spontanee

Tesi di dottorato della Dott.ssa Sandra Sivilia

Settore disciplinare "VET01"

Tutor:
Chiar.ma Prof.ssa
Laura Calzà

Coordinatore:
Chiar.ma Prof.ssa
Maria Luisa Lucchi

Anno Accademico 2005-2006

Al mio Nicola

ELENCO DEI LAVORI INCLUSI NELLA TESI

I) **Sivilia S**., Paradisi M., D'Intino G., Fernandez M., Pirondi S., Lorenzini L., Calzà L. Skin homeostasis during inflammation: a role for Nerve Growth Factor. Histology and Histopathology, 2007, *in press*

II) **Sivilia S**., Giuliani A., Del Vecchio G., Fernandez M., Turba M., Forni M., Giardino L., Calzà L. Intravitreal NGF administration partially counteracts retina and optic nerve degeneration after 2VO ligation in rat, by regulating proapoptotic gene expression. *Manuscript draft*

III) D'Intino G., Vaccari F., **Sivilia S**., Scagliarini A., Gandini G., Giardino L., Calzà L. A molecular study of hippocampus in dogs with convulsion during canine distemper virus encephalitis. Brain Res 2006, 1098:186-195

IV) Paradisi M., Fernandez M., **Sivilia S**., Marucci GL, Giulioni M, Pozzati E, Zucchelli M, Calbucc F, Antonelli T., Giardino L., Calzà L. In vitro assay for neurogenesis and gliogenesis in adult human dentate gyrus. *Manuscript Submitted*

V) **Sivilia S**., Giuliani A., Del Vecchio G., Giardino L., Calzà L. Age-dependent impairment of hippocampal neurogenesis in chronic cerebral hypoperfusion. *Manuscript Submitted*

Questi lavori sono stati finanziati da:
Università di Bologna
MIUR (COFIN e FIRB)
ASC-Lab (Azioni PRRIITT Regione Emilia-Romagna)
Associazione Italiana per la lotta alle Sindromi Atassiche, Regione Emilia-Romagna
LIONS CLUB BOLOGNA
LIONS CLUB BOLOGNA SAN LAZZARO

ABBREVIAZIONI

BDNF	Fattore neurotrofico derivato dal cervello
CFA	Adiuvante completo di Freund
CGRP	peptide correlato al gene calcitonina
CREB	proteina legante l'elemento di risposta al cAMP
DRG	Gangli della radice dorsale
EAE	Encefalomielite autoimmune sperimentale
EGF	Fattore di crescita epidermico
FGF	Fattore di crescita dei fibroblasti
IFN	Interferone
IL	Interleuchine
IP3	Inositol(1,4,5)trifosfato
JNK	Jun amino-terminale chinasi
MAG	Inibitori di crescita correlati alla mielina
MAPK	Protein chinasi mitogene-attivate
NADE	*Death effector* associato al recettore di neurotrofine
NADPH	Nicotinamide adenina dinucleotide idrogeno fosfato
NGF	Fattore di crescita nervoso
nNOS	Sintasi dell'ossido nitrico neuronale
NRAGE	Membro della famiglia MAGE
NRIF	Fattore di interazione col recettore delle neurotrofine
NT	Neurotrofine
PDGF	Fattore di crescita derivato dalle piastrine
RGC	Cellule gangliari retiniche
SNC	Sistema nervoso centrale
SNP	Sistema nervoso periferico
SP	Sostanza P
TGFb	Fattore di crescita trasformante beta
TNF	Fattore di necrosi tumorale
TNFR	Recettore del Fattore di necrosi tumorale

TRAF6	Fattore associato al complesso TNF-recettore
Trk	Tirosin chinasi tropomiosina correlata
TRPV1	Recettore della vanilloidina
VEGF	Fattore di crescita endoteliale vascolare

ELENCO LAVORI INCLUSI NELLA TESI

ABBREVIAZIONI

INDICE

1. INTRODUZIONE

1.1 NGF e recettori

Il fattore di crescita nervoso (NGF) è stato scoperto da Rita Levi Montalcini più di 50 anni fa. È il membro capostipite di una famiglia di sostanze analoghe definite neurotrofine (NT). Sono molteplici le funzioni biologiche attribuite a queste sostanze nello sviluppo, per la funzione nella vita adulta, per la protezione e la riparazione mediante complessi meccanismi molecolari che regolano ad esempio il *survival* neuronale, la plasticità sinaptica, la crescita assonale e dendritica (Aloe and Calzà, 2004). NGF, come le altre NT, viene sintetizzato come precursore (pro-NGF) nel reticolo del Golgi e, dopo scissione da parte di pro-convertasi intracellulari e di metalloproteinasi della matrice extracellulare, diventa una proteina matura (Pattarawarapan and Burgess, 2003; Schor, 2005). Dal punto di vista strutturale è costituito da un monomero avente forma allungata con un nucleo costituito da foglietti beta ripiegati e da un motivo ricco in cisteina formato da tre ponti disolfuro che stabilizza la conformazione della molecola stessa, la forma biologicamente è rappresentata dal dimero di questa struttura (McDonald *et al*., 1991).

Gli altri membri delle NT sono il *brain derived neuronal factor* (BDNF), la neurotrofina-3 (NT-3), e le neurotrofine –4 e –5 (NT-4/5) (Pattarawarapan and Burgess, 2003).

L'azione biologica di tutti i membri della famiglia delle NT è mediata dall'interazione con due tipi di recettori transmembrana: i recettori *tropomyosin-related kinasi* (Trk) di cui si riconoscono le isoforme A (per NGF), B (per BDNF) e C (per NT), che legano i rispettivi legandi con alta affinità ed il recettore p75, membro della super famiglia dei recettori per il *tumor necrosis factor* (TNF) che lega tutti i membri della famiglia delle NT con bassa affinità (Nykjaer *et al*., 2005).

Negli ultimi anni si sono aggiute molte informazioni riguardo al ruolo biologico di queste classi di recettori e della loro interazione molecolare. Se per i recettori Trk si riconoscono ruoli primari nello stimolare la sopravvivenza neuronale, la differenziazione, la crescita neuritica, la mielinizzazione e la plasticità sinaptica, il ruolo del p75, considerato fino ad alcuni anni fa ancillare rispetto al TrkA, è attualmente

oggetto di profonda rivalutazione ed alquanto controverso, in quanto può indurre sopravvivenza o apoptosi a seconda del tipo cellulare in cui è espresso, dello stato funzionale della cellula, della presenza o assenza e della tipologia del ligando (Pattarawarapan and Burgess, 2003; Schor, 2005).

La struttura molecolare del recettore Trk comprende una porzione extracellulare ed una citoplasmatica collegate tra loro da un segmento transmembrana. La prima è caratterizzata dalla presenza di cinque domini extracellulari: un dominio ricco in leucina (d2) fiancheggiato da cluster di cisteina (d1 e d3), seguiti da due domini d4 e d5 immunoglobuline simile (Ig1 e Ig2) localizzati più vicino alla membrana cellulare; la porzione intracellulare invece rappresenta il dominio tirosin chinasi (Pattarawarapan and Burgess, 2003). Il dominio d5 (Ig2) è coinvolto nel legame specifico con le NT che porta all'attivazione del Trk (Pattarawarapan and Burgess, 2003; Schor, 2005). Il legame recettore-ligando induce una dimerizzazione del recettore stesso e successivo innesco dell'attività tirosin chinasica. Il recettore Trk attivo fosforila due residui tirosinici: Y-490 prossimo alla membrana intracellulare e Y-785 localizzato presso il residuo carbossilico terminale (Segal, 2003). Questi generano rispettivamente un sito di attacco per le proteine Shc e per la fosfolipasi C (PLC-g1) che a loro volta fungono da substrati per le chinasi (Segal, 2003). La PLC-g1 catalizza l'idrolisi del fosfatidilinositolo in diacil glicerolo e inositol(1,4,5)trifosfato (IP3): il diacil glicerolo attiva una serie di chinasi, mentre IP3, promuovendo il rilascio di Ca^{2+} dalle riserve intracellulari, induce un aumento di Ca^{2+} che va a potenziare la liberazione dei neurotrasmettitori. In tal modo questo *pathway* modula la plasticità e la funzione sinaptica. La fosforilazione di Shc promuove una serie di reazioni attraverso la cascata Ras/MAPK e la via PI3K/Akt (*Phosphatidylinositol-3-OH kinase*). Le MAP chinasi (protein chinasi mitogene-attivate) devono il loro nome al fatto che sono in grado di mediare gli effetti proliferativi (Segal, 2003). Possono trasmettere i segnali dal citoplasma al nucleo influendo così nella trascrizione ma possono anche agire a livello citoplasmatico, fosforilando proteine del citoscheletro, svolgendo quindi una funzione essenziale nella crescita assonale. Le PI3 chinasi sono coinvolte in diversi *pathways* che regolano la sopravvivenza neuronale. Un esempio è dato dall'enzima Akt che inattiva, mediante fosforilazione, una proteina pro-apoptotica (Bad) promuovendo il *survival* bcl2–dipendente; attiva il fattore NF-kB che promuove la sopravvivenza neuronale;

inoltre inibisce il fattore di trascrizione Forkhead che controlla l'espressione di geni promuoventi l'apoptosi ed anche la proteina p53 capace di indurre apoptosi (Segal, 2003) (Fig. 1).

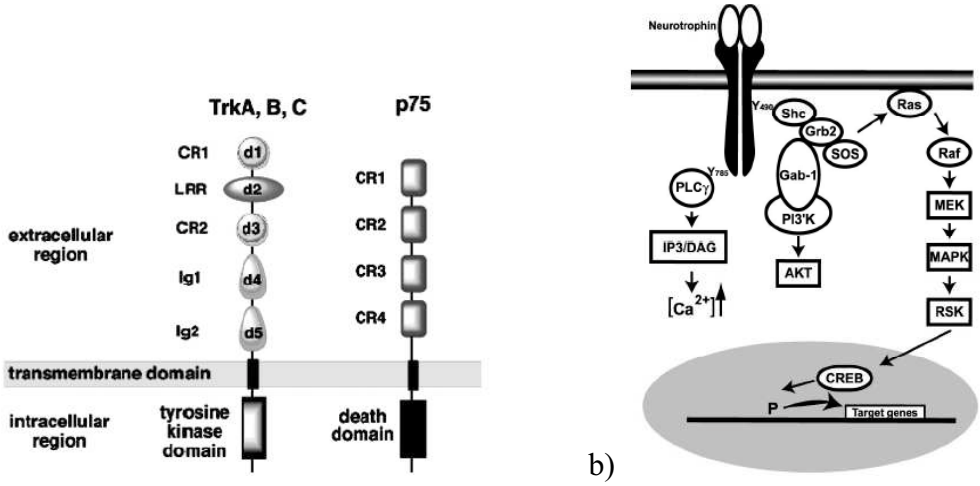

a) b)

Fig. 1: rappresentazione schematica dei recettori Trk e p75 (a); meccanismo d'azione del recettore Trk (b). (a): tratta da Pattarawarapan and Burgess, 2003; (b): tratta da Segal, 2003

Nelle cellule neurali che lo esprimono, TrkA può essere presente sulla membrana plasmatica del soma, dei dendriti ed anche dell'assone. Si ritiene che queste localizzazioni subcellulari possano mediare azioni cellulari diverse attraverso differenti meccanismi. L'attivazione del TrkA situato lungo l'assone può, ad esempio, promuovere la crescita assonale agendo localmente attraverso il *pathway* Erk 1/2 e PI3-K, oppure può mediare il *survival* e il differenziamento neuronale, coinvolgendo le proteine Erk5, PI3-K e CREB (proteina legante l'elemento di risposta al cAMP) a livello del corpo cellulare (Miller and Kaplan 2001; Ye *et al*., 2003). Quindi, NGF che lega il recettore TrkA situato lungo i terminali nervosi, deve essere in grado in qualche modo di trasmettere i propri segnali al corpo cellulare. Da qui la "teoria endosomica", in base alla quale NGF induce una internalizzazione, mediante endocitosi, del complesso NGF-TrkA che viene trasportato in modo retrogrado fino al pirenoforo dove interagisce con altri elementi che a loro volta mediano la risposta cellulare (McPherson *et al*., 2001;

Barker *et al*., 2002; Ye *et al*., 2003). Il meccanismo di endocitosi avviene attraverso la formazione di vescicole rivestite di clatrina che poi si muovono grazie all'interazione con i microtubuli e la proteina dineina che può iniziare il trasporto retrogrado (Miller and Kaplan, 2001).

Alcuni autori (MacInnis and Campenot, 2002) hanno dimostrato che per il segnale di *survival* non è necessaria l'internalizzazione di NGF, mentre è essenziale l'attivazione del recettore TrkA che, con la sua porzione citoplasmatica orientata all'esterno della vescicola, è in grado di interagire con i substrati PLC-g1 e le proteine Erk1/2 e PI3-kinase (Miller and Kaplan 2001; 2002). Quindi diversi possono essere i meccanismi che regolano la trasmissione del segnale: a) NGF potrebbe essere trasportato in modo retrogrado per poi legarsi ad un recettore intracellulare; b) il TrkA, una volta attivato da NGF, potrebbe raggiungere il corpo cellulare da solo o sotto forma di complesso NGF-TrkA; c) NGF, dopo aver interagito con il TrkA, attiverebbe una serie di proteine in grado di fornire esse stesse il segnale retrogrado (Miller and Kaplan 2001).

Un altro meccanismo riguarda l'attivazione del TrkA in assenza di NGF: quando la concentrazione del recettore TrkA supera una certa soglia (come può accadere all'interno delle vescicole), può dimerizzare attivandosi e quindi essere trasportato (Miller and Kaplan 2002).

Anche il recettore p75, insieme alle NT, può essere internalizzato in vescicole di clatrina, associato anche alla proteina MAGE, in modo da trasmettere il segnale retrogrado (Bronfman *et al*., 2003). Gli endosomi contenenti il segnale di p75 si distinguono da quelli del TrkA sia in modo temporale (cinetica differente) che spaziale (Bronfman *et al*., 2003). Secondo Saxena e coll. (2005), NGF induce l'internalizzazione sia di TrkA che di p75 negli endosomi primari, supponendo quindi l'esistenza di diverse popolazioni di vescicole che fanno divergere il destino dei due recettori (Delcroix *et al*., 2003; Saxena *et al*., 2005). Infatti, nelle cellule PC12 si è osservato che, in presenza di NGF, il p75 ed il TrkA inizialmente si trovano insieme all'interno delle vescicole rivestite di clatrina, quindi passano negli endosomi primari dove, per diversa sensibilità di ciascun recettore al pH, si ha la separazione dei due recettori: mentre il p75 muove in endosomi che consentono il reciclo dello stesso che torna sulla superficie di membrana, il TrkA subisce una degradazione enzimatica che avviene all'interno dei lisosomi (Saxena *et al*., 2005).

Il p75 è costituito da un dominio extracellulare ricco in cisteina coinvolto nel legame con le NT; una regione transmembrana contenente il sito di clivaggio per la gamma-secretasi ed un dominio intracellulare tipico della famiglia recettoriale per TNF, dominio "*death*" responsabile dell'attività apoptotica (Pattarawarapan and Burgess, 2003). A differenza del recettore Trk (dimero), il p75 è un monomero, per cui quando NGF (dimero) si lega al TrkA non può contemporaneamente legare il p75 (Schor, 2005). Tuttavia quest'ultimo è in grado di interagire con il complesso TrkA-NGF regolando così il *survival* cellulare (Huang and Reichardt, 2003) (Fig. 2).

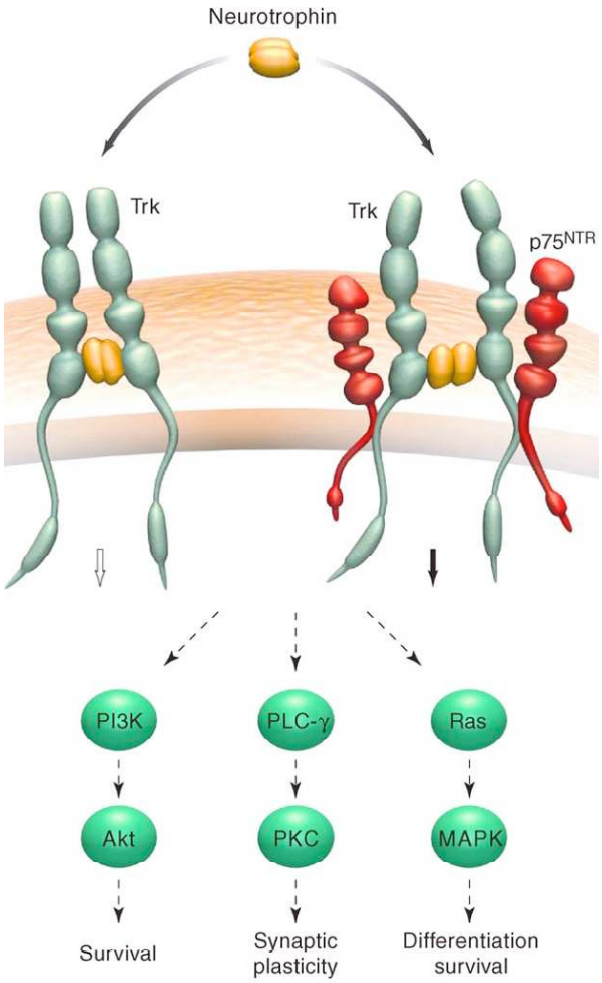

Fig. 2: i possibili *pathway* in seguito all'attivazione di Trk in presenza o assenza di p75 (tratta da Nykjaer *et al.*, 2005)

L'effetto biologico mediato da p75 molto dipende dal contesto cellulare in cui è espresso. Studi recenti hanno infatti dimostrato che p75, in assenza del TrkA, è responsabile dei processi di apoptosi che coinvolgono l'attivazione delle chinasi *Jun amino-terminal kinase* (JNK). Questo porta alla fosforilazione del c-jun e, mediante l'attivazione delle proteine p53, Bad e Bim, alla traslocazione mitocondriale di Bax con rilascio del citocromo c dal mitocondrio stesso e successiva attivazione delle caspasi 3, 6 e 9 (Nykjaer *et al.*, 2005). Inoltre, altri *pathways* possono interagire contemporaneamente: l'attivazione di NF-kB, mediata da uno dei tanti attivatori delle JNK, TRAF6 (fattore associato al complesso TNF-recettore), paradossalmente potrebbe promuovere il *survival* piuttosto che l'apoptosi, mentre l'attivazione delle MAP chinasi può indurre morte in alcuni tipi cellulari e sopravvivenza in altri (Nykjaer *et al*., 2005).
Il p75 può essere sottoposto anche ad un processo proteolitico da parte delle alfa- e gamma- secretasi dando origine rispettivamente ad un dominio extracellulare ed uno intracellulare: il primo, sottraendo le NT al p75, potrebbe prevenire il segnale apoptotico; invece il dominio intracellulare potrebbe essere traslocato all'interno del nucleo regolando la trascrizione (Nykjaer *et al*., 2005) (Fig. 3).

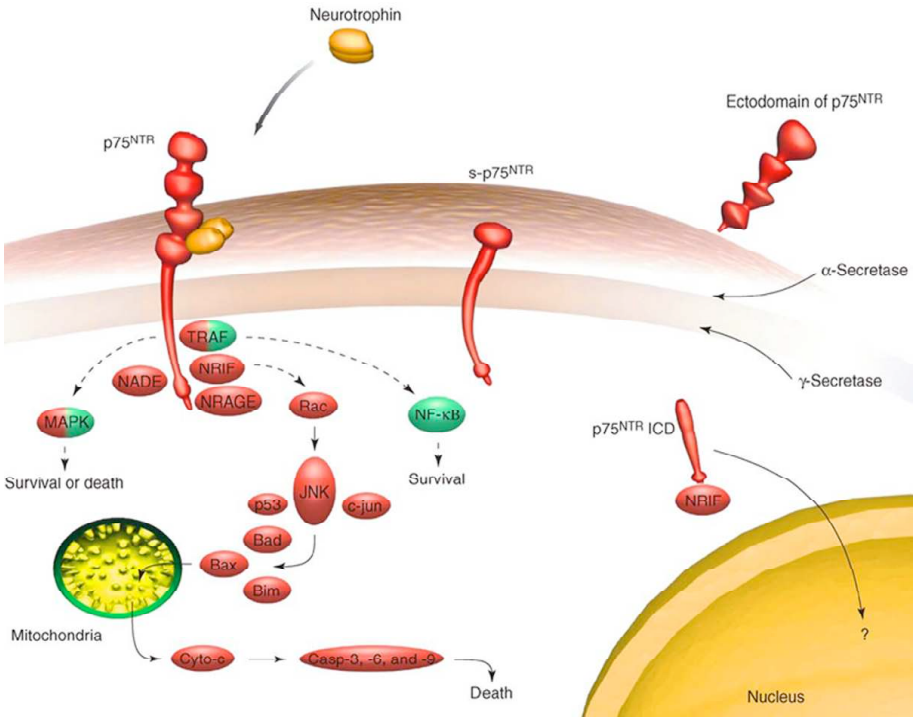

Fig. 3: *pathway* attivato dal p75. (tratta da Nykjaer *et al*., 2005)

Nuovi studi hanno dimostrato che NGF, nella sua forma immatura (pro-NGF), ha una maggiore affinità per il p75, mentre non interagisce affatto con il TrkA, suggerendo quindi una sua potente azione come induttore di apoptosi p75-dipendente (Nykjaer *et al*., 2005). Sono state inoltre identificate numerose proteine in grado di interagire con p75, mediandone i diversi effetti cellulari, fra queste la sortilina, membro della famiglia VPS10, che è in grado di interagire con il p75 favorendo il legame di quest'ultimo con il pro-NGF e formando così un complesso terziario (Nykjaer *et al*., 2005). Il complesso pro-NGF/sortilina potrebbe formarsi già a livello del Golgi, trasferirsi sulla superficie cellulare e diventare co-recettore per il p75 oppure, se sottoposto a scissione proteolitica, potrebbe staccarsi dalla membrana e venire rilasciato nello spazio extracellulare come complesso solubile (riserva di pro-NGF) (Bronfman and Fainzilber, 2004; Schor, 2005). In assenza di Sortilina invece, il pro-NGF viene attivato ad NGF che va poi a stimolare il recettore trkA (Bronfman and Fainzilber, 2004; Nykjaer *et al*., 2005). Un altro co-recettore per il p75 può essere NogoR-lingo1 la cui attivazione in presenza dei ligandi quali NOGO, MAG (*myelin-based growth inhibitors*) e OmGP (*oligodendrocyte myelin glycoprotein*) inibisce la rigenerazione assonale promuovendo il collasso del cono di crescita di assoni danneggiati (Barker, 2004; Nykjaer *et al*., 2005) (Fig. 4).

Infine Bex1 (*Brain-Expressed X-linked 1*) di recente identificato come possibile traslocatore nucleare del dominio intracellulare di p75 dopo clivaggio ad opera delle secretasi. Questa proteina appartiene ad una famiglia di piccole proteine di cui non è ben chiara la funzione, ma alcuni esperimenti hanno confermato il fatto che siano adattatori o modulatori intracellulari di *pathway* di segnalazione (Vilar *et al.,* 2006). In particolare, si è notato che Bex1 interagisce con la porzione intracellulare di p75NTR indipendentemente dalla presenza o meno del legame del recettore stesso con NGF ma ne risulta in qualche modo condizionata. Quando p75NTR lega NGF, la proteina Bex1 viene esportata dal nucleo e si localizza nel citoplasma per interagire con p75NTR. La concentrazione di questa proteina è molto bassa in fase G_1 del ciclo, ma aumenta in fase S; come se seguisse parallelamente l'andamento d'espressione del p75NTR. Allo stesso tempo, Bex1 non ha un ruolo principale sul ciclo cellulare, ma agisce in secondo piano: non è determinante per la progressione del ciclo cellulare, ma previene l'uscita dal ciclo in fase S-G_2-M, infatti una grande diminuzione di tale proteina accelera l'uscita dal

ciclo cellulare e una progressione più veloce verso il differenziamento (Vilar *et al*., 2006).

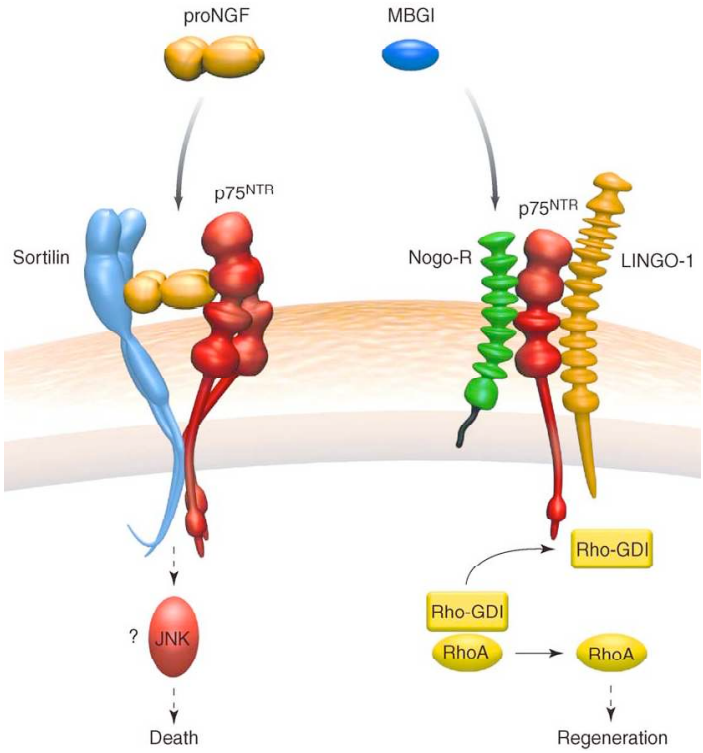

Fig. 4: *pathway* in seguito all'interazione del p75 con Sortilin, NOGO-R e LINGO-1. (tratta da Nykjaer *et al*., 2005).

1.2 NGF e morte cellulare

L'apoptosi neuronale insieme alla sinaptogenesi è uno dei più importanti eventi nello sviluppo del sistema nervoso, ma si verifica anche in seguito ad un trauma, ad una malattia neurodegenerativa, all'esposizione a tossici, ecc. Il recettore delle neurotrofine p75 è altamente espresso in neuroni durante lo sviluppo ed è *down*-regolato nel periodo seguente ma, dopo un insulto, viene riespresso notevolmente. Il p75 è coinvolto nella regolazione della morte cellulare soprattutto quando il recettore Trk è assente.

Il p75, per analogia di struttura, fa parte della superfamiglia recettoriale del TNF. Infatti, in comune con questi recettori, ha un dominio intracellulare prossimo al C-terminale nominato dominio *death*, maggiormente coinvolto nel processo apoptotico; mentre l'omologia extracellulare è basata su regioni ricche in cisteina che sono coinvolte

nell'interazione con i ligandi. Esistono comunque delle differenze che distinguono il p75 dagli altri recettori della *superfamily*: riconosce ligandi che sono fattori solubili anziché di membrana e che sono dimeri anziché trimeri (Barrett, 2000). Qualche variazione strutturale riguarda anche il dominio *death*, in quanto tutte le proteine intracitoplasmatiche, ad eccezione di NF-kB, che interagiscono con il dominio *death* del recettore per TNF (TNFR), non instaurano alcun tipo di contatto con il p75 (Barrett, 2000). Quindi il segnale apoptotico mediato dal p75 non seguirebbe lo stesso *pathway* attivato da TNF. Il recettore p75 presenta un altro dominio citoplasmatico, nella regione iuxtamembrana, noto come dominio *Chopper*, che sembrerebbe il responsabile della morte cellulare (Sofroniew *et al*., 2001; Coulson *et al*., 2004). Infatti, mentre la delezione del dominio *death* non riduce affatto la morte cellulare, l'assenza del dominio *Chopper* la previene; il dominio *death* agirebbe in modo da regolare o modulare la via apoptotica iniziata dal dominio *Chopper*, piuttosto che promuoverla esso stesso (Coulson *et al*., 2004).

Proteasi apoptotiche, caspasi e calpaine giocano un ruolo essenziale nella regolazione della plasticità sinaptica che viene controllata anche da un aumento extracellulare di ioni K^+ ed un aumento intracellulare di ioni Ca^{2+}. Tuttavia, è risultato evidente che ridotti livelli intracellulari di K^+ possono mediare anche apoptosi, come è stato confermato da Coulson e coll. (2004), i quali hanno osservato una correlazione tra una forma di morte cellulare mediata dal p75, attraverso il dominio *Chopper*, ed un flusso verso l'esterno del neurone di ioni K^+ (Coulson *et al*., 2004).

Un grande numero di proteine intracellulari interagiscono con il segmento intracellulare del p75. Alcune promuovono la morte cellulare come NRIF (fattore di interazione col recettore di neurotrofine); TRAF (fattore associato a TNFR); NADE (*death effector* associato al recettore di neurotrofine); NRAGE (membri della famiglia MAGE); Rac (membro della famiglia GTPase). Altre invece mediano processi cellulari riguardanti il *survival* cellulare mediante l'attivazione di NF-kB che induce la sintesi di proteine antiapoptotiche (IAP). Queste sono rappresentate da sc-1 (proteina legante zinco); caveolina; altre proteine TRAF; RhoA (membro della famiglia GTPase); RIP2 (proteina-2 che interagisce col recettore).

Il punto di arrivo della cascata apoptotica consiste nell'attivazione delle caspasi. Esistono varie isoforme di caspasi, ma quelle coinvolte nel meccanismo mediato dal

p75 sono le caspasi –3 e –9 indotte rispettivamente dalle proteine NADE e NRAGE. Quest'ultima, più precisamente, è in grado di antagonizzare una delle proteine anti-apoptotiche (XIAP) che solitamente controlla l'attività dell'apoptosoma. Si tratta di un complesso ternario costituito da APAF-1 (fattore-1 attivante le proteasi apoptotiche), caspase-9 e Bcl-$_{xL}$ (membro anti-apoptotico appartenente alla famiglia di Bcl-2). I primi due si legano tra di loro in presenza di dATP e di citocromo c rilasciato dai mitocondri, evento questo che attiva le caspasi-9 che a loro volta attivano le caspasi-3. Le caspasi-3 e la proteina apoptotica Bax attivano le JNK (Jun kinasi) che insieme alla proteina p53 partecipano alla cascata apoptotica promossa dall'apoptosoma (Coulson *et al*., 2004). L'attivazione di questo complesso richiede, oltre al rilascio di citocromo c dal mitocondrio, anche una riduzione dei livelli di K^+ intracellulare, poiché a normali concentrazioni intracellulari dello stesso ione, non avviene l'assemblaggio delle tre proteine. Già in precedenza è stato riportato che l'efflusso di K^+ è una delle prime risposte apoptotiche nei neuroni, nei linfociti ed in altri tipi cellulari. Contribuisce alla perdita del volume cellulare, alla comparsa di annexina V sulla membrana extracellulare ed inoltre promuove l'attivazione di endonucleasi che frammentano il DNA. GIRK sono canali di K^+ che normalmente si aprono in presenza di PIP2 (fosfatidilinositolo), la cui sintesi è sostenuta dalla proteina Rac e per interazione con le subunità b/g delle proteine G in seguito all'attivazione di un recettore (accoppiato a proteine G) da parte del neurotrasmettitore. Le proteine G possono attivare anche la fosforilazione del recettore Trk che a sua volta fa prevalere il *pathway* del *survival* su quello di morte cellulare mediato dal p75, in quanto, attivando la PLC (fosfolipasi C), provoca idrolisi di PIP2 e quindi inattiva il canale GIRK. In assenza di neurotrasmissione e del Trk, il p75 attivato stimola l'apertura dei canali GIRK iniziando così la cascata della via apoptotica (Coulson *et al*., 2004) (Fig. 5).

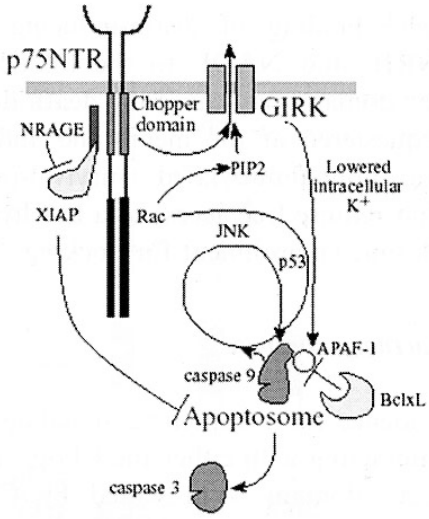

Fig. 5: schema riassuntivo della cascata apoptotica mediata dall'interazione del dominio *Chopper* ed il canale GIRK. (tratto da Coulson *et al*., 2004)

Un altro *pathway* coinvolto nel *signaling* apoptotico, in seguito all'attivazione del p75, consisterebbe nella formazione del lipide ceramide ottenuto per idrolisi della sfingomielina ad opera della sfingomielinasi. Questi enzimi sono presenti nelle membrane cellulari e si pensa che siano attivate da diversi stimoli come shock termico, radiazione ultravioletta, stress ossidativo (Barrett, 2000). Nei neuroni sensitivi però si è trovato che la somministrazione di ceramide esogena provoca un aumento del *survival* cellulare confutando così l'ipotesi di partenza (Barrett, 2000). La spiegazione a ciò è che in normali condizioni la ceramide viene metabolizzata dall'enzima ceramidasi in sfingosina, responsabile del *survival* cellulare. Quindi si ha morte cellulare in caso di inibizione della ceramidasi e conseguente accumulo di ceramide (Barrett, 2000).

Per approfondire lo studio sulla morte cellulare programmata nel SNC, molti autori utilizzano il modello rappresentato dalle cellule gangliari retiniche (RGC) (Cellerino *et al*., 2000), in quanto la retina è una struttura semplice, facente parte del SNC: il nervo ottico è mielinizzato da oligodendrociti e le RGC hanno le loro proiezioni interamente contenute nel SNC. Esse ricevono input eccitatori glutamatergici dalle cellule bipolari, input eccitatori (colinergici) ed inibitori (GABAergici e Glicinergici) dalle cellule amacrine. Tutte le RGC inviano i loro assoni al nervo ottico e proiettano ai primi centri visivi del cervello, localizzati nel talamo e nel mesencefalo. Principalmente nel ratto la

maggior parte delle RGC proiettano al collicolo superiore ed ai nuclei pretettali, con circa un 30% che invia collaterali al nucleo genicolato nel talamo.

Nel ratto circa il 50% delle RGC neoformate muoiono subito dopo aver raggiunto il proprio *target*, e molte altre anche prima che la migrazione nello strato retinico sia completa. Recenti investigazioni indicano che la morte cellulare delle RGC avvenga per apoptosi e che questa sia regolata dagli stessi *pathways* indotti da una lesione del nervo ottico (Cellerino *et al*., 2000) oppure da glaucoma o assotomia (Qin *et al*., 2004). Una sezione del nervo ottico induce cambiamenti nell'omeostasi cellulare con perdita del supporto trofico e di sensibilità dei neuroni e conseguente morte delle RGC. Il processo apoptotico coinvolge due principali meccanismi: uno estrinseco scatenato dall'attivazione dei recettori della famiglia di TNF, ed uno intrinseco dovuto alla deprivazione dei fattori di crescita, a vari tipi di stress ed all'attivazione della proteina p53 (Qin *et al*., 2004).

Le molecole pricipalmente coinvolte sono la proteina bcl-2 essenziale nel *survival* e Bax induttore apoptotico. In seguito ad un trauma aumenta l'attività di Bax che viene traslocato nel mitocondrio e dimerizzando, forma dei pori nella membrana esterna mitocondriale che consentono il rilascio del citocromo c nel citoplasma. Il citocromo c e ATP sono cofattori dell'attivazione del fattore APAF-1, quest'ultimo attivato forma l'apoptosoma, insieme al citocromo c ed alla procaspasi-9, portando alla cascata delle caspasi. Bax prende parte anche al *pathway* estrinseco attraverso la proteina Bid che è un membro della famiglia di bcl-2. L'attivazione di Bid, in seguito all'attivazione del recettore di TNF, come risulta da lavori in vitro, potrebbe essere un meccanismo con cui Bax, inserito nella membrana mitocondriale esterna, ne facilita la permeabilizzazione (Qin *et al.,* 2004).

Nelle RGC durante lo sviluppo si ha una *down*-regulation dell'espressione di bcl-2 così che nelle cellule adulte è presente una piccola quantità della proteina. Al contrario, l'espressione di bax è molto variabile. In presenza di una lesione del nervo ottico si ha una scomparsa di bcl-2 ed un aumento di Bax. Da studi eseguiti su retine embrionali di pollo (animali E6), è risultato che NGF, legandosi al recettore p75, può regolare il processo apoptotico. Infatti, l'uso di anticorpi anti-NGF o anti-$p75^{NTR}$ ha ridotto fortemente il numero di cellule apoptotiche; si è ottenuto lo stesso risultato anche in topi transgenici $ngf^{-/-}$ e negli embrioni $p75^{NTR-/-}$. Tuttavia, la somministrazione di NGF

esogeno non aumenta l'apoptosi: poiché NGF endogeno è legato alle cellule microgliali nel primo sviluppo della retina, NGF esogeno potrebbe semplicemente non essere presentato in modo appropriato da attivare il recettore p75 (Cellerino *et al*., 2000).
Recenti studi hanno proposto che, nella retina di pollo, le RGC stratificate controllano il numero delle stesse mediante secrezione di NGF che a sua volta elimina le RGC migratorie, interagendo con il p75 espresso da queste ultime. D'altro canto, le RGC stratificate possono sopravvivere all'effetto apoptotico di NGF, in quanto esprimono il recettore TrkA responsabile appunto di un effetto neurotrofico (Harada *et al*., 2006).
Invece, nella retina di topo, l'espressione dei due recettori per NGF nelle RGC migratorie e in quelle stratificate è invertita. Il p75 regola il processo apoptotico nella prima fase dello sviluppo retinico, successivamente intervengono altre molecole a regolare il numero delle cellule gangliari (Harada *et al*., 2006). Tra queste sono essenziali i fattori trofici come NGF, BDNF e NT-4, infatti le RGC esprimono anche il recettore TrkB che promuove il *survival* delle RGC neonatali. Quindi un bilancio tra l'effetto neuroprotettivo di BDNF e di NT-4, e quello apoptotico da parte di NGF può influenzare l'espressione dei recettori Trk e p75, determinando così il destino delle RGC. Tuttavia, l'effetto di BDNF è transiente in quanto un trattamento continuo con BDNF esogeno può provocare desensitizzazione del recettore ed inoltre induce un aumento di ossido nitrico dannoso per le stesse RGC (Cellerino *et al*., 2000).
Pichè in altre situazioni il p75 può fungere da molecola neuroprotettiva e necessaria per la rimielinizzazione, sono necessari ulteriori studi per rivelare il preciso ruolo del recettore.

1.3 NGF e angiogenesi

Con il termine "angiogenesi" si indica la formazione di nuovi vasi da una rete vascolare pre-esistente, regolata dal bilancio locale di molecole in grado di indurla o inibirla; per "vasculogenesi" si intende, invece, il processo di formazione di nuovi vasi a partire dagli angioblasti, precursori delle cellule endoteliali. Vari sono i segnali che provocano angiogenesi: dai parametri metabolici dovuti ad una ridotta pressione di O_2 , ad un basso pH, a processi infiammmatori, a varianti genetiche, etc.

Negli ultimi anni è stato da diversi gruppi dimostrato un coinvolgimento di NGF nei processi di angiogenesi e vasculogenesi in diversi tessuti, compreso il nervoso. Il nostro laboratorio ha dimostrato (Calzà *et al*., 2001) che la somministrazione di NGF nell'immediato post-natale influenza la crescita dei gangli cervicali simpatici anche attraverso la regolazione della vascolarizzazione, effetto questo esaltato dalla lesione con 6-idrossi dopamina (Calzà *et al*., 2001). Questo effetto sembrerebbe mediato a breve termine da un'aumentata produzione neuronale dell'enzima di sintesi dell'ossido nitrico, a più lungo termine da un'aumentata espressione neuronale del peptide angiogenico fattore di crescita andoteliale vascolare (VEGF). Questo dato è stato interpretato come un effetto diretto di NGF sul trofismo delle cellule gangliari, che aumentano di numero e di dimensione, a seguito dell'azione della neurotrofina, provvedendo contemporaneamente alla sintesi di fattori vasodilatatori e pro-angiogenetici, proprio per garantire l'adeguato supporto metabolico al ganglio ipertrofico.

Oltre che ad agire direttamente o indirettamente sull'angiogenesi, NGF è anche in grado di esercitare un effetto mitogenico diretto sulle cellule endoteliali (Cantarella *et al*., 2002). Studi in vitro hanno portato ad ipotizzare che questo effetto sia di tipo autocrino. Le cellule endoteliali della vena ombelicale umana (HUVEC), infatti, esprimono NGF (RNAm e proteina) ed anche TrkA, attraverso la cui fosforilazione induce la proliferazione cellulare. E' stato quindi ipotizzato che in caso di privazione del siero, condizione che in vitro mima una deplezione di nutrienti e supporto trofico, l'aumento di NGF possa promuovere la proliferazione di cellule endoteliali e quindi il ripristino di un adeguato supporto metabolico (Cantarella *et al*., 2002).

Un altro tessuto preso in considerazione per studiare l'effetto di NGF sulla formazione di nuovi vasi, è il tessuto adiposo bruno (BAT) che è presente nella maggior parte di animali che vanno in letargo ed anche nei neonati. Si tratta di un tessuto altamente specializzato in quanto produce calore in risposta al freddo o in seguito al consumo di cibo. La termogenesi è attivata dalla norepinefrina secreta dalle terminazioni nervose simpatiche che a loro volta sono sotto il controllo di NGF. E' stato dimostrato che l'*over*-espressione di NGF nel tessuto adiposo grigio (in topi che *over*-esprimono diffusamente NGF), provoca un aumento di VEGF e dei suoi recettori, effetto questo bloccato da anticorpi anti NGF. L'aumento della densità delle fibre nervose associata

con la vascolarizzazione rafforza l'ipotesi che l'irrorazione del tessuto adiposo sia regolata da un controllo nervoso dei vasi e che la stretta correlazione tra NGF e VEGF rappresenti un fattore chiave per attivare il fenomeno dell'angiogenesi (Hansen-Algenstaedt *et al*., 2006).

Il ruolo di NGF nella stretta correlazione fra innervazione e angiogenesi, è suggerita anche da studi sulla cute di soggetti affetti da diabete di Tipo I. Sia nei roditori che nell'uomo, può causare la formazione di ulcere mediante alterazioni delle cellule endoteliali, dovute ad una ridotta proliferazione e ad un aumento dell'apoptosi (Graiani, *et al*., 2004). In questa condizione è stato riscontrato non solo un basso livello di NGF, ma anche una riduzione di circa 100 volte del rapporto TrkA/p75 espressi dall'endotelio. Si è osservato che più del 90% delle cellule endoteliali apoptotiche, nelle ulcere da diabete, sono p75-positive. In questi casi il trattamento con NGF ha migliorato la vascolarizzazione, probabilmente attraverso la stimolazione della proliferazione delle cellule endoteliali e l'inibizione della loro morte per apoptosi, grazie all'aumento dell'espressione dei recettori TrkA. Anche in questo studio è stata evidenziata l'azione indiretta di NGF sull'endotelio attraverso la stimolazione di mitogeni endoteliali quali VEGF e modulatori della vasodilatazione come NO (Graiani *et al*., 2004).

Questi esperimenti ed altri prima di questo, volti allo studio del possibile effetto riparatore di NGF su lesioni ulcerative e cutanee e della cornea, hanno in realtà aperto una nuova prospettiva sulla molteplicità dei possibili bersagli cellulari dell'azione di NGF. Le ulcere cutanee, sono infatti associate ad un danno strutturale e funzionale che coinvolge numerose cellule e diversi processi fisiopatologici: vi si osserva un'alterata innervazione periferica sensitiva e simpatica; l'attivazione delle cellule infiammatorie; il rilascio di vari fattori di crescita come il PDGF (fattore di crescita derivato dalle piastrine), EGF (fattore di crescita epidermico), FGF (fattore di crescita dei fibroblasti), TGFβ (fattore di crescita trasformante beta) e NGF da parte di cheratinociti e fibroblasti (Aloe, 2004). NGF può essere secreto dai fibroblasti/miofibroblasti, dalle cellule epiteliali, dai cheratinociti, dalle cellule immunitarie e dalle cellule endoteliali. Tutte queste, insieme alle fibre nervose periferiche sensitive e simpatiche, sono in grado di rispondere agli stimoli di NGF, confermando l'ipotesi che NGF agisce meccanismi autocrino e/o paracrino.

Nelle ferite cutanee, NGF oltre ad indurre la proliferazione delle cellule endoteliali,

promuove anche l'espressione della metalloproteinasi 9 di matrice nelle cellule muscolari lisce vascolari. Questo enzima contribuisce alla migrazione delle cellule muscolari dalla matrice extracellulare verso lo spazio interno ai due lembi della ferita favorendone la contrazione (Nockher and Renz, 2006).

1.4 NGF ed infiammazione

NGF è essenziale nell'organizzare e nel mantenere funzionanti i neuroni ed i circuiti neurali ad esso sensibili. Gioca un ruolo chiave nell'indurre differenziazione, promozione del survival e prevenzione dell'apoptosi in neuroni del sistema nervoso centrale e periferico. Ma oltre alla sua attività neurotrofica, negli anni recenti è stato sottolineato il suo ruolo nella regolazione delle risposte infiammatorie ed immunitarie (Micera *et al*., 2003), al punto da diventare un possibile bersaglio dellla regolazione farmacologica di questi processi. Il coinvolgimento di NGF in diverse malattie infiammatorie periferiche, quali l'asma, allergie da contatto, psoriasi, dermatite atopica, è stato ampiamente dimostrato nella specie umana (Renz *et al*., 2004).
NGF è sintetizzato e rilasciato da cellule infiammatorie quali i lifociti T e B, i mastociti, gli eosinofili, i monociti, oltre che da cellule epiteliali e fibroblasti (Lipnik-Stangelj, 2006). La sintesi e la secrezione di NGF è regolata da vari meccanismi molecolari a cui prendono parte molte sostanze (neurotrasmettitori, fattori di crescita, citochine, steroidi). Inoltre, le interleuchine (IL-1β e IL-6) e l'istamina sono riconosciute come potenti induttori della sintesi e del rilascio di NGF sia a livello centrale che periferico (Lipnik-Stangelj, 2006). Tutte le cellule infiammatorie esprimono TrkA e p75, garantendo quindi un loop autocrino/paracrino. Il TrkA è stato trovato nelle mast cellule umane di cui promuove l'attivazione e la degranulazione; nei linfociti-B aumentandone la proliferazione e stimolando la risposta anticorpale; nei linfociti-T, nei macrofagi alveolari e nei basofili, attivandone il differenziamento ed il *survival* (Freund and Frossard, 2004). Il p75 viene espresso per la maggior parte dalle cellule strutturali: nella cute media i segnali apoptotici dei fibroblasti soprattutto nell'ultima fase riparatrice e di rimodellamento tissutale (Kawamoto e Matsuda, 2004). NGF può a sua volta promuovere il rilascio di istamina con un meccanismo a *feed-back* positivo, andando così ad amplificare la risposta infiammatoria (Lipnik-Stangelj, 2006).

In condizioni infiammatorie croniche, quali allergie ed asma, vi è una complessa alterazione strutturale dei tessuti coinvolti che comprende anche un'alterazione dell'innervazione sensitiva e simpatica. Genericamente l'espressione di neurotrofine NGF e BDNF, è fortemente aumentata in corso di infiammazione cronica e tutti gli elementi cellulari ricordati (neuroni, cellule endoteliali, fibroblasti, cellule immuntarie, cellule infiammatorie) sono identificate non solo come fonte ma anche come target delle neurotrofine (Nockher and Renz, 2006). Nelle patologie infiammatorie delle vie respiratorie, l'iperreattività bronchiale è ad esempio correlata ad un aumento dell'innervazione sensitiva dovuta alla presenza di elevati livelli di NGF che viene rilasciato dalle cellule infiammatorie. NGF a sua volta, stimola molte di queste cellule a rilasciare anche le citochine pro-infiammatorie che possono indurre ulteriore produzione dello stesso fattore di crescita da parte di altre cellule. Ad esempio, IL-1β e TNF-α (fattore di necrosi tumorale alfa) possono aumentare la secrezione di NGF da parte di fibroblasti, cellule epiteliali polmonari e cellule muscolari liscie bronchiali.

NGF partecipa anche al fenomeno della "infiammazione neurogenica". È noto infatti che l'attivazione delle fibre sensitive periferiche, che mediano la percezione del dolore, e la cui attività è esaltata in corso di infiammazione, rilasciano alcuni neuropeptidi (sostanza P, CGRP) non solo a livello di midollo spinale, ma anche e soprattutto, nei tesssuti periferici, dove questi peptidi svolgono una potente azione vasodilatatoria e di attrazione chemotattica di cellule infiammatorie. NGF ha diversi effetti sui neuroni sensitivi nocicettivi nell'adulto: induce una *up-regulation* dei recettori TrkA e p75, aumenta l'espressione di CGRP (*calcitonin gene related peptide*) e di tachichinine, modula l'attività cellulare ed il rilascio di neuropeptidi (McMahon, 1996).

Numerosi dati su modelli animali anche trangenici, modelli di patologie dolorose acute a croniche e studi sull'uomo hanno indicato un importante ruolo di NGF nella genesi del dolore in condizioni infiammatorie sia acute che croniche (Hefti *et al*., 2006). NGF è responsabile dell'iperalgesia si termica che meccanica nella fase acuta dell'infiammazione, come è dimostrato dalla sua soppressione in seguito alla somministrazione di anticorpi anti-NGF (Shu and Mendell, 1999). NGF altera la risposta dei nocicettori agli stimoli dolorosi, inducendo la degranulazione dei mastociti con conseguente rilascio di istamina, serotonina ed NGF stesso e *up*-regola la produzione ed il rilascio di neuropeptidi vasoattivi (CGRP, SP e BDNF) (Shu and

Mendell, 1999).

Ma l'azione di NGF sul primo neurone in corso di patologie infiammatorie media anche effetti adattivi a più lungo termine. Il legame NGF-TrkA favorisce la fosforilazione del canale TRPV1 (*vanilloid receptor*) e successiva traslocazione sulla superficie cellulare. Si tratta di un canale cationico identificato inizialmente come recettore della capsacina (alcaloide presente nel peperoncino piccante) che, una volta attivato, porta ad un aumento intracellulare di cationi mono- e di-valenti (principalmente Ca^{2+}) con successiva depolarizzazione e quindi aumentata eccitabilità cellulare (Hefti *et al*., 2006). Il trasporto retrogrado del segnale, mediante via endosomica, dal terminale periferico al corpo cellulare dei neuroni nocicettivi promuove l'espressione di molte proteine che sensitizzano maggiormente i neuroni stessi e facilitano l'attivazione di neuroni secondari nel SNC. Queste proteine includono: la sostanza P e il CGRP; il canale del Na^+ ($Na_v1.8$) che viene espresso esclusivamente dai nocicettori ed è coinvolto nell'iperalgesia NGF-indotta; il canale ionico 3 acido-sensibile che è attivato nel dolore ischemico e infiammatorio; il canale TRPV1; e BDNF che è trasportato alle sinapsi centrali dove aumenta l'eccitabilità nocicettiva riflesso-spinale. BDNF e TRPV1 successivamente possono anche essere trasportati in modo anterogrado (Hefti *et al*., 2006).

NGF è prodotto anche nell'ippocampo adulto, interviene nel prevenire la degenerazione di neuroni colinergici e contrasta l'atrofia degli stessi nel forebrain basale del cervello di ratto adulto. NGF è in grado sia di prevenire la degenerazione colinergica che stimolare la produzione ed il rilascio di acetilcolina dai neuroni rimanenti (Tuszynski and Blesch, 2004).

2. SCOPO DELLA RICERCA

Il nostro laboratorio è da diversi anni impegnato nello studio del ruolo di NGF in diversi processi patologici sperimentali e spontanei nell'animale da laboratorio, negli animali domestici e nella specie umana. Focus primario di questo lavoro è l'indagine di processi patogenetici responsabili della evoluzione temporale di patologie, nell'intento di definire se NGF può candidarsi come molecola chiave per il controllo della

progressione di patologie croniche. In particolare in questa tesi vengono riportati dati relativi al possibile intervento di NGF in 3 diverse condizioni sperimentali a carico del sistema nervoso periferico e sistema nervoso centrale:

1. transizione da dolore acuto a dolore cronico in un modello di flogosi articolare cronica (artrite da *Complete Freund Adjuvant*). In questo modello, già ampiamente caratterizzato dal nostro laboratorio (Calzà *et al.,* 1998; 2000), per la transizione fenotipica del primo neurone che suggerisce la sua evoluzione temporale da modello di dolore infiammatorio acuto a modello di dolore neuropatico, viene studiata l'espressione di NGF e dei suoi recettori nel distretto cutaneo interessato dall'infiammazione, e correlato con processi proliferativi cellulari e innervazione;
2. ipoperfusione cerebrale cronica, indotta dalla occlusione bilaterale delle carotiti comuni nel ratto. Questo modello è caratterizzato da una duplice lesione: l'atrofia del nervo ottico e della retina, e la compromissione ippocampale, che porta nel tempo ad un difetto colinergico, di espressione di NGF e cognitivo (apprendimento e memoria). Nello sviluppo e caratterizzazione del modello, mai prima utilizzato dal nostro laboratorio, è stata studiata la variazione età-dipendente della neurogenesi ippocampale indotta dal difetto vascolare cronico. Con riferimento a NGF, è stata studiata la capacità di questa neurotrofina di interferire con il processo di apoptosi e di neoangiogenesi, quando iniettata in singola dose nella camera posteriore dell'occhio;
3. NGF ed epilessia. La corteccia ippocampale rappresenta una struttura cerebrale altamente sensibile a stimoli lesivi, che rappresentano un potente induttore della sintesi locale di NGF. In particolare, in corso di epilessia sperimentale si osserva un drammatico aumento della sintesi di neurotrofine ippocampali, espresse a bassissimo livello in condizioni basali (Calzà *et al*., 1996). In un primo lavoro eseguito su cani soppressi in corso di crisi convulsiva intrattabile (da infezione da virus del cimurro), a confronto con animali di controllo, abbiamo studiato mediante immunoistochimica la neurochimica della corteccia ippocampale, nell'intento di verificare se le alterazioni nell'espressione di neurotrasmettitori, neuropeptidi e neurotrofine descritte dalla letteratura nei modelli sperimentali di crisi convulsiva fossero presenti anche nella patologia spontanea di una specie animale con importanti affinità rispetto all'umana, relativamente a ptologie neurologiche. È stato

poi sviluppato il sistema in vitro di isolamento delle cellule staminali neurali da ippocampo umano prelevato da pazienti con epilessia farmacoresistente, nell'intento di sviluppare un modello di studio *ex vivo* per l'interazione di NGF con i neurotrasmettitori chiave della funzione ippocampale (glutammato e GABA).

3. MATERIALI E METODI

Per una descrizione più dettagliata dei metodi si rimanda ai singoli lavori

3.1 Esperimenti in *vivo*

3.1.1 Animali e trattamenti

Animali

Sono stati utilizzati animali della Charles River Laboratories Italia (Calco, Lecco) ed in particolare: ratti maschi adulti Sprague Dowley apatogeni di età 2, 3 e 12 mesi all'inizio degli esperimenti. Tutti gli animali sono stati stabulati in gabbie di plexiglas in numero e in condizioni conformi alle norme vigenti, in condizioni standard di luce e buio (luce dalle 7.00 a.m. alle 7.00 p.m.), temperatura 19-22 °C, umidità 45 %, cibo e acqua ad libitum.

Per gli esperimenti riguardanti lo studio dell'ippocampo in corso di encefalite da virus del cimurro sono stati utilizzate le seguenti razze di cane:

ID	**Breed**	**Sex**	**Age (months)**
1	English setter	F	6
2	Mixed	M	12
3	Mixed	M	3
4	Mixed	F	3
5	Yorkshire	F	2
6	Corso	F	15
7	German shephered	F	2

8	Mixed	F	
10	Bulldog		

Tutte le sperimentazioni sono state eseguite dopo approvazione dei comitati etici e comunque in accordo con le "*European Community Council Directives"* del 24 Novembre 1986 (86/609/EEC. Per ogni sperimentazione ciascun gruppo di animali varia da 3 a 10.

Induzione dell'ipoperfusione

I ratti utilizzati sono maschi Sprague Dowley apatogeni di 3 e 12 mesi. Dopo anestesia con ketamina cloridrato (equivalente a ketamina 1mg/bw), si esegue un'incisione ventrale sulla linea mediana e si espongono bilateralmente le arterie carotidi che vengono separate delicatamente dal nervo vago, dopo essere state isolate dalla guaina connettivale. Segue una doppia legatura ad entrambi i lati con un filo di seta 5-0: la prima approssimativamente 8-10 mm inferiore alla biforcazione dell'arteria carotide comune (Davidson *et al*., 2000), la seconda 2-5 mm al di sotto della prima.

Durante l'operazione la temperatura corporea viene mantenuta a 37°C ponendo l'animale su una coperta termo-riscaldata fino alla completa ripresa di conoscenza.

Iniezione intravitreo

24 h dopo l'intervento, si anestetizza il ratto con ketamina cloridrato (1mg/bw) e dopo aver instillato in ciascun occhio del collirio anestetico (Ossibuprocaina 4mg/ml) si procede all'iniezione intravitreo mediante l'utilizzo di un microscopio operatorio (Wild Heerbrugg M651). L'iniezione viene effettuata a livello della pars plana utilizzando un ago (butterflay) 27 gauge (PIC) collegato ad una siringa Hamilton da 25 □l. L'ago, prima di essere rimosso, viene lasciato in sede per due minuti agevolando la diffusione delle soluzioni all'interno dell'umor vitreo ed evitandone la fuoriuscita.

Il volume iniettato è di 3 □l di soluzione salina sterile nell'animale controllo, e di 5 □g di NGF in 3 □l di soluzione fisiologica nell'animale trattato.

Alla fine dell'iniezione si instillano alcune gocce di collirio antibiotico (Tobromicina 3gr/100ml), per evitare insorgenza di infezioni.

Induzione CFA

L'artrite da adiuvante è stata indotta in animali di 125-150 g dalla Charles River Francia mediante una singola iniezione intradermica di 0,1 ml alla base della coda sul lato dorsale di *Mycobacterium butyricum* inattivato al calore ad una concentrazione di 40 mg/ml sospeso in olio di paraffina.

3.1.2 Test comportamentali

Valutazione del riflesso pupillare

L'effettiva ipoperfusione, viene valutata mediante perdita del riflesso pupillare. Gli animali vengono adattati al buio per 5 minuti, quindi con un otoscopio si dirige un raggio luminoso prima su di un occhio (riflesso diretto) e subito dopo sull'altro (riflesso consensuale). Segue il buio per un altro minuto e si ripete la procedura partendo questa volta dall'altro occhio. La perdita del riflesso pupillare consiste nella non costrizione della pupilla dopo un'esposizione di 10 sec. alla luce.

Il test del riflesso pupillare va eseguito quotidianamente, a partire dal giorno dopo l'iniezione intravitreo, per almeno 7 giorni (periodo massimo entro cui l'animale può perdere il riflesso), segue un'osservazione a settimana fino al sacrificio.

Valutazione dell' edema (Pletismometro)

L'edema è stato valutato utilizzando il pletismometro (Ugo Basile Italia). Il pletismometro è un strumento in grado di determinare il volume di una zampa basandosi sul principio di Archimede; è costituito da una cella nella quale è contenuta acqua ad una temperatura di circa 37°C e un trasduttore in grado di determinare la variazione del volume di acqua nella cella. Lo strumento è stato tarato ad ogni utilizzo mediante gli appositi standard a volumi noti. La zampa posteriore degli animali è stata immersa fino all'altezza del calcagno nella cella. Sono stati raccolti tre valori per ciascuna delle zampe posteriori per ciascun animale ed è stata ottenuta la media dei tre.

Sensibilità a stimoli termici (Plantar Test)

La soglia di sensibilità al dolore per stimoli termici è stata valutata utilizzando lo

strumento “plantar test” (Ugo Basile Italia). Il plantar test è uno strumento in grado di valutare il tempo impiegato dagli animali liberi di muoversi per sottrarre la zampa esposta ad una sorgente puntiforme di calore; è costituito da tre compartimenti fra loro separati che posano su una superficie di vetro, al di sotto della quale è presente un generatore infrarosso mobile dotato di sensore in grado di arrestare il timer nel momento in cui l’animale solleva la zampa. Gli animali CFA sono stati sistemati e lasciati ambientare per alcuni minuti in appositi compartimenti. Sotto la superficie d’appoggio, in corrispondenza delle zampe posteriori, è stato posizionato un generatore infrarosso mobile in grado di determinare calore in un punto specifico. Il test consiste nel valutare il tempo in secondi impiegato dall’animale dal momento in cui parte il fascio luminoso al momento in cui solleva la zampa. Il test è stato ripetuto cinque volte, a distanza di cinque minuti l’una dall’altra, su ciascun animale per ciascuna delle zampe posteriori. Dai valori ottenuti è stata effettuata la media per ogni singola zampa.

3.1.3 Istologia ed Immunoistochimica

Fissazione in vivo

Gli animali sono stati anestetizzati con Cloralio Idrato (350 mg/Kg/ml, Sigma). Quando l’animale è profondamente addormentato viene perfuso attraverso l’aorta ascendente con soluzione salina calda (37°C), seguita da Lana’s (paraformaldeide 4% (w/v), soluzione satura di acido picrico, tampone Sörensen 0.4 M a pH 6.9, H_2O bidistillata). Dopo la decapitazione il cervello e il midollo vengono rimossi e immersi per un tempo che varia dai 90 minuti alle 24 ore in paraformaldeide 4% a 4°C e successivamente immersi per almeno 48 ore in saccarosio al 5% in tampone fosfato Sörensen 0.1M.

Acetilcolinesterasi

Dopo la perfusione e il congelamento con neve carbonica dell’area di interesse, le sezioni sono allestite al criostato (14 mm di spessore; Kriostat 1720, Leitz). Dopo essere state portate a temperatura ambiente per circa 15 minuti vengono immerse in tampone acetato (0.1M, pH 6) 2x2 min. Si esegue poi l’incubazione a 37°C per 30 min in una soluzione contenente: sodio acetato 0.1M pH 6, sodio citrato 0.1M, solfato di rame 0.03M, ferrocianuro di potassio 0.1mM. Seguono 5 passaggi da 1 min. in tampone

acetato (0.1M, pH 6), 1 min. in solfuro di ammonio (1%), 5 passaggi da 1 min. in nitrato di sodio (0.1M), 1 min. in nitrato di argento (0.1%), 5 passaggi da 1 min. in nitrato di sodio (0.1M), e 2 min. in tampone acetato (0.1M, pH 6). Dopo disidratazione in alcool le sezioni si montano in Eukitt (Kindler, Freiburg, Germany).

Colorazione nucleare con Hoechst-33258

Per evidenziare lo stato di condensazione della cromatina è stata utilizzata la colorazione con Hoechst-33258. Il protocollo prevede l'allestimento di sezioni al criostato dello spessore 14mm. Si idratano le sezioni con PBS e si effettuano tre lavaggi di 10 min. ciascuno in PBS-Triton$_{x\text{-}100}$ 0.2%. Successivamente il colorante Hoechst-33258 (1mg/ml PBS) viene fatto reagire con le sezioni per 20 minuti a temperatura ambiente; seguono tre lavaggi da 10 min. in PBS-Triton$_{x\text{-}100}$ 0.2% ed infine si montano i vetrini con una soluzione contenente glicerolo 50% v/v, citrato 0.044M, tampone fosfato 0.111M, pH 5.5.

La coesistenza di un antigene specifico con la frammentazione nucleare viene evidenziata con una doppia colorazione. Dopo la visualizzazione dell'antigene con la tecnica dell'immunofluorescenza indiretta viene eseguita la colorazione con il colorante nucleare, come sopra descritta, preceduta da tre lavaggi da 10 minuti in PBS-Triton$_{x\text{-}100}$ 0.2%. I vetrini vengono montati con fenilendiammina.

Immunofluorescenza Indiretta

Dopo la perfusione (vedi sopra) e il congelamento della regione d'interesse con neve carbonica, le sezioni vengono allestite al criostato, 14 mm di spessore e tenute a -20°C fino al momento dell'uso. I vetrini vengono portati a temperatura ambiente per 30 minuti e viene eseguita un'idratazione con PBS per 15-30 minuti. Segue l'incubazione delle sezioni con anticorpo primario diluito in PBS-Triton$_{x\text{-}100}$ 0.3% (a 4°C, per tutta la notte in camera umida). Dopo il lavaggio con PBS, le sezioni vengono incubate a 37°C per 30 min con l'anticorpo secondario, coniugato con una molecola fluorescente (Jackson Immuno Research Laboratories, INC, PA), diluito in PBS-Triton$_{x\text{-}100}$ 0.3%. Dopo aver effettuato 2 lavaggi di 15 min. in PBS, i vetrini vengono montati con fenilendiammina (fenilendiammina 0.1% glicerina-PBS 50% tampone borato, pH 8.6). Gli anticorpi utilizzati sono indicati nella seguente tabella (**TAB I**).

TAB I

Anticorpi primari

Anticorpo	**Specie**	**Diluizione**	**Ditta**
P75	Goat	1:100	S.Cruz biotechnology,U.S.
CGRP	Rabbit	1:2000	Peninsula
PGP 9.5	Rabbit	1:1000	Biogenesis
β−tubulina	Mouse	1:600	R&D Systems
MBP	Rabbit	1:100	DAKO
OX42	Mouse	1:300	Serotech
Laminina	Rabbit	1:25	Sigma
CDV	Mouse	1:5	Biodesign
NG2	Rabbit	1:250	Chemicon
c-fos	Rabbit	1:100	S.Cruz biotechnology,U.S.
NFkB	Rabbit	1:100	S.Cruz biotechnology,U.S.
BDNF	Rabbit	1:500	Chemicon
NGF	Rabbit	1:200	S.Cruz biotechnology,U.S.
Neuronal glutamate transporter	Goat	1:3000	Chemicon
Met-ENK	Rabbit	1:750	Chemicon
Galanin	Rabbit	1:500	Peninsula
MOR1	Guinea pig	1:500	Chemicon
MAP-2	Rabbit	1:300	S.Cruz biotechnology,U.S.
GFAP	Mouse	1:600	Sigma
MCM2	Goat	1:150	S.Cruz biotechnology,U.S.
DCX	Goat	1:150	S.Cruz biotechnology,U.S.
NeuN	Mouse	1:100	Chemicon
BrdU	Rat	1:100	ImmunologicalsDirect
S100	Rabbit	1:50	Incstar

NG2	Mouse	1:100	Chemicon

Anticorpi secondari

Anticorpo	**Specie**	**Diluizione**	**Fluorocromo**	**Ditta**
Rabbit IgG	Donkey	1:75	Cy2	Jackson Immuno Research Laboratories
Mouse IgG	Donkey	1:50	Cy2	Jackson Immuno Research Laboratories
Goat IgG	Donkey	1:100	Cy2	Jackson Immuno Research Laboratories
Rat IgG	Donkey	1:100	RRX	Jackson Immuno Research Laboratories
Rabbit IgG	Donkey	1:75	RRX	Jackson Immuno Research Laboratories
Mouse IgG	Donkey	1:100	RRX	Jackson Immuno Research Laboratories
Goat IgG	Donkey	1:100	RRX	Jackson Immuno Research Laboratories

Up-take di bromodesossiuridina (BrDU)

La BrDU è un analogo nucleotidico della timina che si intercala nel DNA cellulare in fase di divisione. Veine iniettata intraperitoneo due volte al giorno (75 mg/kg, Sigma, St. Louis, MO) per 3 giorni , e l'animale viene perfuso 9 giorni dopo l'ultima iniezione di BrdU. La regione d'interesse viene macroscopicamente tagliata e immediatamente congelata con CO_2. Le sezioni, 14 m di spessore, sono allestite al criostato e vengono processate mediante la tecnica di immunofluorescenza indiretta (IF) secondo il seguente protocollo. Dapprima si esegue l'idratazione del tessuto con PBS 0,1M a temperatura ambiente per 30 min, e dopo l'incubazione a 37°C per 30 min con HCL 2N. Dopo lavaggio con PBS, le sezioni vengono incubate a 37°C per 4 min con pepsina 0,025% e quindi processate per la visualizzazione della BrdU usando l'anticorpo primario rat anti-

BrdU diluito in PBS/Triton 0,3% che viene lasciato agire a 4°C overnight. In seguito a due lavaggi con PBS, le sezioni vengono incubate, per un'ora a temperatura ambiente, con l'anticorpo secondario anti-Rat IgG (H+L) Donkey coniugato con il fluorocromo Rhodamine Red^{TM}–X (Jackson Immunoresearch West Grove PA) diluito con PBS/Triton 0,1%. Infine le sezioni vengono montate con coprioggetto in fenilendiammina (50mg fenilendiammina in 5ml PBS + 45ml glicerina + 10 gocce di tampone carbonato).

Intensificazione mediante TSA

Le sezioni allestite al criostato vengono reidratate in PBS per cinque minuti. Si bloccano le perossidasi endogene con acqua ossigenata 0.1% in PBS e si procede all'incubazione *overnight* con l'anticorpo primario diluito in PBS-Triton$_{x\text{-}100}$ 0.3% e BSA 0.1%. Per il protocollo di intensificazione si utilizza il kit TSA (Tyramide Signal Ampification: TSA –Plus Cyanine 3; Fluorescein Sistem Perkin Elmer; Boston, MA. USA).

Si lavano le sezioni in TNT (temperatura ambiente) e si blocca la reazione con TNB. Quindi si procede all'incubazione delle sezioni con l'anticorpo secondario coniugato con *horseradish peroxidase* (HRP) per 30 minuti a temperatura ambiente. Segue un lavaggio in TNT e l'incubazione della Tiramide fluorescinata diluita nella soluzione di amplificazione. Si immergono nuovamente in TNT e si montano i vetrini con fenilendiammina.

Metodo Avidina-Biotina (ABC)

Dopo la perfusione il cervello viene rimosso ed immerso nel fissativo freddo per 2 ore e quindi immerso per 48 ore in saccarosio 5% in tampone fosfato 0.1M, a 4°C. Sezioni coronali di 50 m di spessore contenenti le aree di interesse sono state allestite utilizzando un vibratomo (Vibratome Series 1000, Lancer Sectioning System, St Louis, MO. USA) ed immediatamente processate per la tecnica *avidin-biotin peroxidase complex*. Le sezioni, *free-floating*, vengono immerse in PBS 0.1M a temperatura ambiente per 10-30 minuti, pretrattate con H_2O_2 per bloccare l'attività delle perossidasi endogene, e quindi incubate con *normal serum* 1.5-2%. Segue l'incubazione a 4°C con gli anticorpi primari diluiti in PBS-Triton$_{x\text{-}100}$ 0.3%. La specificità della colorazione del

peptide è stata accertata dopo una preincubazione *overnight* dell'antisiero (2 mg/ml) diluito alla normale concetrazione di lavoro in una soluzione contenente *normal serum* 1% della stessa specie in cui è stato prodotto il secondario, albumina di siero bovino (BSA) e PBS-Triton$_{x\text{-}100}$ 0.3%. Le sezioni vengono lavate in PBS per 30 minuti e quindi incubate con l'immunoglobulina biotinilata (anti-topo o anti-pecora) (Dako, Denmark) diluita in PBS-*normal serum* 1% per 2 ore a temperatura ambiente. Le sezioni vengono quindi nuovamente lavate in PBS ed infine incubate utilizzando il complesso *horseradish peroxidase* (HRP; Amersham, UK) diluita in PBS per 30 minuti a temperatura ambiente. Per evidenziare l'immunocomplesso si è utilizzata la 3.3'-diaminobenzidina (Sigma St. Louis, MO, USA; 0.5mg/ml in Tris-HCl 0.1M, pH 7.5 + H_2O_2 0.03%). Dopo un lavaggio in PBS, le sezioni vengono montate su vetrino gelatinizzato, fatte asciugare e montate con Eukitt.

3.1.4 Western blot

Gli animali sono stati sacrificati per decapitazione previa anestesia con cloralio idrato. La cute è stata congelato immediatamente in azoto liquido e conservata a –80°C. Al momento dell'uso i campioni sono stati omogeneizzati meccanicamente mediante un *potter* con tampone di lisi (Hepes 10mM, pH 7.5, DTT 1mM e un mix di inibitori di proteasi (*Protease Inhibitor Coktail,* SIGMA, MO). La separazione delle proteine è stata effettuata mediante SDS-PAGE (SDS-*Poliacrilamide gel electroforesis*) l 15%, utilizzando 75 g di proteina, la cui concentrazione è stata determinata con il metodo di Lowry (1951). La elettroforeresi si è svolta sotto l'azione di una differenza di potenziale di 120V per tre ore. Al termine della separazione delle proteine queste sono state trasferite su una membrana di nitrocellulosa con l'applicazione di corrente di 180mA per 30 minuti. Il bloccaggio die siti aspecifici delle proteine trasferite sulla membrane è stato effettuato con la blocking solution (Pierce), per due ore a temperatura ambiente. Si procede poi all'incubazione con l'anticorpo primario anti-Ki67 (anticorpo policlonale prodotto nel coniglio, Novocastra, NE) diluito 1:2500, *overnight* a 4°C. Al termine dell'incubazione le membrane sono state lavate con TTBS 0,05% (TBS 0.05M-0.1%, Tween-20) per 60 minuti e incubate con l'anticorpo secondario, anticorp anti coniglio

(prodotti in capra Santa Cruz Biotechnology) coniugato con l'enzima *Horseradish peroxidase* (HRP) diluito 1:4000, per 30 minuti a temperatura ambiente. Al termine dell'incubazione le membrane sono state lavate con TTBS 0,05% (TBS 0.05M-0.1%, Tween-20) per 60 minuti a temperatura ambiente. Le proteine sono state evidenziate mediante chemioluminescenza (ECL, Pierce), impresse in lastre fotografiche e poi sviluppate. Le bande corrispondenti alla proteina Ki67 sono state densitometrate mediante il software AIS Imaging System (Ontario, Canada). I risultati sono presentati come il valore medio della densità ottica relativa ± SEM (Standard error median) di tre animali per gruppo. Gli esperimenti sono stati fatti in duplicato.

3.1.5 RT-PCR

Estrazione del RNA

L'estratto di RNA messaggero della cute è stato preparato secondo il protocollo indicato dal Kit "mRNA Isolation Kit" (Roche). Tale metodica si basa sull'appaiamento tra i residui di adenosina al terminale 3' dei mRNA e sonde oligo dT coniugate con biotina che a loro volta si legano a particelle magnetiche marcate con streptavidina. In questo modo il mRNA può essere separato dal tRNA e dal rRNA e quindi eluito dal supporto solido abbassando la concentrazione dei sali.

L'RNA totale della retina è stato estratto utilizzando il "High pure RNA tissue kit" (Roche). Questa metodica si basa sull'interazione specifica fra l'RNA totale in una soluzione molto concentrata in sali (guanidina HCl) e la lana di vetro della colonnina. L'RNA totale viene eluito con acqua grado biologia molecolare.

La concentrazione dell'RNA viene poi valutata con lo spettrofotometro (Eppendorf) ad una lunghezza d'onda λ= 260 nm e l'RNA retro-trascritto in un volume finale di 20 µl.

Trascrizione Inversa (RT)

In primo luogo, l'eventuale DNA genomico presente nel RNA estratto viene eliminato trattando il campione con l'enzima Deossiribonucleasi I libera da RNasi (Promega) 0,1 U/ µl in presenza di un inibitore delle ribonucleasi (Ribonuclease inhibitor, Fermentas) 4 U/ µl, a 37°C per 30 min, quindi l'enzima viene denaturato a 95 °C per 5 min. La

reazione di trascrizione inversa è stata condotta secondo le condizioni indicate per l'enzima trascrittasi inversa M-MLV (Moloney murine leukemia virus reverse transcriptase) (GIBCO BRL), in una mix di reazione formata da Oligo$(dT)_{23}$ 1 μM, $p(dN)_6$ 5 μM, $d(NTP)_s$ 1 mM, Buffer dell'enzima (1x), enzima retrotrascrittasi 10 U/μl, incubando a 37 °C per 50 minuti e successiva denaturazione a 70°C per 15 min. Il cDNA così ottenuto è stato utilizzato per l'amplificazione di diversi geni di ratto mediante reazioni di PCR semiquantitativa o PCR quantitativa relativa in tempo reale. In questa fase sono stati preparati campioni in cui non è stato aggiunto l'enzima retrotrascrittasi come controllo d'una eventuale contaminazione dei campioni di RNA con DNA genomico.

RT-PCR semiquantitativa

Per lo studio dell'espressione dei messaggeri, sono state usate le seguenti coppie di primers: per l'*NGF* (Nerve Growth Factor), senso: 5'-ccaaggacgcagctttctat-3', antisenso: 5'-ctccggtgagtcctgttgaa-3' (Scott et al., 1983), ottenendo un frammento di 402 paia di basi; per il *p75* (recettore ad alta affinità dell'NGF), senso: 5'-gtcgtgggccttgtggcc-3'e antisenso: 5'-ctgtgagttcacactgggg-3' (Troy et al., 2002), ottenendo un frammento di 497 paia di basi; per la GADPH (glyceraldehyde 3-phosphate deshydrogenase), senso: 5'-tccatgacaactttggcatcgtgg-5', antisenso: 5'-gttgctgttgaagtcacaggagac-3' (Lobsiger *et al*., 2000), ottenendo un frammento di 376 paia di basi. L'amplificazione del *house keeping gene* GAPDH è stata usata come controllo interno per correggere le quantità di mRNA trascritto a cDNA che abbiamo amplificato per ciascun campione.

Il volume finale della mix di reazione per la PCR è 25 μl e contiene: TRIS-HCl 670 mM pH 8.8, $(NH_4)SO_4$ 160 mM, Tween-20 0.1% , $MgCl_2$ 2 mM, dNTPs 0.2 mM, i corrispondenti primers senso e antisenso ad una concentrazione finale di 0.4 μM e 1.25 Unità dell'enzima Taq DNA polimerasi (EuroClone).

Per l'amplificazione dell'*NGF* è stata usata una quantità di cDNA equivalente a 23 ng di mRNA trascritto. Le condizioni d'amplificazione sono state: denaturazione iniziale a 95°C per 5 min, 40 cicli di 30 secondi a 95°C, 1 minuto e 30 secondi a 52°C e 1 minuto e 30 secondi a 72°C, infine allungamento della catena per 10 minuti a 72°C. Per

l'amplificazione del *p75* è stata usata una quantità di cDNA equivalente a 50 ng di mRNA trascritto. Le condizioni d'amplificazione sono state: denaturazione iniziale a 95°C per 5 min, 40 cicli di: 30 secondi a 95°C, 1 minuto a 54°C, 1 minuto e 30 secondi a 72°C, infine allungamento della catena per 10 minuti a 72°C. Per la GADPH, è stata usata una quantità di cDNA equivalente a 18,5 ng di mRNA trascritto. Le condizioni d'amplificazione sono state: denaturazione iniziale a 95°C per 5 min, 30 cicli di: 30 secondi a 95°C, 30 secondi a 60°C e 30 secondi a 72°C, infine allungamento della catena per 10 minuti a 72°C.
I prodotti di PCR sono stati analizzati mediante elettroforesi su gel di agarosio al 2%, fotografati, quindi le bande ottenute densitometrate mediante il *Software* AIS *Immaging Sistem* (St. Catharines, Ontario, Canada).

RT-PCR quantitativa

Mediante questa tecnica, utilizzando il SYBR-green I come colorante fluorescente, abbiamo studiato la possibile alterazione nei livelli di espressione dei geni BAX e Bcl-2, pro- e anti-apoptotico, rispettivamente; uno dei così chiamati *Inmediately Early Gene* (*IEG*), *c-jun*; NGF e i suoi recettori ad alta e bassa affinità, p75 e trk-A, rispettivamente; l'enzima gliceraldeide 3-fosfato desidrogenasi (GAPDH) è stata utilizzata come *housekeeping gene*. I *primers* per l'amplificazione d'un frammento dei sopraccitati geni sono stati disegnati mediante il software Beacon Designer 4.0 (Premier Biosoft International, Palo Alto, CA, USA), a partire della sequenza completa del loro cDNA, descritta nella banca di dati *Pub Med Nucleotide* nella specie animale *Rattus norvegicus*. L'amplificazione dei frammenti desiderati, così come la specificità delle reazioni d'amplificazione sono state controllati sia mediante la *curva di melting*, sia mediante elettroforesi in gel d'agarosio al 2.5%. La descrizione della sequenza dei *primers* senso e antisenso, il numero d'accessione alla banca di dati *Pub Med Nucleotide* e la dimensione in paia di basi (bp -*base pair*-) dei frammenti amplificati sono stati riportati nella tabella:

Primer	N° accessione	Sequenza (5'-3')	Prodottoamplificato (pb)
BAX	AF235993	5'-tgctacagggtttcatccag-3'	135
		5'-ccagttcatcgccaattcg-3'	

Bcl-2	NM_031535	5’-tggaaagcgtagacaaggagatgc-3’	88
		5’-caaggctctaggtggtcattcagg-3’	
c-jun	X17163	5’- aacgaccttctacgacgatg-3’	140
		5’-ggtgcggcttcagattgc-3’	
NGF	M36589	5’- acctcttcggacactctgg-3’	165
		5’- cgtggctgtggtcttatctc-3’	
P75	NM_012610	5’- agtggcatctctgtggac-3’	130
		5’- ctacctcctcacgcttgg-3’	
Trk-A	NM_021589	5’- aagccgtggaacagcatc-3’	91
		5’- agcacagagccgttgaag-3’	
GAPDH	M17701	5’-ggcaagttcaatggcacagtcaag-3’	125
		5’-acatactcagcaccagcatcacc-3’	

Nel caso dei *primers* BAX, Bcl-2, *c-jun*, NGF, P75, Trk-A e GAPDH le reazioni d’amplificazione in tempo reale sono state realizzate con lo strumento Mx3005*P*™ real-time PCR system (Stratagene, CA, USA), in un volume finale di 25 µl con una mix di reazione costituita da: master mix 1x, (Brilliant SYBR-green QPCR master mix, Stratagene), colorante di riferimento Rox 16 nM (Stratagene), *primers* senso e antisenso (0.4 µM). Le reazioni sono state realizzati in tre *step* o tappe. Nel : 1. denaturazione a 95°C per 10 minuti; 2. 40 cicli di 95°C per 15 secondi, 60°C per 30 secondi; 3. *melting*, in cui i campioni di DNA amplificati vengono scaldati progressivamente da 55°C a 95°C con un incremento della temperatura di 0.5°C per secondo. Nel caso dei *primers* VEGF-A, FLT-1 e FLK-1, le reazioni sono state realizzate con lo strumento real-time PCR della BioRad, in un volume finale di 25 µl con una mix di reazione contenente SYBR-gree, BioRad) e i *primers* senso e antisenso (0.5 µM). Il programma d’amplificazione per VEGF-A, FLT-1 e GAPDHè stato: 1. denaturazione a 95°C per 1 minuto e 50 secondi; 2. 40 cicli di 95°C per 15 secondi, 60°C per 1 minuto; 3. *curva di melting*, in cui i campioni di DNA amplificati vengono scaldati progressivamente da 55°C come sopra descritto. Nel caso del FKL-1, il programma eseguito è stato: 1.

denaturazione a 95°C per 1 minuto e 50 secondi; 2. 40 cicli di 95°C per 15 secondi, 58°C per 20 secondi, 72°C per 20 secondi; 3. *curva di melting* da 53°C.

La quantità relativa di mRNA viene determinata dal ciclo soglia Ct (threshold cycle) o ciclo d'amplificazione a partire del quale il sistema comincia a rivelare il segnale fluorescente emesso dal colorante SYBR-green che si lega al DNA amplificato. Il valore del Ct è in correlazione inversa con la quantità di mRNA del gene di studio nel campione. La GAPDH è stata utilizzata come *housekeeping gene* per la normalizzazione della quantità di RNA retrotrascritto di partenza dei campioni.

L'espressione relativa dei geni oggetto di studio è stata calcolata mediante la formula:

$$\Delta\Delta Ct = \Delta Ct \text{ (gene animale operato)} - \Delta Ct \text{ (gene animale controllo)}$$

ΔCt (gene animale operato)=Ct (gene animale operato)-Ct (GAPDH animale operato)

ΔCt (gene animale controllo) = Ct (gene animale controllo)- Ct (GAPDH animale controllo)

formula applicata ad ogni gruppo di trattamento che si vuole confrontare. I risultati vengono dati come il numero di volte che cambia il livello d'espressione dei geni oggetto di studio, calcolato mediante la formula: $X = 2^{-\Delta\Delta Ct}$, espressione matematica semplificata dalla formula:

$$X = (1+E \text{ gene})^{-\Delta Ct \text{ gene}} / (1+E \text{ normalizzatore})^{-\Delta Ct \text{ normalizzatore}}$$

La forma semplificata è possibile applicarla quando l'efficienza della reazione d'amplificazione del gene oggetto di studio e quella del *housekeeping gene* sono simili e uguale a 1. L'efficienza viene calcolata a partire della pendenza della curva standard data dallo strumento dopo che sono state amplificate quantità di cDNA corrispondenti a diluizioni seriali con ciascuno dei geni sopraccitati, nelle condizioni d'amplificazione (composizione della *mix* di reazione e profilo termico) precedentemente descritte, mediante la formula: Efficienza = [10(-1/pendenza)]-1. Per tutti i geni studiati abbiamo ottenuto un'efficienza di 1 quindi abbiamo applicato la formula

$X = 2^{-\Delta\Delta Ct}$ per calcolare l'espressione relativa dei sopraccitati geni.

I risultati dell'espressione del'RNA negli animali controlli e patologici è stata riportata nella tabella, dove si presenta la media dei valori ± l'errore standard della media (SEM) e nel caso dell'espressione relativa anche il *range* calcolato a partire dell'espressione: $2^{-(\Delta\Delta Ct-SEM)}$, $2^{-(\Delta\Delta Ct+SEM)}$

Analisi statistica

Per l'analisi dei risultati sono stati utilizzati lo Student's t test (confronto fra due gruppi), e l'analisi della varianza a una vi, ANOVA, seguita da un post hoc test per l'analisi fra gruppi multipli.

3.2 Esperimenti *in vitro*

3.2.1 Reperimento pazienti

La neurogenesi nel giro dentato è stata studiata in 4 pazienti la cui diagnosi clinica era di epilessia farmacoresistente del lobo temporale (ELT). La durata prechirurgica dell'epilessia era di 33, 30, 20 e 25 anni e l'età al momento dell'intervento era rispettivamente di 39, 41, 32, 27 anni. Due dei pazienti erano right sided e due left sided. Due erano maschi e due femmine. Tutti i pazienti reclutati nello studio presentavano sclerosi ippocampale (SI) e una rilevante storia di attacchi febbrili (FS) era presente nei casi 1, 3 e 4. I dati clinici dei pazienti inclusi nello studio sono riportati in tabella I. Il consenso informato era stato ottenuto da tutti i pazienti. Dopo l'intervento, il campione di tessuto incluso il giro dentato dell'ippocampo è stato suddiviso e destinato all'istopatologia e alla coltura cellulare per la generazione di neurosfere.

3.2.2 Allestimento di colture primarie di cellule staminali neurali da umano

I campioni di tessuto raccolti dal giro dentato dell'ippocampo sono stati trasferiti al laboratorio di colture cellulari in HBSS (Hanks Balanced Salt Solution -INVITROGEN) freddo, 100U-100 g/mL di soluzione a base di Penicillina-Streptomicina e processati entro un'ora dall'intervento. Il tessuto è stato, poi, incubato con una soluzione di Tripsina (1,3 mg/ml) e Ialuronidasi (0,7 mg/mL) in HBSS/5,4 mg/mL D-glucosio / 15 mM HEPES (Invitrogen), a 37°C per 45 min e successivamente trattati con DNasi (1000 U) per digerire l'eccesso di DNA. La sospensione così ottenuta è stata filtrata attraverso filtro in nylon (70 mm di diametro- Falcon-) e lavata con una soluzione composta da 40 mg/mL BSA (Sigma), 20mM HEPES, 1x EBSS (Earle's Balanced Salt Solution -Invitrogen-) e centrifugata a 1500 rpm per 5 min. Il pellet è stato, poi, lavato

con una soluzione di 0,5x HBSS/0,3mg/mL saccarosio (Merck) al fine di rimuovere i frammenti di mielina. Il pellet cellulare è stato risospeso in medium di coltura privo di siero, DMEM:F12 GlutaMAX I (Invitrogen) addizionato di 8mM HEPES, 2% B27 (Invitrogen), 0,5% N2 (Invitrogen) e 100U-100 g/mL di penicillina/streptomicina. Le cellule ottenute sono state contate e piastrate ad una densità di 2,4 x 10^4 cell/cm^2. I mitogeni, EGF (20ng/mL) e bFGF (10ng/mL) sono stati aggiunti ogni 48 ore e la metà del medium è stata cambiata una volta per settimana, osservando la formazione di neurosfere entro la prima settimana.

Le neurosfere sono state splittate dopo 22-28 DIVs e le cellule ottenute sono state seminate su coverslips trattati con poli-L-Lisina (50 g/mL -SIGMA-) ad una densità fra 6 e 10 X10^3 cellule/cm^2 Per i dettagli della procedura di splitting si veda Paragrafo precedente. Le cellule sono state poste in coltura nello stesso medium senza aggiungere i mitogeni e mantenute in queste condizioni per 12 giorni di differenziamento spontaneo.

3.2.3 Immunofluorescenza indiretta su colture cellulari

Le neurosfere e le cellule da esse derivate seguono la medesima procedura di immunofluorescenza indiretta. Esse vengono lavate con PBS freddo e fissate con paraformaldeide 4% in tampone Sørensen per 20 minuti a temperatura ambiente e poi lavate ancora con PBS per altri 15 minuti a RT (3 lavaggi da 3 minuti ciascuno). L'incubazione con anticorpi primari diluiti in PBS-Triton X-100 0.3%, è stata effettuata *overnight* a 4 °C.

Sono stati utilizzati gli anticorpi primari indicati nelle tabelle riportate per ciascun lavoro. Dopo aver lavato le cellule o le sfere con PBS per 15 minuti a RT (3 lavaggi da 3 minuti ciascuno), sono state incubate con anticorpi secondari diluiti in PBS-Triton X-100 0.3% per 30 minuti a 37 ° C. Sono stati utilizzati gli anticorpi primari indicati nelle tabelle riportate per ciascun lavoro. Sono state eseguite sia reazioni di immunofluorescenza singole che doppie. Dopo questa seconda incubazione, le cellule sono state incubate con Hoechst33258 per colorarne i nuclei (1mg/ml in PBS 0.2% TRITON X-100) per 20 minuti a Temperatura ambiente. A questo punto i *coverslips*

sono stati tolti dal fondo dei pozzetti e montati su vetrini con fenilendiammina e coprioggetto (**TAB II**).

TAB II

Anticorpi Primari

Anticorpo	**Specie**	**Diluizione**	**Ditta**	**Reattività crociata**
CNPasi 2',3'-ciclico nucleotide 3'-fosfodiesterasi umana, purificata	Topo	1:1000	CHEMICON, International, Inc. Temecula, CA	Uomo, bovino, ratto, can pecora, topo, coniglio
MAP2 Proteina associata ai microtubuli, bovino, cervello	Coniglio	1:350	CHEMICON, International, Inc. Temecula, CA	Uomo, bovino, ratto, topo, poll
Vimentina Vimentina umana	Topo	1:20	NEN Products, Boston	Uomo, ratto, capra, coniglio bovino
βIII-tubulin Derivata dai microtubuli, cervello di ratto	Topo	1:1000	R&D system Minneapolis, MN	Mammiferi, pollo
GFAP Frammento gliale purificato	Topo	1:200	CHEMICON, International, Inc. Temecula, CA	Uomo, maiale, pollo, ratto
MCM2 human mini-chromosome maintenance	Capra	1 : 150	Santa C Biotechnology, Santa Cruz, CA	Topo, Ratto, Uomo

protein type 2, amino terminal				
Doublecortina Umana, C-Terminal	Capra	1:100	Santa C Biotechnology, Santa Cruz, CA	Topo, Ratto, Uomo
NeuN Nuclei cellulari purificati da cervello di topo	Topo	1:250	CHEMICON, International, Inc. Temecula, CA	Uomo, ratto, topo, poll salamandra
Nestina Rat-401	Topo	1:500	BD Pharmingen San Diego, CA	Rat
Rip Bulbo Olfattorio di ratto	Topo	1:2500	CHEMICON, International, Inc. Temecula, CA	Ratto, criceto
NG2 Linea cellulare che esprime forma troncata di NG2	Topo	1:75	CHEMICON, International, Inc. Temecula, CA	Ratto, probabilmente uomo
Musashi Peptide sintetico di AA 5-21 of Musashi	Coniglio	1:100	CHEMICON, International, Inc. Temecula, CA	Uomo, roditore

Anticorpi Secondari

Affinipure Anti Rabbit IgG (H+L)	Donkey	1:75	Cy2	Jackson Immuno Research Laboratories West Grove PA
Affinipure Anti Mouse IgG (H+L)	Donkey	1:50	Cy2	Jackson Immuno Research Laboratories West Grove PA
Affinipure Anti Goat IgG (H+L)	Donkey	1:100	Cy2	Jackson Immuno Research Laboratories West Grove PA

3.2.4 Analisi delle neurosfere

Il numero e le dimensioni delle sfere sono stati valutati durante i giorni di coltura mediante conta e analisi morfometrica a 3, 6, 16 e 22 DIVs (days in vitro) tramite il software Image-Pro Plus. Entrambi i parametri, il numero e le dimensioni delle neurosfere formatesi, sono stati considerati per calcolare il rate di proliferazione tramite la formula:

diametro medio x n° neurosfere

4. RISULTATI e DISCUSSIONE

Come riportato nell'introduzione, NGF originariamente identificato come fattore di protezione delle cellule nervose, ha visto negli ultimi anni ampliare enormemente non solo le conoscenze sulla sua biologia, ma anche le implicazioni per la patologia e forse la farmacologia di molte malattie della specie umana (Aloe and Calzà, 2004). Interesse del nostro laboratorio è la comprensione del ruolo patogenetico di NGF in condizioni di malattia che prevedono il ruolo di una componente nervosa, confrontando condizioni anche fra loro molto diverse, quali infiammazione neurogenica, dolore neuropatico,

neuroinfiammazione, le degenerazioni età-dipendenti di popolazioni neuronali e regioni cerebrali specifiche.

I lavori presentati in questa tesi sono pertanto relativi a:

1. ruolo di NGF nell'infiammazione periferica (paper **I**, in press)
2. lesione vascolare cronica (di retina e ippocampo) e ruolo di NGF nella protezione retinica (paper **II**, manuscript draft; paper **V**, submitted paper)
3. modelli di epilessia in vivo e in vitro, per lo studio del ruolo di NGF nella protezione dei circuiti ippocampali (paper **III**, in press; paper **IV**, submitted)

4.1 Ruolo di NGF nell'infiammazione periferica

Paper I

Skin Homeostasis during inflammation: a role for Nerve Growth Factor. **Sivilia S.**, Paradisi M., D'Intino G., Fernandez M., Pirondi S., Lorenzini L., Calzà L., Histology and Histopathology, 2007, *in press*

La cute rappresenta un organo immunitario e neuroendocrino le cui differenti componenti cellulari contribuiscono a determinarne il comportamento in condizioni fisiologiche e patologiche come nell'infiammazione periferica e nell'insorgenza del dolore somatico. In questo contesto, le cellule del derma e dell'epidermide, le terminazioni nervose sensitive e simpatiche, i vasi e le cellule infiammatorie comunicano in maniera bidirezionale attraverso un ampio spettro di mediatori molecolari. L'attivazione delle terminazioni nervose induce vasodilatazione e richiama le cellule immunitarie generando infiammazione (Infiammazione Neurogenica) mentre, a loro volta, le terminazioni nervose risentono del rilascio di molecole infiammatorie modificando la propria eccitabilità. In questo contesto fisiopatologico, lo studio dei mediatori chimici che intervengono, può portare all'individuazione di *targets* molecolari che consentano interventi terapeutici efficaci. NGF è stato originariamente definito come fattore di sopravvivenza neuronale e successivamente gli è stato attribuito un ruolo nei tessuti maturi, nell'infiammazione e anche nella fisiologia della cute, candidandosi come possibile *target* per nuovi agenti terapeutici nel dolore acuto e

cronico. Scopo di questo lavoro è lo studio delle variazioni di espressione di NGF e dei suoi recettori nella cute, correlato a fenomeni proliferativi e a variazione della densità dell'innervazione terminale, in un modello di cui è ben caratterizzato il ramo centrale, ma non il periferico, del primo neurone sensitivo. Il modello scelto è l'infiammazione periferica indotta dall'iniezione di adiuvante completo di Freund (CFA) alla base della coda di ratto, che induce una severa poliartrite con interessamento anche della cuta relativa, che appare arrossata e assottigliata. In questo modello, era già stato descritta dal nostro laboratorio la transizione da una condizione di dolore acuto a una di dolre cronico (come definite dal profilo comportamentale e dalla neurochimica del primo neurone sensitivo), confermata in questo studio dalla sostanzaiale riduzione delle densità delle fibre sensitive nervose epidermiche (PGP 9.5 e CGRP-immunoreattive), che suggerisce lo sviluppo di una degenerazione delle piccole fibre terminali. In questo contesto, abbiamo descritto un aumento dell'espressione di NGF e di p75 (mRNA e proteina) nella cute durante la fase acuta e cronica avanzata dell'infiammazione da CFA. L'espressione di TrkA, invece, si correla inversamente all'espressione di NGF e p75. Questa condizione si associa ad un'aumentata attività proliferativa della cute come mostra l'espressione di Ki67, proteina correlata al ciclo cellulare. Nel complesso questi risultati suggeriscono un ruolo di NGF nell'infiammazione cronica da CFA, anche se sono necessari esperimenti farmacologici per confermare questa ipotesi ed identificare il o i processi fisiopatologici e il/i tipi cellulari che coinvolgono NGF.

4.2 Lesione vascolare cronica (di retina e ippocampo) e ruolo di NGF nella protezione retinica

La letteratura è molto ricca di risultati ottenuti su modelli di lesione vascolare cerebrale acuta, sia localizzata, quali la occlusione dell'arteria cerebrale media nel ratto o nel topo, sia globale, quali la legatura di arterie carotidi e vertebrali nel topo e nel ratto, che mimano condizioni di patologia umana molto diffuse e altamente invalidanti. Questi studi, molti dei quali mirano ad identificare i processi fisiopatologici e molecolari che portano alla morte neuronale nell'intento di sviluppare terapie neuroprotettive, hanno anche contribuito allo studio della neurogenesi ippocampale, sostanzialmente aumentata in queste condizioni sperimentali.

Molti meno sono invece studi che utilizzano modelli di deficit vascolare cronico, a mimare condizioni altrettanto diffuse nelle patologie umane, quali restrizioni carotidee a seguito di placche ateromasiche, o da minore gittata cardiaca, ecc. il nostro laboratorio, nell'intento generale di esplorare l'impatto della ipoperfusione cronica sulla qualità dell'invecchiamento cerebrale e sulla vulnerabilità di selettive popolazioni e regioni, prime fra tutti il sistema colinergico e la corteccia ippocampale, ha sviluppato il modello della legatura bilaterale e permanente della carotide comune nel ratto, caratterizzandone fino ad oggi alcuni aspetti. In questa tesi sono inclusi due lavori, l'uno mirato a studiare le variazioni età-dipendenti della neurogenesi ippocampale in ratti portatori di legatura bilaterale della carotide comune. Il secondo, che sfrutta lo sviluppo di una grave lesione della retina e del nervo ottico che si sviluppa rapidamente, volto a studiare la possibile azione di NGF nell'interferire con la morte per apoptosi di cellule retiniche.

paper V

caratterizzazione del modello:

Age-dependent impairment of hippocampal neurogenesis in chronic cerebral hypoperfusion. **Sivilia S**., Giuliani A., Del Vecchio G., Giardino L., Calzà L., *Manuscript submitted*, 2007

Nel cervello adulto dei roditori ma anche dei primati compreso l'uomo, permangono aree di attiva neurogenesi, in particolare nella zona subventricolare (SVZ) a livello telencefalico ed il giro dentato (DG) dell'ippocampo. Nell'ippocampo di ratto ogni giorno si formano circa 9000 cellule nuove nella zona subgranulare del giro dentato, da qui migrano per differenziarsi in cellule granulari che iniziano ad inviare le proiezioni assonali verso l'area CA3 integrandosi nei circuiti esistenti. La neurogenesi ippocampale è regolata da vari stimoli (età, ormoni, fattori di crescita e trattamenti farmacologici) che possono influenzarne le diverse tappe, alterando ad esempio la velocità di proliferazione, l'equilibrio *survival*-apoptosi, la differenziazione. Inoltre, molti lavori hanno riportato che danni cerebrali di natura ischemica, ma anche crisi convulsive, stimolano la nascita di nuove cellule che tendono a dirigersi verso l'area danneggiata per una eventuale riparazione.

In questo studio, si è voluto indagare la proliferazione e la differenziazione dei neuroblasti nel DG dell'ippocampo di ratto, una volta sottoposto ad ipoperfusione cerebrale cronica, ottenuta mediante la doppia legatura bilaterale delle carotidi comuni (2VO). Poiché la riduzione di apporto sanguigno cerebrale è una condizione osservata soprattutto nell'uomo a partire dalla mezza età, lo studio è stato rivolto sia sul ratto adulto (3 mesi) che anziano (12 mesi). Due sono stati i tempi di osservazione: uno a breve (8 giorni) ed uno a lunga termine (75 giorni) dall'intervento. Negli animali giovani, è stata osservata un'intensa attività proliferativa valutata sia con un marcatore di proliferazione (MCM2), sia con un marcatore di neuroblasti (doblecortina) nel giro dentato dell'ippocampo a 8 giorni dalla legatura, che si è nettamente ridotta nell'animale anziano. Inoltre usando la BrdU (intercalante del DNA nella fase S del ciclo cellulare) abbiamo potuto caratterizzare le cellule in proliferazione come neuroblasti (DCX + BrdU immunoreattivi) e neuroni maturi (NeuN + BrdU immunoreattivi), confermado che questo fenomeno proliferativo esitava in neurogenesi. In questo studio non è stata indagata la sopravvivenza dei neuroni neoformati.

paper II

Intravitreal NGF administration partially counteracts retina and optic nerve degeneration after 2VO ligation in rat, by regulating proapoptotic gene expression, Factor. **Sivilia S**., Giuliani A., Del Vecchio G., Fernandez M., Turba M., Forni M., Giardino L., Calzà L., *Manuscript draft*

L'ipoperfusione cerebrale cronica indotta nel ratto mediante legatura bilaterale delle arterie carotidi comuni (2VO), provoca una rapida degenerazione retinica. In questo lavoro abbiamo voluto caratterizzare la degenerazione retinica (misura dello spessore degli strati retinici e stima del numero di profili nucleari riferibili a cellule gangliari) e del nervo ottico (diametro, valutazione semiquantitativa della colorazione immunoistichimica di beta-tubulina, MBP, laminina), e testare se una singola somministrazione di NGF 24h ore dopo l'occlusione carotidea era in grado in indurre una protezione sia a livello di retina che di nervo ottico. Sono stati studiati tre tempi (8, 30 e 75 giorni) dall'intervento 2VO. La lesione retinica, evidenziata dalla perdita del

riflesso pupillare, si accompagna alla riduzione di spessore degli strati plessiforme interno ed esterno e dello strato delle cellule gangliari già a 8 giorni. La degenerazione del nervo ottico, che inizia con la disaggregazione della beta-tubulina a 8gg dalla legatura, accompagnata da un significativo aumento dell'immunoreattività per la laminina morfologicamente riferibile alla densità capillare, si manifesta con una sostanziale riduzione del diametro del nervo a 30gg. La somministrazione di NGF sembra parzialmente proteggere sia la retina che il nervo ottico, come osservato a 75 gg dopo la legatura studiando i parametri sopra indicati (spessore degli strati retinici, numero di cellule gangliari, diametro del nervo ottico), ed a questo effetto protettivo non è probabilmente estraneo l'aumentata produzione intraoculare di NGF, osservata in tutti i gruppi sperimentali (escluso controllo) e riferibile sia alla condizione di ipoperfusione sia alla lesione da sclerotomia prodotta dalla iniezione di NGF o di veicolo. Abbiamo quindi studiato il bilancio di geni pro- e anti-apoptotici nella retina a 8gg dalla legatura, osservando che la somministrazione di NGF negli animali con legatura provoca la sovraespressione dell'mRNA del gene antiapoptotico bcl-2 contro una ridotta espressione dell'mRNA di BAX, gene proapoptotico. Non è stato osservato invece nessun effetto di NGF sull'espressione di VEGF che sembra essere regolata soltanto dalla legatura delle arterie carotidi.

4.3 Modelli di epilessia in vivo e in vitro, per lo studio del ruolo di NGF nella protezione dei circuiti ippocampali

L'ippocampo è una regione cerebrale altamente sensibile a stimoli lesivi di varia natura, da quelli ormonali a quelli metabolici, rappresentando quindi un modello preferenziale per studi di neuroprotezione. E' in particolare una regione di elezione per lo studio della eccitotossicità, la lesione cioè prodotta da stimoli incontrollati dei sistemi glutamatergici, condizione riscontrabile in molte forme di epilessia spontanea e sperimentalmente indotta. E' inoltre la regione cerebrale dove la sintesi di neurotrofine, ed in particolare NGF, è più rapidamente e drasticamente regolata, con un aumento di sintesi di decine di volte rispetto al controllo entro pochi minuti dalla somministrazione

dello stimolo eccitotossico (Calzà *et al*., 1996). Il suo ruolo nei processi di apprendimento e memoria e più in generale nei fenomeni cognitivi, e la recnte scoperta di una intensa neurogenesi nella vita adulta, regolata sia da paradigmi sperimentali capaci di influenzare la performance cognitiva, sia da condizione di patologia, prima fra tutte l'epilessia, la rendono regione cerebrale di estremo interesse.

paper III

A molecular study of hippocampus in dogs with convulsion during canine distemper virus encephalitis. D'Intino G., Vaccari F., **Sivilia S**., Scagliarini A., Gandini G., Giardino L., Calzà L. Brain Res. 1098:186-195, 2006

Lo studio di patologie neurologiche nel cane è di grande interesse per le strette somiglianze fra quest'ultimo e la specie umana in alcune condizioni di neuropatologia, quali epilessia intrattabile e invecchiamento patologico. L'encefalite dovuta al virus del cimurro (CDV) rientra in queste condizioni sia perché è stata anche associata alla sclerosi multipla a causa della estensiva demielinizzazione, sia per il frequente sviluppo di epilessia intrattabile che comporta eutanasia dell'animale.

Abbiamo studiato i cambiamenti di espressione molecolari nell'ippocampo del cane in seguito ad crisi convulsiva intrattabile in corso di encefalite da cimurro mediante immunoistochimica e valutazione semiquantitativa, nell'intento di valutare se le alterazioni descritte nell'epilessia sperimentale dell'animale da laboratorio corrispondessero a quelle osservate in patologia spontanea. La sequenza di eventi molecolari descritti nel modello sperimentale indica un aumento nella trasmissione in sistemi eccitatori, in particolare nel sistema glutamatergico, producea over-eccitazione neuronale, sia il trigger per la scarica epilettica. L'eccesso di glutammato extracellulare causa una over-stimolazione dei recettori ionotropi e metabotropi del glutammato, con l'innesco di una catena di eventi molecolari e genici ben caratterizzati. La prima risposta genetica descritta nei roditori coinvolge una aumentata trascrizione e traduzione dei fattori di trascrizione della famiglia degli "*immediate-early genes*" (IEG) i cui membri Fos e Jun sono espressi nel nucleo dei neuroni. Una volta indotti, si pensa che questi IEGs vadano a regolare una ritardata ma più prolungata espressione di geni effettori interagendo con il sito AP-1 nella regione regolatoria di questi ultimi. L'espressione di

questi geni bersaglio potrebbe codificare per la sintesi di proteine strutturali, enzimi, canali ionici, neurotrasmettitori, neuropeptidi e fattori di crescita risultando in cambiamenti permanenti nella morfologia, struttura e funzione del tessuto nervoso.
In cani spontaneamente epilettici c'è una up-regolazione della proteina Fos nello strato piramidale, così come del fattore di trascizione NF-kB. Abbiamo inoltre osservato una forte sovra-espressione di neurotrofine. BDNF sembra accumularsi nei corpi cellulari ma principalmente nei dendriti apicali nei neuroni piramidali. La sua up-regolazione durante l'attacco epilettico potrebbe indicare un coinvolgimento sia nel promuovere l'eccitabilità nell'ippocampo, che nel mantenere l'integrità dendritica e favorire la crescita assonale.
Infine la immunoreattività alla galanina è regolata nei cani epilettici, dove aumenta rispetto a quelli di controllo. In questo studio abbiamo quindi tracciato la sequenza di cambiamenti neurochimici determinati nell'ippocampo in seguito agli attacchi determinati da epilessia mediata da CDV, descrivendo una up-regolazione dell' "*immediate-early genes*" (IEG) c-Fos, NfkB, NGF e BDNF. Inoltre abbiamo riscontrato una up-regolazione del trasportatore del glutammato e dell' encefalina, ed infine una down-regolazione della galanina.
Questi risultati forniscono una validazione dei dati ottenuti sull'animale da esperimento, in una specie animale di grande interesse per la neuropatologia umana.

Paper IV

<u>*sviluppo di modello:*</u>

In vitro assay for neurogenesis and gliogenesis in adult human dentate gyrus. Paradisi M., Fernandez M., **Sivilia S**., Marucci GL, Giulioni M, Pozzati E, Zucchelli M, Calbucci F, Antonelli T., Giardino L., Calzà L., *Manuscript submitted*, 2007

Esistono nella specie umana alcune forme di epilessia farmacoresistenti, per le quali esiste l'indicazione terapeutica di completa asportazione dell'ippocampo. Abbiamo sviluppato una collaborazione con la Divisione di neurochirurgia dell'Ospedale Bellaria di Bologna, al fine di studiare neurochimica e neurogenesi nell'ippocampo umano, in questi campioni confrontati, quando possibile, con ippocampi di controllo (derivati ad esempio da asportazione per tumori cerebrali). Viene qui presentato l'allestimento del

modello per lo studio in vitro di cellule staminali neurali umane derivate da questi campioni.

Alcuni dati della letteratura suggeriscono che una alterazione della neurogenesi ippocampale nell'adulto possa essere coinvolta nella fisiopatologia di alcune forme di epilessia farmacorestistenti. Diversi studi fatti su modelli animali indicano che le crisi epilettiche possono indurre neurogenesi e al contrario che uno stato epilettico di lunga durata può inibire la neurogenesi stessa. Comunque il ruolo della neurogenesi nel cervello affetto da epilessia è oscuro. In questo lavoro abbiamo ricercato la presenza di cellule staminali neurali nel giro dentato mettendo in coltura tessuto derivato dall'ippocampo di pazienti affetti da epilessia farmacoresistente sottoposti a resezione temporale antero-mesiale. I pazienti sono stati sottoposti a risonanza magnetica ed è stato evidenziato che tutti i casi mostravano sclerosi ippocampale che è caratterizzata da perdita neuronale nelle regioni CA1, CA2, CA3 dell'ippocampo e da gliosi fibrillare. Abbiamo dunque messo in coltura il tessuto in presenza di mitogeni per un tempo sufficiente ad osservare la presenza di cellule in proliferazione che hanno dato origine ad aggregati chiamati neurosfere. L'espansione nel tempo di questi aggregati, in assenza e in presenza di diversi mitogeni è stata quantificata mediante misure morfometriche. Abbiamo poi indotto il differenziamento di tali cellule togliendo i mitogeni dal mezzo di coltura, e dopo 12 giorni in coltura abbiamo osservato la formazione di cellule con fenotipo neurale e oligodendrogliale, come evidenziato da antigeni specifici. Questo lavoro dimostra che è possibile coltivare aggregati di cellule staminali umane a partire da giro dentato dell'ippocampo, quantificarne il potenziale proliferativo e la capacità di *lineage*, indicando il sistema delle neurosfere come buon candidato per lo studio di processi patologici anche della specie umana.

5. BIBLIOGRAFIA

1. Aloe L. *Nerve growth factor, human skin ulcers and vascularization. Our experience.* Progress in Brain Research 2004; 146:515-522
2. Aloe L, Calzà L. *NGF and related molecules in health and disease.* Progress in Brain Research 2004; 146
3. Barker PA, Hussain NK e McPherson PS. *Retrograde signaling by the neurotrophins follows a well-worn Trk.* TRENDS in Neurosciences 2002; 25:379-380
4. Barker PA. *p75NTR is positively promiscuous: novel partners and new insights*. Neuron 2004; 42:529-533
5. Barrett GL. *The p75 neurotrophin receptor and neuronal apoptosis.* Prog Neurobiol. 2000; 61:205-229
6. Bronfman F, Fainzilber M. *Multi-tasking by the p75 neurotrophin receptor: sortilin things out?* European Molecular Biology Organization 2004; 5:867-871
7. Bronfman FC, Tcherpakov M, Jovin TM, Fainzilber M. *Ligand-induced internalization of the p75 neurotrophin receptor: a slow route to the signaling endosome*. The Journal of Neuroscience 2003; 23:3209-3220
8. Calzà L, Giardino L, Ceccatelli S, Hokfelt T. *Neurotrophins and their receptors in the adult hypo- and hyperthyroid rat after kainic acid injection: an in situ hybridization study*. Eur J Neurosci 1996; 8:1873-1881
9. Calzà L, Pozza M, Zanni M, Manzini CU, Manzini E, Hokfelt T. Peptide plasticity in primary sensory neurons and spinal cord during adjuvant-induced arthritis in the rat: an immunocytochemical and in situ hybridization study. Neuroscience 1998; 82:575-589
10. Calzà L, Pozza M, Arletti R, Manzini E, Hokfelt T. *Long-lasting regulation of galanin, opioid, and other peptides in dorsal root ganglia and spinal cord during experimental polyarthritis.* Exp Neurol 2000; 164:333-343
11. Calzà L, Giardino L, Giuliani A, Aloe L, Levi-Montalcini R. Nerve growth factor control of neuronal expression of angiogenetic and vasoactive factors. Proc Natl Acad Sci USA 2001; 98:4160-4165
12. Cantarella G, Lempereur L, Presta M, Ribatti D, Lombardo G, Lazarovici P,

Zappalà G, Pafumi C, Bernardini R. *Nerve growth factor-endothelial cell interaction leads to angiogenesis in vitro and in vivo. Faseb J 2002; 16:1307-1309*

12 Cellerino A, Bähr M, Isenmann S. *Apoptosis in the developing visual system.* Cell Tissue Res 2000; 301:53-69

13. Coulson EJ, Reid K, Shipham KM, Morley S, Kilpatrick TJ, Bartlett PF. *The role of neurotransmission and the Chopper domain in p75 neurotrophin receptor death signaling*. Prog Brain Res. 2004; 146:41-62

14. Davidson CM, Pappas BA, Stevens WD, Fortin T, Bennet SAL. *Chronic cerebral hypoperfusion: loss of pupillary reflex, visual impairment and retinal neurodegeneration.* Brain Res 2000; 859:96-103

15. Delcroix JD, Valletta JS, Wu C, Hunt S, Kowal AS, Mobley WC. *NGF signaling in sensory neurons: evidence that early endosomes carry NGF retrograde signals.* Neuron. 2003; 39:69-84

16. Freund V, Frossard N. *Expression of nerve growth factor in the airways and its possible role in asthma.* Progress in Brain Research 2004; 146:335-346

17. Graiani G, Emanueli C, Desortes E, Van Linthout S, Pinna A, Figueroa CD, Manni L, Madeddu P. *Nerve growth factor promotes reparative angiogenesis and inhibits endothelial apoptosis in cutaneous wounds of Type 1 diabetic mice.* Diabetologia 2004; 47:1047-1054

18. Hansen-Algenstaedt N, Algenstaedt P, Schaefer C, Hamann A, Wolfram L, Cingöz G, Kilic N, Schwarzloh B, Schroeder M, Joscheck C, Wiesner L, Rüther W, Ergün S. *Neural driven angiogenesis by overexpression of nerve growth factor.* Histochem Cell Biol 2006; 125:637-649

19. Harada C, Harada T, Nakamura K, Sakai Y, Tanaka K, Parada LF. *Effect of $p75^{NTR}$ on the regulation of naturally occurring cell death and retinal ganglion cell number in the mouse eye.* Developmental Biology 2006; 290:57-65

20. Hefti FF, Rosenthal A, Walicke PA, Wyatt S, Vergara G, Shelton DL, Davies AM. *Novel class of pain drugs based on antagonism of NGF.* TRENDS in Pharmacological Sciences 2006; 27:86-91

21. Huang EJ, Reichardt LF. *TrK receptors: roles in neuronal signal transduction*. Annu Rev Biochem 2003; 72:609-642

22. Kawamoto K e Matsuda H. *Nerve growth factor and wound healing.* Progress in Brain Research 2004; 146:369-384

23. Lipnik-Stangelj M. *Multiple role of histamine H_1-receptor-PKC_MAPK signalling pathway in histamine-stimulated nerve growth factor synthesis and secretion.* Biochemical Pharmacology 2006; 72:1375-1381

24. Lobsiger CS, Schweitzer B, Taylor V, Suter U. *platelet-derived growth factor-BB supports the surviaval of cultured rat Schwann cell precursors in synergy with neurotrophin-3*. Glia 2000; 30:290-300

25. Lowry O.H., Rosebrough N.J., Farr A.L. and Randall R.J. (1951). *Protein Cyclic AMP decreases the expression of a neuronal marker measurement with the Folin phenol reagent.* J. Biol. Chem. 193 265–275.

26. MacInnis BL e Campenot RB. *Retrograde support of neuronal survival without retrograde transport of nerve growth factor.* Science 2002*;* 295:1536-1539

27. McDonald N.Q., Lapatto R., Murray-Rust J., Gunning J., Wlodawer A. and Blundell T.L. *New protein fold revealed by a 2.3-A resolution crystal structure of nerve growth factor.* Nature 1991; 354:411-414

28. McMahon SB. *NGF as a mediator of inflammatory pain*. Philos Trans R Soc Lond B Biol Sci. 1996*;* 351:431-40

29. McPherson PS, Kay BK, Hussain NK. *Signaling on the endocytic pathway.* Traffic 2001; 2:375-384

30. Micera A, Puxeddu I, Aloe L, Levi-Schaffer F. *New insights on the involvement of Nerve Growth Factor in allergic inflammation and fibrosis*. Cytokine Growth Factor Rev 2003; 14:369-374

31. Miller FD e Kaplan DR. *On Trk for retrograde signaling.* Neuron. 2001; 32:767-770

32. Miller FD e Kaplan DR. *Trk makes the retrograde.* Science 2002; 295:1471-1473

33. Nockher WA, Renz H. *Neurotrophins in allergic diseases: From neuronal growth factors ti intracellular signaling molecules.* J Allergy Clin Immunol 2006; 117:583-589

34. Nykjaer A., Lee R., Teng K.K., Jansen P., Madsen P., Nielsen M.S., Jacobsen C., Kliemannel M., Schwarz E., Willnow T.E. et al. *Sortilin is essential for proNGF-induced neuronal cell death.* Nature 2004; 427:843-848
35. Nykjaer A., Willnow T.E. and Petersen C.M. *$p75^{NTR}$-live or let die.* Current Opinion in Neurobiology 2005; 15:49-57
36. Pattarawarapan M, Burgess K. Molecular basis of neurotrophin-receptor interactions. Journal of Medicinal Chemistry 2003; 46:5277-5291
37. Qin Q, Patil K, Sharma SC. The role of Bax-inhibiting peptide in retinal ganglion cell apoptosis after optic nerve transection. Neuroscience Letters 2004; 372:17-21
38. Renz H, Kerzel S, Nockher WA. *The role of neurotrophins in bronchial asthma: contribution of the pan-neurotrophin receptor p75.* Progress in Brain Res. 2004; 146:325-334
39. Saxena S, Howe CL, Cosgaya JM, Steiner P, Hirling H, Chan JR, Weis J, Krüttgen A. *Differential endocytic sorting of p75NTR and TrkA in response to NGF: a role for late endosomes in TrkA trafficking.* Mol.Cell. Neurosci. 2005; 28:571-587
40. Schor NF. *The p75 neurotrophin receptor in human development and disease.* Progress in Neurobiology 2005; 201-214
41. Segal RA. *Selectivity in neurotrophin signaling: theme and variations.* Annu Rev Neurosci 2003; 26:299-330
42. Shu XQ, Mendell LM. *Neurotrophins and hyperalgesia.* Proc Natl Acad Sci U S A. 1999; 96:7693-7696
43. Sofroniew MV, Howe WC, Mobley WC. *Nerve growth factor signaling, neuroprotection and neural repair.* Annu Rev Neurosci 2001; 24:1217-1281
44. Tabakman R, Lecht S, Sephanova S, Arien-Zakay H, Lazarovici P. *Interactions between the cells of the immune and nervous system: neurotrophins as neuroprotection mediators in CNS injury*. Prog Brain Res. 2004; 146:387-401
45. Troy CM, Friedman JE, Friedman WJ. *Mechanisms of p75-mediated death of hippocampual neurons*. *Role of caspases*. J Biol Chem 2002; 277:34295-34302
46. Tuszynski MH, Blesch A. *Nerve growth factor: from animal models of*

cholinergic neuronal degeneration to gene therapy in Alzheimer's disease. Prog Brain Res. 2004; 146:441-449

47. Vilar M, Murillo-Carretero M, Mira H, Magnusson K, Besset V and Ibanez CF. (2006) *Bex1, a novel interactor of the p75 neurotrophin receptor, links neurotrophin signaling to the cell cycle*. The EMBO Journal 25:1219-1230
48. Villoslada P, Genain CP. *Role of nerve growth factor and other trophic factors in brain iflammation.* Prog Brain Res. 2004; 146:403-414
49. Ye H, Kuruvilla R, Zweifel LS e Ginty DD. *Evidence in support of signaling endosome-based retrograde survival of sympathetic neurons.* Neuron. 2003; 39:57-68

6. Ringraziamenti

Ringrazio le mie *prof* Luciana e Laura per avermi dato la possibilità di conoscere il nuovo mondo della RICERCA scientifica che avevo sempre sognato. Una realtà tanto dura quanto bella ed entusiasmante. Devo ammettere che non ho mai incontrato due persone appartenenti al mondo universitario dai grandi valori umani che sinceramente hanno contribuito a voler vivere questa realtà. Ho incontrato un caloroso ed attivo gruppo di lavoro che sicuramente rappresenta il pilastro dell'intero laboratorio. Ringrazio prima di tutti la mia *insegnante* Giulia che oltre ad avermi istruito su come muovermi in lab (dal momento che sono arrivata qui senza alcuna esperienza), mi ha trasmesso anche dei valori umani che hanno arricchito la mia personalità. La sua risata è una vera forza! Ma non sottovaluto l'ingenua follia di Michy che non fa altro che riempirmi di COMPLIMENTI! Anzi quando mi rivolge una parola carina devo stare attenta perché ci sarà qualcosa sotto! (…SCHERZO!). Ringrazio Stefy che vorrebbe essere tanto come… senza rendersi conto che già lo è…ed ecco che arriva con la sua calma e serenità il Badrone Ale (tornato dal periodo di studio in Stoccolma) che purtroppo si becca tutte le paranoie di noi ragazze ma che per fortuna sarà salvato dall'arrivo di altri tre ragazzi: Marco, Alex e Luca.

Ringrazio Mercy che con la sua precisione professionale è una vera macchina da guerra! Mi ha aiutato ad avvicinarmi al campo della biologia molecolare per me veramente difficile da capire. Ringrazio Giovanna che mi ha dato una grande mano nel fare con grande pazienza numerevoli analisi mentre io ero spaparanzata al sole lungo le coste della bella Creta. Non posso dimenticare Ale che mi ha sostenuto nei momenti di crisi che mi assalivano quando il povero rattino non si addormentava dopo l'anestesia facendomi ritardare l'intervento chirurgico! Ringrazio Marco che mi ha seguito nei successivi interventi sacrificando anche diversi sabati e domeniche.

E Nadia? Da non dimenticare i suoi consigli ed i suoi rimproveri sul disordine da noi creato e che …NON SI PUO' ANDARE AVANTI COSI'…!

E come posso non ringraziare il grande Libi che ogni giorno vuole farmi ricordare le mie origini della *Terronia* di cui vado fiera e Luca il *permaloso* (oh quanto mi diverto a prenderlo in giro!!) però tanto caro ed affettuoso anche se con me non prova

soddisfazione dato che quando mi abbraccia (come è solito fare con tutti al mattina al suo arrivo) resto impassibile… e che ci posso fare sono tutta strana!
Infine ringrazio Nicola che sopportando i miei sbalzi d'umore mi ha sempre sostenuto in questa avventura, credendoci come me e che nei momenti più difficili non ha fatto altro che incitarmi a non mollare *"perché chi si estranea dalla lotta è..."*

Skin homeostasis during inflammation: a role for Nerve Growth Factor

Sivilia S., Paradisi M., D'Intino G., Fernandez M., Pirondi S., Lorenzini L., Calzà L.
Department of Veterinary Morphophysiology and Animal Production (DIMORFIPA),
University of Bologna, 40064 Ozzano Emilia (Bologna), Italy

Short running title: NGF in the skin during CFA inflammation

correspondence:
Laura Calzà, MD
DIMORFIPA
University of Bologna
Via Tolara di Sopra 50
40064 Ozzano Emilia (Bologna), Italy
phone +39-051-792950
fax +39-051-792956
Email laura.calza@unibo.it

ABSTRACT

The skin is a neuroendocrine immune organ in which many different molecules operate in autocrine-paracrine manner to guarantee tissue homeostatsis in physiological and pathophysiological conditions. In this paper we examined NGF and p75 receptor expression in the skin, during CFA induced inflammation, in a time-course study. We also examined cutaneus innervation and proliferation, by means of immunohistochemistry and quantitative image analysis, RT-PCR and Western blot. Spontaneous and evoked pain-behavior was also measured in experimental rats. The main results can be summarized as follows: 1. a peripheral sensory neuropathy develops in this condition, as indicated by thermal hyperalgesia, thus leading to a sensory denervation of the hind-paw skin as indicated by disappearance of CGRP and PGP9.5-IR fibers; 2. NGF and p75 expression (mRNA and protein) increases in the skin (keratinocytes) in the acute phase of CFA inflammation; 3. at this stage, a higher proliferative activity is observed in the skin, as defined by the expression of cell cycle-associated protein Ki67; 4. in the long-lasting chronic phase there is a further up-regulation of NFG and p75 expression in the skin; 5. trkA mRNA expression inversely correlates with p75 and NGF mRNA expression. These results suggest that CFA chronic inflammation evolves from inflammation to a small fibers sensory neuropathy and NGF seems to play a role in both events.

KEY WORDS

Skin, NGF, CGRP, p75, CFA

INTRODUCTION

A growing body of evidence indicates that the bidirectional communication between the different histological components of the skin, e.g. epidermal and dermal cells, sensory and sympathetic nerve endings, vessels and inflammatory cells, plays a key role in the physiology of the skin, in the pathophysiology of peripheral inflammation and in somatic pain generation (Zimmerman, 2001; DeLeo and Yezierski, 2001; Smith and Liu, 2002; Marchand et al., 2005; McMahon et al., 2005). The activation of sensory nerve endings leads to vasodilation and inflammatory cells recruitment into peripheral tissues (neurogenic inflammation)(Schmelz and Petersen, 2001; Richardson and Vasko, 2002). Moreover, the cellular release of cytokines and neuroactive substances that modify excitability of peripheral nerve endings is involved in neuropathic pain generation and maintenance (Moalem and Tracey, 2005; Richardson and Vasko, 2002; Marchand et al., 2005). Thus, a number of chemical mediators present in the skin influence physiological (embryogenesis, vasoconstriction, vasodilatation, body temperature, barrier function, secretion, growth, differentiation, cell nutrition, nerve growth) and pathophysiological (inflammation, immune defense, apoptosis, proliferation, wound healing) functions within the skin, which acts as a true neuroimmune endocrine organ (Roosterman et al., 2006).

In this complex context, selected molecular players could interact with more than one type of cell, thus also becoming preferential targets for therapeutic intervention. Nerve growth factor (NGF) seems to be a good candidate for this possibility. NGF was first defined as an important survival factor in the development and proliferation of neurons of the nervous system, including sensory neurons of the dorsal root ganglia (DRG) (Levi-Montalcini and Angeletti, 1968). More recently, NGF has been identified as having a role in mature tissue and organs (Aloe and Calzà, 2004) as it is also a significant mediator in inflammation and skin physiology (McMahon, 1996; Roosterman et al., 2006), and the low- (p75) and high- (trkA) affinity NGF receptors have been postulated as also being involved in inflammation modulation (Allen and Dawbarn, 2006).

In order to highlight NGF's role in skin pathophysiology, we investigated NGF and p75 expression in the skin during different phases of paw inflammation induced by complete Freund's adjuvant (CFA) injection in the rat. CFA injection, which is a widely used model for peripheral inflammation, results in a severe cutaneous paw inflammation with skin thinning,

polyarthritis and the final alteration of joint structure (Calzà et al., 2000; Holmdahl et al., 2001).

MATERIALS AND METHODS

Animals

Male, pathogen free, 2 month-old, Sprague Dawley rats (Charles River, Varese, Italy) were used. The animals were housed under standard light/dark conditions (light on 7.00, off 19.00) in polypropylene cages. Paw inflammation was induced by a single intradermal injection (150µl) of heat-killed *Mycobacterium butyricum* (DIFCO) suspended in complete Freund's adjuvant on the upper side of the tail under brief fentanyl/midazolam anesthesia (performed at the breeding center, Charles River, Saint Aubin Les Elfreuf, France). Paw inflammation was evaluated by clinical examination of the animals by two investigators blind to the animals' condition and by paw oedema measurement. A numerical score was attributed to oedema and reddening observed in the anterior and posterior paws and scrotum (0=absence; 1=low; 2=moderate; 3=severe) (Calzà et al., 1998, 2000). Animal evaluation started 3 days after the adjuvant injection. A total score (sum of the score attributed to the different areas for the symptoms evaluated) was then assigned to the animals during each observation. Only animals with signs of inflammation (score $\geq$1 for at least two body segments) 5 days after CFA-injection were included in the study. Animals developing skin lesions were excluded from the study. The volume for both hind paws in CFA-injected animals, such as control animals, was measured in triplicate using a water displacement plethysmometer (UGO BASILE, Italy) on day 3, 12 and 17 after CFA-injection. No further measurements were possible due to severe pain and joint stiffness. Data were plotted as volume (ml) of each paw at each time point.

Immunohistochemical and molecular biology experiments were carried out in groups of animals sacrificed 21, 52 and 88 days after CFA injection (Calzà et al., 1998, 2000, Giuliani et al., 2004). Five (immunohistochemical) and 4 (molecular biology) animals were included in each time-point group.

Experiments were conducted in accordance with current European Union and Italian law, with Italian Ministry of Health authorization number 123/2004-B. All experiments were designed to minimize the number of animals used as well as their discomfort. All

algesiometric assays were conducted in accordance with the ethical guidelines set out by the International Association for the Study of Pain (IASP) (Zimmermann, 1983).

Immunocytochemical studies

Indirect immunofluorescence technique was performed on cryostat sections as previously described (Calzà et al., 2000). Briefly, after paraformaldehyde fixation, skin biopsy from the plantar surface of both hind-paws were removed, post-fixed, rinsed, quickly frozen and cryostat sections (14μm) immediately processed for the immunofluorescence procedure. Slides from all animals were run in the same assay. The following primary antisera have been used in the study: goat anti p75 (Santa Cruz C-20, Santa Cruz CA), rabbit anti NGF (Santa Cruz M-20), rabbit anti CGRP (Peninsula Lab, Bubendorf, Switzerland), rabbit anti PGP 9.5 (Biogensesis, Kingston, NH). Fluorescein isothiocyanate- (FITC), cyanine- (Cy2) and rodamine red-x succinimidyl- (RRX) conjugated secondary antisera were used, and slices were mounted in glycerol and PBS (3:1, v/v) containing 0.1% 1,4-phenylenediamine to minimize fluorescence decay.

Images were collected using a Nikon Eclipse fluorescence microscope equipped with a Nikon DXM1200F camera (x125 final magnification) and quantification of skin immunocytochemical staining was carried out using Image Pro Plus software (Media Cybernetics, Silver Spring, MD). Five animals/group/time were used in each analysis. All samples were collected using the same exposure time and analyzed at the same time by a blind observer. For skin analysis, 5 sections/animal were used. Once all images had been collected, they were subjected to a normalization procedure in order to equalise background levels across sections. The entire epidermis included in the field (area of 100000 square microns) was then evaluated by measuring the total length of immunoreactive fibres, the epidermis area and thickness. Due to variation in epidermis thickness in the different CFA phases, the innervation index was calculated as follows: fibre length/epidermis area x epidermis thickness.

RNA isolation and reverse transcription

Messenger RNAs (mRNA isolation kit, Roche Molecular Biochemicals) obtained from skin were subjected to DNase treatment (1U/μl, Roche Molecular Biochemicals), 10mM DTT (GIBCO BRL) and 4U/μl RNase inhibitor (PROMEGA), at 37°C for 30 min. First

strand cDNAs were obtained using 200U of the M-Moloney murine leukaemia virus (MuLV) reverse transcriptase enzyme (GIBCO/ BRL), 1x First Strand Buffer, 0.5mM of each d(NTP)s (Roche Molecular Biochemicals) and 50μM of the $p(dN)_6$ random primers (Roche Molecular Biochemicals), incubation at 37°C for 50 min and 70°C for 15 min.

Semiquantitative traditional PCR

Before setting the amplification conditions for each pair of primers used, linear regression curves assaying different amounts of retrotranscribed mRNA (cDNA) (Fig. 3) and different numbers of cycles of amplification (data not shown) were performed. Both of these parameters (cDNA amount and number of cycles of amplification) were chosen in the linear range. The oligonucleotides used as specific primers were: *NGF*, forward 5'-ccaaggacgcagctttctat-3', reverse 5'-ctccggtgagtcctgttgaa-3' (Scott et al., 1983) (402 bp); *p75*, forward 5'-gtcgtgggccttgtggcc-3', reverse 5'-ctgtgagttcacactgggg-3' (Troy et al., 2002) (497bp); *GADPH* (glyceraldehyde phosphate deshydrogenase), forward 5'-tccatgacaactttggcatcgtgg-5', reverse 5'-gttgctgttgaagtcacaggagac-3' (Tso J.Y. et al. 1985) (376bp). Amplifications were performed in a mixed reaction medium consisting of 670 mM Tris-HCl pH 8.8, 160 mM $(NH_4)_2SO_4$, 0.1% Tween-20, 2 mM $MgCl_2$, 0.2 mM dNTPs, 0.05U/μl of Taq DNA polymerase (EuroClone) and the corresponding oligonucleotides (forward and reverse) at a final concentration of 0.4μM. Amplification parameters were: for NGF, 95°C 30 sec, 60°C 1 min 30 sec, 72°C 1 min 30 sec, 40 cycles; for p75, 95°C 30 sec, 54°C 1 min, 72°C 1 min, 40 cycles; for GAPDH, 95°C 30 sec, 60°C 30 sec, 72°C 30 sec, 30 cycles. The analysis of GAPDH mRNA was used as a control for cDNA quantities used as templates for PCR assays. PCR products were electrophoresed on 2% agarose gels, stained with ethidium bromide (SIGMA) and visualized under UV light. Specificity of amplifications was confirmed by the appearance of a single band of the expected size. The bands obtained were analysed using the AIS Imaging System software (Ontario, Canada). Results are shown as mean ± SEM of two different experiments and at least three different animals per group.

Relative Quantitative real-time PCR reactions

Real time PCR reactions were performed in the Mx3005*P*™ real-time PCR system (Stratagene, CA, USA) using SYBR-green I dye. Rat primers for trk-A and GAPDH real-time PCR were designed for SYBR-green real-time reactions by using the software Beacon

Designer 4.0 (Premier Biosoft International, Palo Alto, CA, USA). The sequences of designed primers for trk-A amplification are: forward 5'-aagccgtggaacagcatc-3', reverse 5'-tgctacagggtttcatccag-3' (accession number MN_021589); the sequences of primers for GAPDH amplification are: forward 5'-ggcaagttcaatggcacagtcaag-3', reverse 5'-acatactcagcaccagcatcacc-3' (accession number M17701). The reactions were performed in a final volume of 25μl consisting of 1x master mix (Brilliant SYBR-green QPCR master mix, Stratagene), 1.6 nM reference dye Rox (Stratagene) and 0.4 μM forward and reverse primers. Two step PCR reactions have been performed: 1. denaturation (95°C, 10 min; 2. annealing/extension (40 cycles of: 95°C for 15 sec, 60°C for 30 sec); At the end of PCR reaction the melting curve of amplified products was performed following this temperature/time scheme: heating from 55°C to 95°C with a temperature increase of 0.5°C/sec. The relative mRNA level of trk-A gene was calculated in the base of the threshold cycles (C_T) values obtained for each sample. The housekeeping gene GAPDH was used to normalize the amount of retro-transcribed mRNA used for PCR reactions.

Before processing the samples corresponding to the different groups of animals, the efficiencies of trk-A and GAPDH real-time PCR reactions were calculated by amplifying cDNA dilution series in the presence of trk-A or GAPDH primers in the conditions above described. Threshold cycle (C_T) values for each pair of primers were used by MxPro QPCR software 3.0 (Stratagene, CA, USA) to calculate standard curves, slopes and efficiencies. As they were near 100% (99,1% for trk-A and 98% for GAPDH), in order to determine the relative amount of trk-A mRNA in each treated group of animals relative to the control group, we could apply the equation $2^{-\Delta\Delta C_T}$ where

$\Delta\Delta C_T = \Delta C_T$ mean value of treated animals - ΔC_T mean value of control animals

ΔC_T treated animals = C_T trk-A - C_T GAPDH

ΔC_T control animals = C_T trk-A - C_T GAPDH

The specificity of real-time PCR reactions was evidenced by the melting curve, obtaining a unique peak at the correspondent melting temperature (Tm). Moreover, we wanted to analyse PCR products by electrophoresis on 2.5% agarose gel stained with ethidium bromide and visualized under UV light. A single band of the expected size was obtained for each pair of primers used (Fig. 3C).

Ki67 Western blotting

Tissue homogenates from hind paws were prepared using a 10mM Hepes, 1mM DTT, pH 7.5 lysis buffer containing a protease inhibitor cocktail (Sigma, St. Louis, MO). Equal amounts of protein (5 μg) were separated in 15% SDS-polyacrylamide gels and electroblotted to nitrocellulose membranes. In order to block non specific protein binding sites, filters were incubated with blocking solution (Pierce) for 2 hours at room temperature and the primary antibody rabbit polyclonal anti-Ki67 1:2500 (Novo Castra) was then incubated overnight at 4°C. After washing for 1 hour with TTBS (TBS-0.05%Tween-20), filters were incubated with the secondary antibody anti-rabbit conjugated to horseradish peroxidase (Dako) 1:4000 for 30 min. at RT and washed again for another hour. The proteins were detected using an ECL chemioluminescent kit (Pierce). Densitometric analysis was performed using the AIS Imaging System.

Statistical Analysis

Descriptive statistics are reported as means±SEM. Data were analyzed with t-test and ANOVA followed by multiple comparison tests. Duncan's test was used to compare experimental (CFA-injected, 21 and 79 days after CFA) and control groups in the ICC and molecular biology experiments; the Tukey multiple comparison test was used for plantar test experiments. Results were considered significant when the probability of them occurring due to chance alone was less than 5%.

RESULTS

CFA injection at the base of the tail results in a severe cutaneous paw inflammation with skin thinning, polyarthritis and the final alteration of joint structure (Calzà et al., 2000). The course of the experimental pathology is illustrated in Fig. 1. The animals' distress was already evident from the body weight curve (A), which indicates a cessation of growth between 5 and 30 days, with corresponding increase in inflammation score (B), paw oedema (C) and thermal hyperalgesia (D). Paw oedema in one paw is evident already 5 days after injection, and at 17 days both hind paws in injected animals had a higher volume than control animals. There was a progressive increase in inflammation (Fig.1B), which peaked 14-16

days after CFA injection and then remained elevated until day 27, after which it slowly decreased.

Hind-paw skin taken from animals without ulcerations was used for both morphological and biomolecular studies. Cutaneous innervation was evaluated by means of immunostaining for the protein gene product 9.5 (PGP9.5), which has been indicated as a sensitive marker for nerve terminals (Johnson et al., 1994) and for calcitonin gene-related peptide (CGRP), which is a marker for sensory innervation (Oaklander and Siegel, 2005). Our observations of PGP9.5 and CGRP-IR fibers in the normal rat footpad skin are consistent with those of previous studies (Ma and Bisby, 2000). PGP9.5-IR fibres are observed in the epidermis and dermis, and thinner fibers extend from the dermoepidermidal junction into the epidermis (Fig. 2A). CGRP-IR fibers are also distributed in the superficial and deeper dermis, and some fibers penetrate into the epidermis, also reaching the superficial layers (Fig. 2D). No nerve fibers were recognized when the first antibody step was omitted. Quantitative analysis of skin innervation was performed in the epidermis in the acute phase (Fig. 2B and E) and at two different times: 55 and 88 days after CFA injection (Fig. 2C and F); results have been normalized according to the epidermis thickness and illustrated by the graphs in Fig. 2. In the epidermis, PGP9.5-IR innervation significantly increases in CFA animals at day 21, when irregular, thin fibres are observed in the most superficial layers, and nerve trunks are found at the dermoepidermal junction. Conversely, at 88 days there is a significant reduction of PGP9.5-IR fibres, and also of CGRP-IR somatosensory innervation compared to control animals.

We then analyzed NGF, p75 and TrkA mRNAs expression in the skin according to the same time-schedule (Fig. 3). In the first phase (21 days after CFA injection), there is an increase in NGF mRNA expression (Fig. 3B), which is followed by protein expression in cells in the dermis but also in the epidermis, where NGF is found in the cytoplasm of single cells or of small cell clusters. There is then a drop in NGF mRNA expression, which is strongly re-expressed in the last phase (88 days after CFA injection). A similar expression profile is shown by p75 mRNA (Fig. 3B), which is expressed by infiltrating cells in the dermis *(not shown)*. Conversely, we found trk-A mRNA expression to be significantly down-regulated 21 and 88 days after CFA injection (28% and 42%, respectively, Table I), being inversely regulated with respect to NGF and p75 mRNAs.

In view of the role of innervation in proliferative rate control of keratinocytes, in order to have an index of cellular activity in the skin during CFA chronic inflammation, we measured the expression of the nuclear proliferation-associated antigen Ki67 (Fig. 4). We found a three-fold increase in the protein expression during the acute phase, whereas it was reduced to a one-fold increase in the chronic phases.

DISCUSSION

The experimental model used in this study is characterized by a severe cutaneous and deep (joint) inflammation involving paw soft tissues and joint structures, which evolves over time. The first phase, corresponding to day 21 after CFA injection, is characterized by severe joint oedema, spontaneous pain and thermal hyperalgesia; the two last phases, corresponding to days 52 and 88 after CFA injection, are identified by decreased inflammation scores and resolution of acute inflammation (Calzà et al., 2000). Here we demonstrated a complex regulation of NFG and p75 receptor expression in the skin during CFA inflammation, characterized by a biphasic expression profile. NGF and p75 mRNAs levels increase in acute inflammation, when NGF-IR cells are observed in the basal and spinal layers of the epidermis and also in a large number of infiltrating cells in the dermis, and in chronic, long-lasting phase, when epidermis sensory innervation disappears. The first increase could be related to the NGF role in inflammation, whereas the increase observed in the long-lasting phase corresponding to sensory neuropathy, could reflect a neurotrophic attempt by NGF. In the acute phase, a higher proliferative activity, as defined by the expression of cell cycle-associated protein Ki67, is also observed in the skin. In the long-term, epidermis sensory innervation disappearance suggests that a small-fibre pathology is present in this chronic inflammatory model. Skin sensory denervation could cause neuropathic pain (Lauria, 2005), as described in postherpethic neuroalgia (Wasner et al., 2005), diabetic painful neuropathy (Shun et al., 2004), Sjogren syndrome (Chai et al., 2005) and also rheumatoid arthritis (Pozza et al., 2000).

NGF is synthesized by a variety of cell types, including cutaneous epithelium (Davies et al., 1987) where proliferating keratinocytes are the main source (Yaar et al., 1991; Albers et al., 1994; Pincelli et al., 1994). However, inflammatory cells as well, such as mast cells,

lymphocytes and eosinophils can release NGF (Raychaudhuri and Raychaudhuri, 2004) and NGF itself stimulates chemotaxis *in vitro* (Gee et al., 1983). NGF tissue level increases in various diseases and inflammatory states of the skin, such as atopic dermatitis (Dou et al., 2006) and the administration of NGF in laboratory animals has been shown to cause neutrophil accumulation at the site of *in vivo* injection (Lewin et al., 1993; Boyle et al., 1985; Bennet et al., 1998). NGF synthesis also correlates with keratinocyte growth *in vitro* (Di Marco et al., 1991) and *in vivo* (Constantinou et al., 1994; Pincelli et al., 1994) and participates in hair growth control (Botchkarev et al., 2004). Here we report that this correlation exists also in this *in vivo* model, as indicated by the high expression of the Ki67 cell cycle-associated protein in acute CFA-induced inflammation. This could reflect skin tropism maintenance during severe inflammatory states that also produce ulcers. It has actually been shown that skin wounding in neonatal rats produces a marked increase in NGF levels (Constantinou et al., 1994), and application of NGF to wound sites can lead to accelerated tissue repair and an enhanced rate of wound healing (Lawman et al., 1985; Matsuda et al., 1998; Aloe, 2004; Kawamoto and Matsuda, 2004). Notably, in the CFA chronic phase, which is also characterized by increased NGF synthesis, the epidermis is thinner than in control animals *(data not shown)*. One possible explanation is that the NGF effect on skin cell proliferation is mediated through nerve endings, which are lacking at this stage, since the keratinocyte mitotic rate is neurally controlled (Hsieh and Lin, 1999).

A large body of evidence supports the role of NGF in inflammatory hyperalgesia (Lewin and Mendell, 1993; McMahon, 1996; Woolf, 1996; Anand, 2004). NGF levels are elevated in injury, inflammation and pain states, skin- (Foster et al., 2002) and endothelia- (Foster et al., 2003) being the main sources; administration of NGF provokes pain and hyperalgesia whereas inhibition of NGF function reduces pain and hyperalgesia in animal models. Genetic disorders, including mutations in the genes that encode trkA and NGF, modify pain perception, so that novel classes of pain drugs based on antagonism of NGF are under development (Hefty et al., 2006; Myers et al., 2006). Also, in this study we found high NGF tissue levels associated with hyperalgesia, as defined by a decreased latency in thermal threshold tests.

The NGF increase observed in the skin 88 days after immunization could be related to sensory neuropathy. In CFA arthritis, small fibers disappear from the synovium (Mapp et al., 1990) and other joint structures, and here we indicate that cutaneous innervation also

decreases. We used CGRP and PGP9.5 to study small fibres in the skin. Both markers recognized small unmyelinated (C) and thinly myelinated (Aδ) fibres, and topical capsaicin studies have indicated that more than 90% of epidermis neurites are C and Aδ fibres that transduce and transmit pain (Oaklander and Siegel, 2005). This indicates that a peripheral sensory neuropathy develops in CFA chronic arthritis. NGF plays a key role in the survival and properties of sympathetic and sensory neurons (Levi-Montalcini, 1987), 40% of which are sensitive to NGF during adulthood (Snider and McMahon, 1998), and peripheral denervation itself induces an increase in NGF expression by target tissues, including keratinocytes, and this sustains neuropathic pain (Li et al., 2003). Moreover, a restorative effect of NGF administration has been reported in diabetes-induced cutaneous axon loss in mice (Christianson et al., 2003), so that NGF present in the skin could prevent complete denervation. An increased expression of NGF is also found in atopic dermatitis lesions, which are characterized by an inflammatory cell infiltrate consisting of eosinophils, lymphocytes, macrophages and increased numbers of mast cell, indicating a pathophysiological participation of these cytokine and cells in this diseases (Gronenberg et al., 2005). In the animal model of the disease (NC/Nga mice) this correlates with increased epidermal nerve fibers density (Horiuchi et al., 2005) and administration of anti-NGF antibodies significantly inhibited development of epidermal hyper-innervation (Takano et al., 2005).

We also studied NGF low- and high- affinity receptor mRNAs expression in skin. p75 in the skin is synthetized by epidermal basal cells (Dou et al., 2006; Roosterman et al., 2006), fibroblasts, keratinocytes, keratinocytes of the hair follicle root (Peters et al., 2006a) where it probably participates in hair cycle progression as growth terminators (Peters et al., 2006b). Parallel regulation that we found in NGF and p75 mRNA expression during CFA supports an autocrine-paracrine role of neurotrophins in regulating skin physiology and pathophysiology. TrkA is also expressed by basal keratinocytes, melanocytes and sweat glands (Adly et al., 2006), and trkA immunostaining could be observed in the Meissner's and Pacinian corpuscles and around small arteries in glabrous digital skin (Vega et al., 1994). A reciprocal regulation between NGF and TrkA proteins leading to parallel variations has been reported in several experimental and spontaneous pathologies including atopic dermatisis (Dou et al., 2006). Here we observed that the TrkA mRNA expression is down-regulated when NGF mRNA is up-regulated. This occurs in tissue samples which pool different cell types. Thus, these changes could be not related. Moreover, differential gene expression pattern of NGF, TrkA

and p75 has been described during differentiation in rat bone marrow stromal cells (Yaghoobi and Mowla, 2006). Both high- (trkA) and low- (p75) affinity receptors seem to take part in mediating the listed NGF effects in the skin, but having different and still partially unknown roles (Hokfelt et al., 1994; Chen et al., 1999; Malik-Hall et al., 2005; Roosterman et al., 2006). Pharmacological experiments aimed to interfere with NGF and specific receptors are needed to clarify this complex scenario.

ACKNOWLEDGMENT

This study has been supported by MIUR (Italian Minister for Instruction, University and Research), FIRB and cofin projects (LC). Technical assistance of Alberto Albanese and Marco Quarta is acknowledged.

REFERENCES

1. Adly M.A., Assaf H.A., Hussein M.R. and Paus R. (2006). Analysis of the expression pattern of glial cell line-derived neurotrophic factor, neurturin, their cognate receptors GFRalpha-1 and GFRalpha-2, and a common signal transduction element c-Ret in the human scalp skin. J. Cutan. Pathol. 33, 799-808.
2. Albers K.M., Wright D.E. and Davis B.M. (1994). Overexpression of nerve growth factor in epidermis of transegenic mice causes hypertrophyof the peripheral nervous system. J. Neurosci. 14, 1422-1432.
3. Allen S.J. and Dawbarn D. (2006). Clinical relevance of the neurotrophins and their receptors. Clin. Sci. (Lond) 110, 175-191.
4. Aloe L. and Calzà L. (2004). NGF and Related Molecules in Health and Disease. Progress in Brain Research, vol. 146. Elsevier, Amsterdam.
5. Aloe L. (2004). Nerve growth factor, human skin ulcers and vascularization. Our experience. Prog. Brain Res. 146, 515-522.
6. Anand P. (2004). Neurotrophic factors and their receptors in human sensory neuropathies. Prog. Brain Res. 146, 477-492.
7. Attal N., Jazat F., Kayser V. and Guilbaud G. (1990). Further evidence for 'pain-related' behaviours in a model of unilateral peripheral mononeuropathy. Pain 41, 235-251.
8. Bennet G., Al-Rashed S., Hoult R.J. and Brain S.D. (1998). Nerve growth factor induced hyperalgesia in the rat hind paw is dependent on circulating neutrophils. Pain 77, 315-322.
9. Botchkarev V.A., Botchkareva N.V., Peters E.M. and Paus R. (2004). Epithelial growth control by neurotrophins: leads and lessons from the hair follicle. Prog. Brain Res. 146, 493-513.
10. Boyle M.D., Lawman M.J., Gee A.P. and Young M. (1985). Nerve growth factor: a chemotactic factor for polymorphonuclear leukocytes *in vivo*. J. Immunol. 134, 564-568.
11. Calzà L., Pozza M., Zanni M., Manzini C.U., Manzini E. and Hokfelt T. (1998). Peptide plasticity in primary sensory neurons and spinal cord during adjuvant-induced arthritis in the rat: an immunocytochemical and in situ hybridization study. Neurosci. 82, 575-589.
12. Calzà L., Pozza M., Arletti R., Manzini E. and Hökfelt T. (2000). Long-lasting regulation of opiate, galanin and other peptides in dorsal root ganglia and spinal cord during experimental polyarthritis**.** Exp. Neurol. 164, 333-343.

13. Chai J., Herrmann D.N., Stanton M., Barbano R.L. and Logigian E.L. (2005). Painful small-fiber neuropathy in Sjogren syndrome. Neurology 65, 925-927.
14. Chen J., Luo C., Li H. and Chen H. (1999). Primary hyperalgesia to mechanical and heat stimuli following subcutaneous bee venom injection into the plantar surface of hindpaw in the conscious rat: a comparative study with the formalin test. Pain 83, 67-76.
15. Christianson J.A., Riekhof J.T. and Wright D.E. (2003). Restorative effects of neurotrophin treatment on diabetes-induced cutaneous axon loss in mice. Exp. Neurol. 179, 188-199.
16. Constantinou J., Reynolds M.L., Woolf C.J., Safieh-Garabedian B. and Fitzgerald M. (1994). Nerve growth factor levels in developing rat skin: upregulation following skin wounding. Neuroreport 21, 2281-2284.
17. Davies A.M., Bandtlow C., Heumann R., Korsching S., Rohrer H. and Thoenen H. (1987). Timing and site of nerve growth factor synthesis in developing skin in relation to innervation and expression of the receptor. Nature 326, 353-358.
18. DeLeo J.A. and Yezierski R.P. (2001). The role of neuroinflammation and neuroimmune activation in persistent pain. Pain 90, 1-6.
19. Di Marco E., Marchisio P.C., Bondanza S., Franzi A.T., Cancedda R. and De Luca M. (1991). Growth-regulated synthesis and secretion of biologically active nerve growth factor by human keratinocytes. J. Biol. Chem. 266, 718-721.
20. Dou Y.-C., Hagstromer L., Emtestam and Johansson O. (2006). Increased nerve growth factor and its receptor in atopic dermatitis: an immunohistochemical study. Arch. Dermatol. Res. 298, 31-37.
21. Foster P.A., Wicks S., Foster M. and Brain S.D. (2002). Cellular pathology changes in rat skin following intradermal injection of nerve growth factor: neutrophil-dependent and –independent events. J. Pathol. 197, 245-255.
22. Foster P.A., Costa S.K.P., Poston R., Hoult J.R.S. and Brain S.D. (2003). Endothelial cells play an essential role in the thermal hyperalgesia induced by nerve growth factor. FASEB J. 17, 1703-1705.
23. Gee A.P., Boyle M.D., Munger K.L., Lawman M.J. and Young M. (1983). Nerve growth factor: stimulation of polymorphonuclear leukocyte chemotaxis *in vitro*. Proc. Natl. Acad Sci. USA 80, 7215-7218.

24. Giuliani A., Fernandez M., Farinelli M., Baratto L., Capra R., Rovetta G., Monteforte P., Giardino L. and Calzà L. (2004). Very low level laser therapy attenuates edema and pain in experimental models. Int. J. Tissue React. 26, 29-37.
25. Groneberg D.A., Serowka F., Peckenschneider N., Artuc M., Grutzkau A., Fischer A., Henz B.M. and Welker P. (2005). Gene expression and regulation of nerve growth factor in atopic dermatitis mast cells and the human mast cell line-1. J. Neuroimmunol. 161, 87-92.
26. Hefty F.F., Rosenthal A., Walicke P.A., Wyatt S., Vergara G., Shelton D.L. and Davies A.M. (2006). Novel class of pain drugs based on antagonism of NGF. Trends Pharmacol. Sci. 27, 85-91.
27. Hokfelt T., Zhang X. and Wiesenfeld-Hallin Z. (1994). Messenger plasticity in primary sensory neurons following axotomy and its functional implications. Trends Neurosci. 17, 22-30.
28. Holmdahl R., Lorentzen J.C., Lu S., Olofsson P., Wester L., Holmberg J. and Pettersson U. (2001). Arthritis induced in rats with nonimmunogenic adjuvants as models for rheumatoid arthritis. Immunol. Rev. 184, 184-202 .
29. Horiuchi Y., Bae S. and Katayama I. (2005). Nerve growth factor (NGF) and epidermal nerve fibers in atopic dermatitis model NC/Nga mice. J. Dermatol. Sci. 39, 56-58.
30. Hsieh S.T. and Lin W.M. (1999). Modulation of keratinocyte proliferation by skin innervation. J. Invest. Dermatol. 113, 579-586.
31. Johnson P.C., Beggs J.L., Olafsen A.G. and Watkins C.J. (1994). Unmyelinated nerve fiber estimation by immunocytochemistry. Correlation with electron microscopy. J. Neuropathol. Exp. Neurol. 53, 176-183.
32. Kawamoto K. and Matsuda H. (2004). Nerve growth factor and wound healing. Prog. Brain Res. 146, 369-384.
33. Lauria G. (2005) .Small fibre neuropathies. Curr. Opin. Neurol. 18, 591-597.
34. Lawman M.J., Boyle M.D., Gee A.P. and Young M. (1985). Nerve growth factor accelerates the early cellular events associated with wound healing. Exp. Mol. Pathol. 43, 274-281.
35. Levi-Montalcini R. (1987). The nerve growth factor 35 years later. Science 237, 1154-1164.
36. Levi-Montalcini R. and Angeletti P.U. (1968). Nerve growth factor. Physiol. Rev. 48, 534-569.

37. Lewin G.R. and Mendell L.M. (1993). Nerve growth factor in nociception. Trends Neurosci. 16, 353-359.
38. Lewin G.R., Ritter A.M. and Mendell L.M. (1993). Nerve growth factor-induced hyperalgesia in the neonatal and adult rat. J. Neurosci. 13, 2136-2148.
39. Li L., Xian C..J, Zhong J.H. and Zhou X.F. (2003). Lumbar 5 ventral root transection-induced upregulation of nerve growth factor in sensory neurons and their target tissues: a mechanism in neuropathic pain. Mol. Cell Neurosci. 23, 232-250.
40. Ma W. and Bisby M.A. (2000). Calcitonin gene-related peptide, substance P and protein gene product 9.5 immunoreactive axonal fibers in the rat footpad skin following partial sciatic nerve injuries. J. Neurocytol. 29, 249-262.
41. Malik-Hall M., Dina O.A. and Levine J.D. (2005). Primary afferent nociceptor mechanisms mediating NGF-induced mechanical hyperalgesia. Eur. J. Neurosci. 21, 3387-3394.
42. Mapp I., Kidd B.L., Gibson S.J., Terry J.M., Revell P.A., Ibrahim N.B., Blaje D.R. and Polak J.M. (1990). Substance P-, calcitonin gene-related peptide- and C-flanking peptide of neuropeptide Y-immunoreactive fibres are present in normal synovium but depleted in patients with rheumatoid arthritis. Neuroscience 37, 143-153.
43. Marchand F., Perretti M. and McMahon S.B. (2005). Role of the immune system in chronic pain. Nat. Rev. Neurosci. 6, 521-532.
44. Matsuda H., Koyama H., Sato H., Sawada J., Itakura A., Tanaka A., Matsumoto M., Konno K., Ushio H. and Matsuda K. (1998). Role of nerve growth factor in cutaneous wound healing: accelerating effects in normal and healing-impaired diabetic mice. J. Exp. Med. 187, 297-306.
45. McMahon S.B. (1996). NGF as a mediator of inflammatory pain. Philos Trans R. Soc. Lond. B Biol. Sci. 351, 431-440.
46. McMahon S.B., Cafferty W.B.J. and Marchand F. (2005). Immune and glial cell factors as pain mediators and modulators. Exp. Neurol. 192, 444-462.
47. Moalem G. and Tracey D.J. (2005). Immune and inflammatory mechanisms in neuropathic pain. Brain Res. Rev. 51, 240-264.
48. Myers R.R., Campana W.M. and Shubayev V.I. (2006). The role of neuroinflammation in neuropathic pain: mechanisms and therapeutic targets. Drug Discov. Tod. 11, 8-20.
49. Oaklander A.L., Siegel S.M. (2005). Cutaneous innervation: form and function. J. Am.

Acad. Dermatol. 53, 1027-1037.

50. Peters E.M., Stieglitz M.G., Liezman C., Overall R.W., Nakamura M., Hagen E., Klapp B.F., Arck P. and Paus R. (2006). p75 Neurotrophin Receptor-Mediated Signaling Promotes Human Hair Follicle Regression (Catagen). Am. J. Pathol. 168, 221-234.
51. Peters E.M., Hendrix S., Golz G., Klapp B.F., Arck P.C. and Paus R. (2006). Nerve growth factor and its precursor differentially regulate hair cycle progression in mice. J. Histochem. Cytochem. 54, 275-288.
52. Pincelli C., Sevignani C., Manfredini R., Grande A., Fantini F., Bracci-Laudiero L, Aloe L., Ferrari S., Cossarizza A. and Giannetti A. (1994). Expression and function of nerve growth factor and nerve growth factor receptor on cultured keratinocytes. J. Invest. Dermatol. 103, 13-18.
53. Pozza M., Guerra M., Manzini E. and Calza L. (2000). A histochemical study of the rheumatoid synovium: focus on nitric oxide, nerve growth factor high affinity receptor, and innervation. J. Rheumatol. 27, 1121-1127.
54. Raychaudhuri S.P. and Raychaudhuri S.K. (2004). Role of NGF and neurogenic inflammation in the pathogenesis of psoriasis. Prog. Brain Res. 146, 433-440.
55. Richardson J.D. and Vasko M.R. (2002). Cellular mechanisms of neurogenic inflammation. J. Pharmacol. Exp. Therapeutics 302, 839-845.
56. Roosterman D., Goerge T., Schneider S.W., Bunnett N.W. and Steinhoff M. (2006). Neuronal Control of Skin Function: The Skin as a Neuroimmunoendocrine Organ. Physiol. Rev. 86, 1309-1379.
57. Schmelz M. and Petersen L.J. (2001). Neurogenic inflammation in human and rodent skin. News Physiol. Sci. 16, 33-37.
58. Shun C.T., Chang Y.C., Wu H.P., Hsieh S.C., Lin W.M., Lin Y.H., Tai T.Y. and Hsieh S.T. (2004). Skin denervation in type 2 diabetes: correlations with diabetic duration and functional impairments. Brain 127, 1593-1605.
59. Smith P.G. and Liu M. (2002). Impaired cutaneous wound healing after sensory denervation in developing rats: effects on cell proliferation and apoptosis. Cell Tissue Res. 307, 281-291.
60. Snider W.D. and McMahon S.B. (1998). Tackling pain at the source: new ideas about nociceptors. Neuron 20, 629-632 .

61. Takano N., Sakurai T. and Kurachi M. (2005). Effects of anti-nerve growth factor antibody on symptoms in the NC/Nga mouse, an atopic dermatitis model. J. Pharmacol. Sci. 99, 277-286.
62. Vega J.A., Vazquez E., Naves F.J., Del Valle M.E., Calzada B. and Represa J.J. (1994). Immunohistochemical localization of the high-affinity NGF receptor (gp140-trkA) in the adult human dorsal root and sympathetic ganglia and in the nerves and sensory corpuscles supplying digital skin. Anat. Rec. 240, 579-588.
63. Wasner G., Kleinert A., Binder A., Schattschneider. and Baron R. (2005). Postherpetic neuralgia: topical lidocaine is effective in nociceptor-deprived skin. J. Neurol. 252, 677-686.
64. Woolf C.J. (1996). Phenotypic modification of primary sensory neurons: the role of nerve growth factor in the production of persistent pain. Philos Trans R. Soc. Lond. B Biol. Sci. 351, 441-448.
65. Yaar M., Grossman K., Eller M. and Gilchrest B.A. (1991). Evidence for nerve growth factor-mediated paracrine effects in human epidermis. J. Cell Biol. 115, 821-828.
66. Yaghoobi M.M. and Mowla S.J. (2006). Differential gene expression pattern of neurotrophins and their receptors during neuronal differentiation of rat bone marrow stromal cells. Neurosci. Lett. 397, 149-154.
67. Yiangou Y., Facer P., Sincropi D.V., Boucher T.J., Bennett D.L., McMahon S.B., Anand P. (2002). Molecular forms of NGF in human and rat neuropathic tissues: decreased NGF precursor-like immunoreactivity in human diabetic skin. J. Peripher. Nerv. Syst. 7, 190-197
68. Zimmermann M. (2001). Pathobiology of neuropathic pain. Eur. J. Pharmacol. 429, 23-37.
69. Zimmermann M. (1983). Ethical guidelines for investigations of experimental pain in conscious animals. Pain 16, 109-110.

Table I. Trk-A mRNA relative expression in treated groups of animals compared with control group.

GROUPS	ΔC_T	$\Delta\Delta C_T$	*Relative Expression to Control (range)*
Control	5.73 ± 0.11	0 ± 0.11	1 (0.93 - 1.08)
21 days	6.21 ± 0.16 *	0.72 ± 0.16	0,72 (0.64 - 0.8)
52 days	6.08 ± 0.17	0.78 ± 0.17	0,78 (0.69 - 0.88)
88 days	6.5 ± 0.15 **	0.58 ± 0.15	0.58 (0.53 - 0.58)

ΔC_T = C_T trk-A average - C_T GAPDH average

$\Delta\Delta C_T$ = ΔC_T mean value of treated animals - ΔC_T mean value of control animals

The S.E.M. (standard error mean) of the difference is calculated from the S.E.M. of the trk-A and GAPDH values. For the calculation of $\Delta\Delta C_T$ a reference group has to be selected in order to subtract this constant value from the rest of the groups. As an arbitrary constant value is subtracted, the S.E.M. of $\Delta\Delta C_T$ is the same as the S.E.M. of ΔC_T (User Bulletin #2, ABI PRISM 7700 Sequence Detection System, 11 December 1997, updated 10/2001). Relative expression is calculated by the equation $2^{-\Delta\Delta C_T}$ and the range for each group (numbers in parenthesis) has been calculated by $2^{\Delta\Delta C_T +SEM}$ and $2^{\Delta\Delta C_T -SEM}$. Student *t* test was used for statistical analysis, *p<0.05, **p<0.01.

FIGURES

Figure 1.

Behavioral characterization of animals used in this study. A. Body weight curve of animals included in the study illustrates distress of CFA animals; statistical analysis ANOVA and post-hoc, ***p<0.001; B. inflammation score, as evaluated throughout the experiment (see text for further explanation). Grey vertical lines indicate the day on which animals were sacrificed; C. paw-edema in CFA animals, as measured 4, 12 and 17 days after CFA injection vs control animals; statistical analysis ANOVA and post-hoc, ***p<0.001; D. latency at thermal stimuli, as measured in freely moving animals 17 days after CFA injection, indicates severe hyperalgesia in CFA animals; statistical analysis: Student's t test, p<0.001.

Figure 2.

Skin innervation in control and experimental animals. A-C: micrographs show PGP9.5-IR innervation of the plantar surface of hind-paw in control (A), CFA acute (B) and CFA chronic, 88 days (C); D-E micrographs show CGRP-IR innervation of the plantar surface of hind-paw in control (D), CFA acute (E) and CFA chronic, 88 days (F); the graph illustrates quantification epidermis sensory innervation, normalized according to epidermis thickness (see text for further details) and expressed as a percentage change compared to control animals (mean±SEM). Five animals were included in each group. Statistical analysis: one-way ANOVA and post-hoc test, *p<0.05, **p<0.01. Bar: 100μm

Figure 3.

p75 and NGF mRNA expression in the skin of all experimental groups. A: standard curves for the semiquantitative RT-PCR assay for NGF, p75 and the internal standard GAPDH; B: the graphs represent the expression of NGF and p75 mRNA levels in the skin of the different groups, as studied by semiquantitative traditional PCR. Agarose gels in the upper part of panel B illustrate one representative PCR experiment with PCR products. Statistical analysis: one-way ANOVA and Dunnet's post-hoc test, *p<0.05, **p<0.01, ***p<0.001. C: shows an agarose gel with the real-time PCR products of trk-A (line 1) and GAPDH (line 3) amplifications. A DNA marker of 100 bp ladder has been used to estimate the size of the obtained PCR products (line 2). In graph D the relative expression of trk-A mRNA in treated

groups of animals compared with control group has been represented. Four animals were included in each group. Student *t* test was used for statistical analysis, *p<0.05, **p<0.01.

Figure 4.

Ki67 protein expression in the skin of all experimental groups, illustrating increased expression in the experimental animals. The blot represents a typical experiment. Four animals were included in each group. Statistical analysis: one-way ANOVA and post-hoc test, *p<0.05

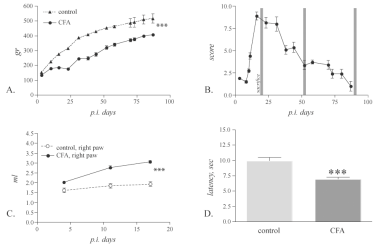
A.
control
CFA
gr
***
p.i. days
B.
score
p.i. days
C.
control, right paw
CFA, right paw
ml
***
p.i. days
D.
latency, sec
***
control
CFA

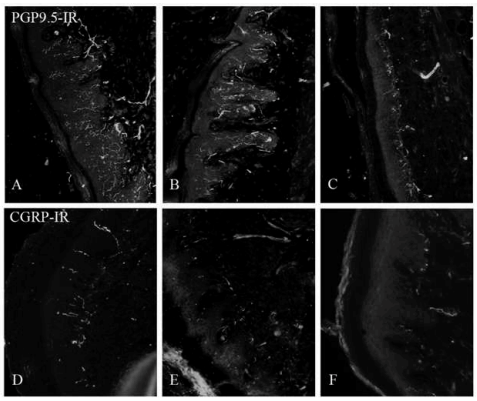
PGP9.5-IR
A
B
C
CGRP-IR
D
E
F

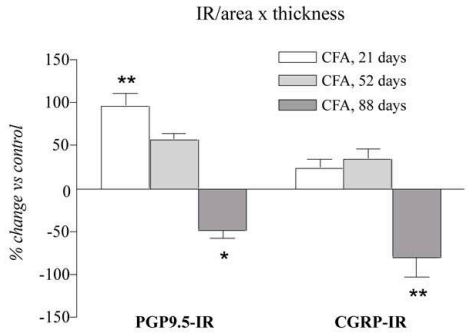
IR/area x thickness
CFA, 21 days
CFA, 52 days
CFA, 88 days
% change vs control
150
100
50
0
-50
-100
-150
**
*
**
PGP9.5-IR
CGRP-IR

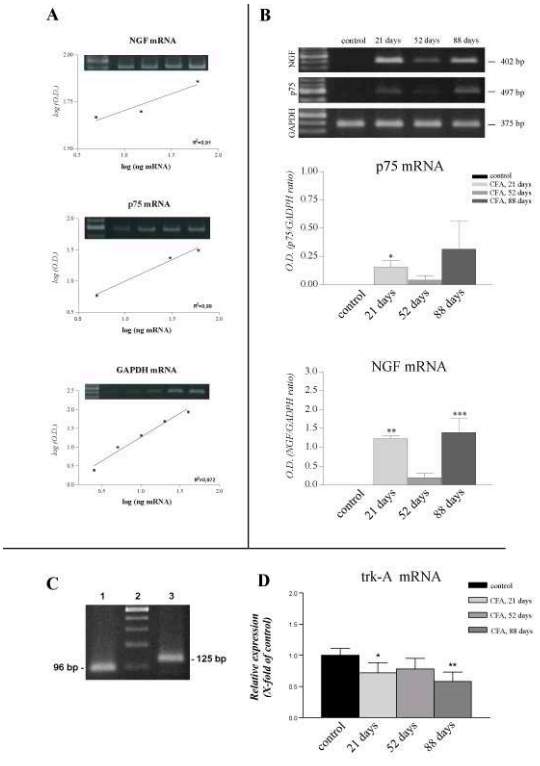
A
NGF mRNA
log (O.D.)
log (ng mRNA)
p75 mRNA
log (O.D.)
log (ng mRNA)
GAPDH mRNA
log (O.D.)
log (ng mRNA)
B
control
21 days
52 days
88 days
NGF
p75
GAPDH
402 bp
497 bp
375 bp
p75 mRNA
O.D. (p75/GADPH ratio)
control
CFA, 21 days
CFA, 52 days
CFA, 88 days
NGF mRNA
O.D. (NGF/GADPH ratio)
control
21 days
52 days
88 days
C
1
2
3
96 bp
125 bp
D
trk-A mRNA
Relative expression
(X-fold of control)
control
CFA, 21 days
CFA, 52 days
CFA, 88 days
control
21 days
52 days
88 days

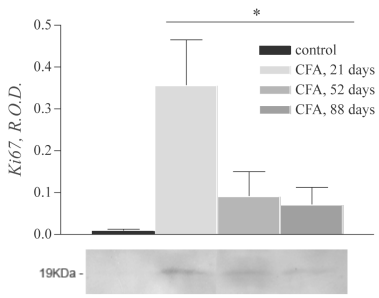
*
0.5
0.4
0.3
0.2
0.1
0.0
Ki67, R.O.D.
control
CFA, 21 days
CFA, 52 days
CFA, 88 days
19KDa -

Intravitreal NGF administration partially counteracts retina and optic nerve degeneration after 2VO ligation in rat, by regulating proapoptotic gene expression

Sivilia S., Fernández M., Giuliani A., Del Vecchio G., Turba M.E., Forni M., Giardino L., Calzà L.

DIMORFIPA, University of Bologna, Via Tolara di Sopra 50, 40064 Ozzano Emilia, Bologna, Italy

Running title:
NGF and retina protection in vascular diseases

Correspondence:
Laura Calzà, MD
DIMORFIPA – University of Bologna
Via Tolara di Sopra 50
40064 Ozzano Emilia (Bologna), Italy
Phone +39 051 2097947
Fax +39 051 2097953
Email laura.calza@unibo.it

ABSTRACT

INTRODUCTION

Nerve growth factor (NGF) is the most well known member of a family of neurotrophins (NT) that regulate neuronal survival also during adult life (Aloe and Calzà, 2004). Signals mediated by NGF are propagated by two distinct receptors: the high affinity receptor tyrosine kinase A (TrkA) and the low-affinity receptor p75, which is a member of the tumor necrosis factor receptor superfamily. TrkA stimulates cell-growth, differentiation and survival, while p75 plays a double role, depending on the cellular context: it can facilitate Trk-mediated cell survival or promote cell death (Nykjaer et al., 2005). The lack of NGF-mediated signalling, either because of the decrease of neurotrophin availability or because of a NGF receptor dysfunction may produce death of sensitive cell population ().

The eye and more generally the visual system are highly sensitive to NGF (Micera et al., 2004). Under normal conditions, NGF and trkA are expressed in the anterior segment of the eye (iris, ciliary body, lens, cornea and conjunctiva), and NGF is released in the aqueous humor. In the retina, NGF is produced and utilized by retinal ganglion cells (RGCs), bipolar neurons as well as glial cells, in a local paracrine/autocrine fashion. During visual system development, NGF, TrkA and p75, as well as other NTs and their related receptors, are localized in numerous visual centers, from the retina to the visual cortex, where NGF appears able to influence neuritis outgrowth, survival and selective apoptosis (Carmignoto et al., 1991; Maffei et al., 1992). A retrograde/anterograde transport along the axons of the RGCs and geniculate nucleus has been also reported (Micera et al., 2004). Finally, NGF seems to also exerts neutrophic effects in vascular and capillary pathologies of the eye, as suggested in experimental diabetes (Hammes et al., 1995) and after ischemia and reperfusion (Tomita et al., 1999).

In order to further explore the NGF role in eye protection during systemic circulatory diseases and in view of the fact that ocular symptoms are a common feature of carotid artery disease, in this study we investigated changes occurring in the retina and optic nerve after permanent bilateral occlusion of the common carotid arteries in rat (2VO) in order to evaluate if a single intravitreal injection of NGF protects the retina and optic nerve. 2VO provides an useful model to investigate mechanisms of therapy for the retinal degeneration associated with this disorder (Stevens et al., 2002).

MATERIALS AND METHODS

Animals and surgery

3-month old male Sprague-Dawley rats (Charles River laboratories Italia, Calco, Lecco) were used for this study. The animals were housed in polypropylene cages, 4 animals in each cage, under standard light/dark conditions (light on 7:00, off 19:00) with food pellets and water ad libitum. Chronic experimental cerebral hypoperfusion was induced by permanent bilateral occlusion of the common carotid arteries (2VO) (Ohta et al., 1997; Steven et al., 2002), with sham-operated animals serving as controls. Prior to surgery, the animals were anesthetized with ketamine hydrochloride (100 mg/kg IP). The common carotid arteries were exposed via a midline ventral cervical incision, carefully separated from their sheaths and vagal nerves, and permanently doubly ligated with 5/0 silk suture approximately 8 to 10 mm below the origin of the external carotid artery. The incision was then sutured. The same procedure was performed on the sham group. Twenty-four hours post surgery, intravitreal injection of saline (3µl) or Nerve Growth Factor (NGF) solution (5µg/3µl) was performed, using a 25µl Hamilton syringe with a 27-gauge needle through the pars plana at the temporal side of the eye (Yan et al., 1998). The classical transcleral approach with the tip of a microsyringe tangentially inserted through a local sclorotomy was used (Dureau et al., 2000). Three different survival times (8, 30 and 75 days) after surgery were investigated. In our laboratory we have a percentage of positive ligation effect (lost of pupillary reflex) of 62 %. The lost of pupillary reflex could be both bilateral and unilateral (Stevens et al.2002). For this reason it has been decided to include into the experiment procedures only the eye that have lost the pupillary reflex. Experimental groups were composed as show table 1.

All animal protocols described herein were carried out according to the European Community Council Directives of 24 November 1986 (86/609/EEC) and approved by our intramural committee and Italian Health Ministry (123/2004-B), in compliance with the guidelines published in the *National Institute of Health Guide for the Care and Use of Laboratory Animals*.

Pupillary reflex

Each animal was first adapted to darkness for at least 5 minutes. One eye was then exposed to a beam of light from an otoscope to assess the direct reflex response. The otoscope was then

immediately directed at the controlateral eye to assess the consensual response. Both eyes were then allowed to readapt to darkness for approximately 1 minute. This procedure was then repeated starting from the controlateral eye. Loss of pupillary reflex has been defined as failure of the pupil to constrict after a 10-second of light exposure. Pupillary reflex were examined each day for the first week after surgery, and at least once for week until animal sacrifice (Stevens et al., 2002).

Immunohistochemistry

All animals were deeply anesthetized with Ketamine (Ketalar, Parke Davis, Italy) 10 mg/kg body weight, i.p. (+ diazepam. 2 mg/kg i.m.) and perfused through the ascending aorta with Tyrode-Ca^{2+} free, pH 6.9 (100 ml; 50 ml at 37°C, 50 ml ice-cold, for adult male rat, 50ml; 25 ml at 37 °C 25 ml ice-cold, for young male rats), followed by 4% paraformaldehyde in Sorensen phosphate buffer 0.1 M pH 7.0. During perfusion, animals were bathed in ice-cold water. The brains were then removed and immersed for 90 min in the same ice-cold fixative, before being rinsed for at least 48 h in 5% sucrose in 0.1M phosphate buffer. Retinas were frozen in CO_2 and 14 μm thick coronal sections were then obtained 300 μm from the optic disk using a cryostat (Kriostat 1750, Leitz) and collected on gelatine coated slides. For immunofluorescence experiments, sections were first incubated in 0.1 M phosphate buffered saline (PBS) at room temperature for 10-30 min, followed by incubation at 4°C for 24h in a humid atmosphere with the primary antibodies diluted in 0.3% PBS-Triton X-100, v/v (see Table 2 for the list of antisera used in this study). After rinsing in PBS for 20 min (2 x10 min), the sections were incubated at 37°C for 30 min in a humid atmosphere with the secondary antisera conjugated with different fluorochromes: Cy™2- conjugated AffiniPure Donkey anti-Mouse IgG (H+L) Jackson Immunoresearch West Grove PA, Cy™2- conjugated AffiniPure Donkey anti-Goat IgG (H+L) Jackson Immunoresearch West Grove PA and Rhodamine Red™–X-conjugated AffiniPure Donkey anti-Rabbit IgG (H+L) Jackson Immunoresearch West Grove PA diluted in PBS triton 0.3%. Sections were then rinsed in PBS (as above) and mounted in glycerol containing 1,4-phenylendiamine 0.1 g/l.

RNA isolation and reverse transcription

Total RNA (total RNA isolation kit, Roche Molecular Biochemicals) was obtained from the retina and subjected to DNase treatment (1U/μl, Fermentas, Life Sciences, Italy) in the

presence of 4U/μl RNase inhibitor (4U/μl, Fermentas), incubating at 37°C for 30 min. First strand cDNAs were obtained after incubation with 200U of the M-Moloney murine leukaemia virus (MuLV) reverse transcriptase enzyme (Fermentas) in a mix reaction composed of 1x First Strand Buffer, 1mM of each d(NTP)s (Fermentas) and 50μM of the $p(dN)_6$ random primers (Roche Molecular Biochemicals), at 37°C for 50 min, followed by a denaturation step heating at 70°C for 15 min.

Relative Quantitative real-time PCR

Relative Quantitative real-time PCR reactions were performed in the Mx3005*P*™ real-time PCR system (Stratagene, CA, USA) using SYBR-green I dye. Rat primers for BAX and Bcl-2, pro- and anti-apoptotic genes, respectively, NGF and its high and low affinity affinità, trk-A and p75, respectively and GAPDH real-time PCR were designed for SYBR-green real-time reactions by using the software Beacon Designer 4.0 (Premier Biosoft International, Palo Alto, CA, USA). The sequences of the designed primers as well as the accession number in the gene bank data base are described in Table 3. For the amplification of NGF, trk-A, p75 and GAPDH, the reactions were performed in a final volume of 25μl consisting on 1x master mix (Brilliant SYBR-green QPCR master mix, Stratagene), 16 nM reference dye Rox (Stratagene) and 0.4μM forward and reverse primers. Two steps PCR reactions have been performed: 1. denaturation (95°C, 10 min; 2. annealing/extension (40 cycles of: 95°C for 15 sec, 60°C for 30 sec); at the end of PCR reaction the melting curve of amplified products was performed following this temperature/time scheme: heating from 55°C to 95°C with a temperature increase of 0.5°C/sec. For the amplification of VEGF-A, FLT-1, FLK-1 and GAPDH, reactions were performed in a final volume of 25μl consisting on 1x mix containing SYBR-green (BioRad) and 0.5μM of correspondent forward and reverse primers. In the case of VEGF-A, FLT-1 and GAPDH, PCR reactions have been performed as follow: 1. denaturation (95°C, 1 min 50 sec; 2. annealing/extension (40 cycles of: 95°C for 15 sec, 60°C for 1 min); at the end of PCR reaction the melting curve of amplified products was performed following the temperature/time scheme above described. In the case of FLK-1, the amplification program was: 1. denaturation (95°C, 1 min 50 sec; 2. annealing/extension (40 cycles of: 95°C for 15 sec, 58°C for 20 sec, 72°C for 20 sec); melting curve of amplified products was this time performed starting from 53°C and following the same temperature/time scheme.

The relative mRNA level of studied genes were calculated in the base of the threshold cycles (C_T) values obtained for each sample. The housekeeping gene GAPDH was used to normalize the amount of retro-transcribed mRNA used for PCR reactions.

Before processing the samples corresponding to the different groups of animals, the efficiencies of BAX, Bcl-2, NGF, p75, trk-A, VEGF-A, FLT-1, FLK-1 and GAPDH real-time PCR reactions were calculated by amplifying cDNA dilution series in the presence of correspondent primers in the conditions above described. Threshold cycle (C_T) values for each pair of primers were used by the correspondent real-time QPCR instruments's softwares (Stratagene, CA, USA or BioRad) to calculate standard curves slopes and efficiencies.

The specificity of real-time PCR reactions was evidenced by the melting curve, obtaining a unique peak at the correspondent melting temperature (Tm) and by agarose gel electrophoresis of PCR products, obtaining a single band of the expected size (results not shown).

Morphometric analysis

Histological and immunohistological images has been captured by Nikon Eclipse E600 microscope equipped with a Nikon color digital camera DXm 1200F. Confocal Laser scanning Microscopy (Olympus IX80 equipped with a FluoView 500 software and 3 laser beam Ar 488, G-HeNe 543, R-HeNe 633μm) has been also used. All misurements have been performed by using the Image Pro-Plus software (Media Cybernetics, MD, USA). For immunohistochemical data in the optic nerve the immunoreactive area has been calculated as percentage of immunoreactive area over the entire transversal section of the optic nerve. Thickness of retina layers has been calculated by dividing each retina, as sampled with coronal sections collected at 300 μm rostral to the optic disk into 4 quadrants. Values present are the mean ± SEM all quadrant. The number of ganglion cells has been estimated along the entire perimeter of the retina by counting nuclear profiles. The diameter of the optic nerve was measured in 5 sections every 150 μm in the stamp (1mm) proximal to the optic bulb.

Statistical analysis

Data are presented in figures as mean ± SEM. statistical analysis was performed by 1 way ANOVA and post-hoc test Tukey and Student's test (see legend to the figures for further details).

RESULTS

Animals.

Bilateral permanent occlusion of the carotid arteries induces a rapid pupillary reflex loss during the first 24 h after legation in a percentage of animals that correspond to 62% in our experiments, which is slightly superior to those reported in other studies (50-54%) (Davidson et al., 2000; Stevens et al., 2002). In order to make more homogeneous experimental groups, only animals with bilateral or unilateral pupillary reflex loss within this post surgical time were included in the study. In case of unilateral lesion, only the lesion eye was considered. Table 1 reports the number of eyes included in the study in the different experimental groups. NGF intravitreal administration 24 h after 2VO ligation failed to induce any functional recovery, as valuated by pupillary reflex.

Retinal and optic nerve degeneration in 2VO

Permanent bilateral occlusion of the common carotid arteries causes a degeneration of the retina and optic nerve, as shown by the histopathology of 2VO *versus* sham operated rat (control) (Fig. 1). In 2VO animals, the OPL of the retina almost completely disappears 8 days after legation, and a reduction of IPL and GCL is also observed (Fig.1B, C). The estimated number of ganglion cells in the whole perimeter of the retina decreases 75 days after 2VO legation. Atrophy of optic nerve, as evaluated by the nerve diameter, is observed 30 and 75 days after surgery (Fig.1F, G). In order to monitor molecular changes induced by the vascular defect in the optic nerve, we analysed beta-tubulin as marker for microtubules, MBP as marker for myelin, laminin as marker for vascular bed and scar formation, MCM2 as marker for proliferating cells, OX42 as marker for activated microglia, NG2 as marker for oligodendrcoyte precursors cells (OPCs). Sample images of the indicated immunohistochemical staining in control sham operated (A, C, E, G, I, M) and 2VO legated (B, D, F, H, L, N) animals at 8 days after surgery are showed in Fig 2. Graphs report the evaluation of immunoreactive areas for beta-tubulin and MBP-immunostaining, showing a rather rapid microtubules disaggregation, which starts from the central portion of the nerve (Fig. 2B) and leading to an almost complete depletion of beta-tubulin in the atrophic nerve

(75 days). Immunostaining for the myelin sheet associated protein MBP decreases more slowly, again starting from the core of the nerve.

NGF administration and retinal and optic nerve degeneration

After extensive characterization of the time-course evolution of the retinal and optic nerve pathology after 2VO legation, we than explored the possible protective effect of a single NGF intravitreal injection. We choose to inject NGF 24 hours after 2VO legation for two main reasons. The first, technical one, was aimed to utilize rather reproducible groups of animals, in view of the inclusion criteria of development of pupillary reflex defect established according to literature 24 hours after 2VO legation (Stevens et al., 2002) The second one, was the specific aim of this part of the study, e.g. to evaluate if NGF is able to interfere with a degenerative process already started.

In this part of the study, we compared 5 experimental groups: sham operated animals, which were intravitreally injected with saline or NGF; 2VO animals, and 2VO animals, which were intravitreally injected with saline or NGF. In order to allow NGF diffusion in the humor vitreo, we used an injection volume of 3 μl, which displays regular reproducibility with minimum loss of injected solution (Dureau et al., 2000) and induced an increase of vitreous humor of about 5% (Laabich and Cooper, 1999). We have evaluated NGF effect on optic nerve diameter, optic nerve beta-tubulin and MBP immunostaining and the extimated number of ganglionic cells 75 days after 2VO legation, and data are presented in Fig 3. While NGF administration had no effect on beta-tubulin immunostaining, a significant preservation of optic nerve fibres myelination and diameter is observed in 2VO-NGF-treated rats. Also the estimated number of ganglion cell profiles indicates a protective effect of NGF administration after 2VO-induced degeneration.

In order to explore the possible molecular mechanism of neuroprotective effect of NGF with respect to retina ganglionic cells degeneration induced by ischemic insult, we investigated expression profile of several genes regulating apoptosis by real-time PCR after 8 days (Fig. 4). In 2VO group, NGF induces a reduction of BAX mRNA expression (Fig. 4C) and a corresponding increase of Bcl-2 mRNA (Fig. 4A).

We also analyzed endogenous NGF synthesis and receptors expression. Intravitreal injection of NGF promotes expression of NGF mRNA (Fig. 5C,D), while no influences expression of NGF receptors mRNA. Expression of TrkA and p75 mRNA are regulated by injection by

itself in both control and 2VO group. TrkA mRNA decreases while p75 mRNA increases (Fig. 5A,B).

To study the possible angiogenic effect of NGF, we investigated expression of VEGF mRNA in retina after 8 days. We have found no effect of NGF, but expression of VEGF mRNA increases after 2VO legation. No significant changes were observed in Flt-1 and Flk-1 mRNA expression level (Fig. 6).

DISCUSSION

Permanent bilateral occlusion of the common carotid arteries is model of chronic cerebral hypoperfusion that affects also retina and optic nerve. It provides an useful model to investigate mechanisms and therapy for the retinal degeneration associated with several visual disorders. In this study we demonstrated a partial protective effect of a single intravitreal injection of NGF, which is able to regulated the expression balance between pre- and anti-apoptotic genes.

Animals and model characterization

Bilateral permanent legation of the carotid arteries causes rapid loss of the pupillary reflex, optic nerve lesion and retrograde degeneration that causes RGCs loss. Only a subset of 2VO rats loses the pupillary reflex and suffers visual system pathology. This is due to the fact that the structure of Willis circle varies considerably among rats. It is possible that in some rats, larger-diameter vessels within the circle of Willis or larger posterior arteries would allow for reverse perfusion of the internal carotid and pterygopalatine arteries and thence retinas. Other rats without this characteristic may suffer more severe ischemia and lose their pupillary reflex (Stevens et al., 2002). We have obtained a percentage of positive ligation effect (lost of pupillary reflex) of 62% vs a percentage of 50-54% reported in precedent studies (Davidson et al., 2000; Stevens et al., 2002).

Anterior ischemic optic neuropathy is an optic nerve stroke, it causes oligodendrocytes dysfunction of the anterior portion of the rodent optic nerve. Because one oligodendrocyte myelinates many axons, demyelination may lead to additional loss of axonal function and, ultimately, to additional RGC death in the ischemic surround. However, RGC loss can led to

axonal degeneration with associated oligodendrocyte dysfunction and demyelination (Goldenberg-Cohen et al., 2005).

Chronic hypoperfusion causes an injury of optic nerve fibers, which results in the progressive retrograde degeneration of axons and death of RGCs (Carmignoto et al., 1989; Goldenberg-Cohen et al., 2005). As already described, a severe reduction in retinal layers thickness, particularly affecting OPL, characterize retinal degeneration (Davidson et al., 2000; Stevens et al., 2002).

NGF and retinal ganglion cell survival

Injury of the optic nerve has served as an important model for the study of cell death and axon regeneration in the CNS. Exogenous application of neurotrophins and other growth factors, like BDNF and GDNF, could attenuate the degeneration of RGCs in adult rats in acute models, like optic nerve transection (Yan et al., 1999). Here we report a protective effect of a single intravitreal injection of NGF was made 24h after induction of a chronic hypoperfusion. NGF induces survival effects on retina and optic nerve only 75 days after carotid arteries occlusion, just when the retina and optic nerve degeneration is more evident. Relevantly, this effect is produced by regulating pro- and anti-apoptitic gene expression. For our knowledge, this is the first report indicating a positive effect of a single NGF injection. Prolonged repetitive intraocular injections of NGF promote the survival of a remarkable number of RGCs, at least for periods as long as 7 weeks from transection of the optic nerve (Carmignoto et al., 1989).

NGF has been implicated as a potent stimulant of the trophism and wound healing process in the eye. Indeed, intraocular injection of NGF promoted recovery of damaged RGCs after ischemic injury, optic nerve transection, and ocular hypertension. NGF expression was found decreased in the retina of mice affected by an inherited retinal degeneration that resembles retinitis pigmentosa (Micera et al., 2004). In diabetic rats, both RGCs and Muller cells underwent apoptosis by overexpression of p75, while exogenous NGF treatment appeared to prevent this RGC, Muller cell and vascular pericyte loss (Micera et al., 2004). NGF also affects retinal plasticity, with massive cell death observed during retinal development associated with a consistent p75 expression. Also in avian retina, which lacks trkA expression, NGF induces local cell death with a p75-mediated (Micera et al., 2004).

Royal College of Surgeons (RCS) rats affected by inherited retinal cell degeneration are characterized by a significant reduction of both NGF protein and mRNA, and injection of NGF enhances the expression of trkA and its mRNA in the retina (Lenzi et al., 2005). Moreover, exogenous NGF causes an increase of others growth factors (FGF-b, BDNF, VEGF) proteins but also an overexpression of their mRNAs (Yan et al., 1999; Lenzi et al., 2005).

Lack of trophic support by NTs has been suggested as a factor of RGC death in glaucoma (Rudzinski et al., 2003). NTs are retrogradely transported from superior colliculus (SC) in the CNS, or are synthetized locally in the retina by amacrine cells and other neighboring cells acting in a paracrine fashion and RGCs themselves acting in an autocrine fashion. Glaucoma could be considered a "physiologic axotomy" because the optic nerve fibers are compressed by high intraocular pressure, producing a disruption of retrograde transport of NTs from SC, along the optic nerve, to the RGC soma (Rudzinski et al., 2003; Micera et al., 2004; Osborne et al., 2005).

REFERENCES

-
- Aloe L, Calzà L. NGF and related molecules in health and disease. *Progress in Brain Research* 2004; 146
- Carmignoto G, Comelli MC, Candeo P, Cavicchioli L, Yan Q, Merighi A. Expression of NGF receptor mRNA in the developing and adult rat retina. *Exp Neurobiol* 1991; 111:302-311
- Carmignoto G, Maffei L, Candeo P, Canella R, Comelli C. Effect of NGF on the survival of rat retinal ganglion cells following optic nerve section. *The journal of Neuroscience* 1989; 9:1263-1272
- Davidson CM, Pappas Ba, Stevens WD, Fortin T, Bennett SAL. Chronic cerebral hypoperfusion: loss of pupillary reflex, visual impairment and retinal neurodegeneration. *Brain Research* 2000; 859:96-103
- Dureau P, Legat L, Neuner-Jehle M, Bonnel S, Pecqueur S, Abitbol M, Dufier JL. Quantitative analysis of subretinal injections in the rat. *Graefe's Arch Clin Exp Ophthalmol* 2000; 238:608-614
- Goldenberg-Cohen N, Guo Y, Morgolis F, Cohen Y, Miller NR, Bernstein SL. Oligodendrocyte dysfunction after induction of experimental anterior optic nerve ischemia. *Investigative Ophthalmology & Visual Science* 2005; 46:2716-2725
- Hammes HP, Federoff HJ, Brownlee M. Nerve growth factor prevents both neuroretinal programmed cell death and capillary pathology in the experimental diabetes. *Mol Med* 1995; 1:527-534 T
- Laabich A. and Cooper NGF. Regulation of Calcium/Calmodulin-Dependent Protein Kinase II in the Adult Rat Retina is Mediated by Ionotropic Glutamate Receptors. *Exp*. *Eye Res*. 1999**;** 68:703±713
- Lenzi L, Coassin M, Lambiase A, Bonini S, Amendola T, Aloe L. Effect of exogenous administration of nerve growth factor in the retina of rats with inherited retinitis pigmentosa. *Vision Research* 2005; 45:1491-1500

- Maffei L, BerardiN, Domenici L, Parisi V, Pizzorusso T. Nerve growth factor (NGF) prevents the shift in ocular dominance distribution of cortical neurons in monocularly deprived rats. *J Neurosci* 1992; 12:4651-4662
- Micera A, Lambiase A, Aloe L, Bonini S, Levi-Schaffer F, Bonini S. Nerve growth factor involvement in the visual system: implications in allergic and neurodegenerative diseases. *Cytokine & Growth Factor Reviews* 2004; 15:411-417
- Nykjaer A., Willnow T.E. and Petersen C.M. *$p75^{NTR}$-live or let die.* Current Opinion in Neurobiology 2005; 15:49-57
- Osborne NN, Chidlow G, Wood JPM. Neuroprotection of retinal ganglion cells: experimental data and significance to glaucoma. *IJNN* 2005; 1:142-151
- Rudzinski M, Wong TP, Saragovi HU. Changes in retinal expression of neurotrophins and neurotrophin receptors induced by ocular hypertension. *Inc J Neurobiol* 2003; 58:341-354
- Stevens WD, Fortin T, Pappas BA. Retinal and optic nerve degeneration after chronic carotid ligation. *Stroke* 2002; 33:1107-1112
- Tomita H, Ishiguro S, Abe T, Tamai M. Administration of nerve growth factor, brain-derived neurotrophic factor and insulin-like growth factor-II protects phosphate-activated glutaminase in the ischemic and reperfused rat retinas. Tohoku J Exp Med 1999; 187:227-236
- Yan Q, Wang J, Matheson CR, Urich JL. Glial cell line-derived neurotrophic factor (GDNF) promotes the survival of axotomized retinal ganglion cells in adult rats: comparison to and combination with brain-derived neurotrophic factor (BDNF). *Inc J Neurobiol* 1999; 38:382-390

TABLE 1.

N° of eyes included in study in the different experimental groups and at the different post surgical times. Only eyes showing lack of pupillary reflex during the first 24h were included in the study. (see text for further details)

Days after Ligation or sham surgery	sham+Saline	sham+NGF	2VO	2VO+saline	2VO+NGF
8	15	10	16	10	18
30	7	7	5	4	4
75	6	6	4	3	4

TABLE 2.

Primary antisera and working conditions used in the study.

ID	Antigens	Hosts	Suppliers	dilution
βIII Tubulin	βIII Tubulin	Rabbit	Santa Cruz	1:300
MBP	myelin basic protein	Rabbit	DAKO	1:100
Mcm-2	mini-chromosome maintenance	Goat	Santa Cruz	1:150
OX42	OX42	Mouse	Serotec	1:300
NG2	NG2 chondroitin sulfate Proteoglycan	Mouse	Chemicon	1:100
Laminin	Laminin	Rabbit	Sigma	1:25

TABLE 3. Primers used for real-time QPCR reactions

Primer	Acc. N°	Sequenze (5'-3')	Amplified product (pb)
BAX	AF235993	5'-tgctacagggtttcatccag-3' 5'-ccagttcatcgccaattcg-3'	135
Bcl-2	NM_031535	5'-tggaaagcgtagacaaggagatgc-3' 5'-caaggctctaggtggtcattcagg-3'	88
NGF	M36589	5'- acctcttcggacactctgg-3' 5'- cgtggctgtggtcttatctc-3'	165
P75	NM_012610	5'- agtggcatctctgtggac-3' 5'- ctacctcctcacgcttgg-3'	130
Trk-A	NM_021589	5'- aagccgtggaacagcatc-3' 5'- agcacagagccgttgaag-3'	91
GAPDH	M17701	5'-ggcaagttcaatggcacagtcaag-3' 5'-acatactcagcaccagcatcacc-3'	125

FIGURES

Fig. 1

A, B: Histological staining (Hematoxylin-Eosin) of the retina of control (A) and 2VO legated animals (B) and thickness of retinal layers (C). The OPL layer almost disappears on 2VO animal 8 days after surgery (C); Student-t test: ***P<0,001. A reduction of the number of ganglion cells 75 days after surgery was also found (D); Student-t test: $^{\#}$P<0,05.

E, F: Histological staining (Masson Trichromic staining) of the optic nerve of control (E) and 2VO animal (F). The atrophic effect of legation is shown as reduction of the optic nerve diameter (G); one-way ANOVA and post hoc Tukey test: *P<0,01 e **P<0,001.

Abbreviations: ONL: outer nuclear layer; *OPL*: outer plexiform layer; *INL*: inner nuclear layer; *IPL*: inner plexiform layer; *GCL*: ganglion cell layer. Bars: 200μm (A, B); 100μm (E, F).

Fig. 2

Optic nerve staining of control (left column, sham) and 2VO operated animal (right colum) for the markers listed in the figure. Images are obtained by conventional fluorescence microscopy, and semiquantitative analysis of relative immunoreactive area. The analysis of the immunoreactive area for the βIII-tubulin (O) shows a strong reduction at 8, 30 and 75 days after legation (one-way ANOVA and post hoc Tukey test: *P<0,05, **P<0,001), such as the analysis of MBP (P) (one-way ANOVA and post hoc Tukey test: *P<0,05; *P<0,01; **P<0,001).

Fig. 3

Morphometric analysis of NGF effect on optic nerve diameter (A), ganglion cells (B), beta-tubulin (C) and MBP (D) immunostaining. See text for details. Statistical analysis: one-way ANOVA and post hoc Tukey test: *P<0,05; *P<0,01 and Student-t test: $^{\#}$P<0,05.)

Fig. 4

Real time PCR of the pro- and anti-apoptotic BAX and Bcl-2 genes. The induction of hypoperfusion induces an increase in the pro-apoptotic gene BAX mRNA when comparing

with its sham group (2VO-saline *versus* sham-saline) (B) which is then diminished after NGF treatment (C). The relative expression of the anti-apoptotic gene Bcl-2 is in contrast increased in the 2VO-NGF group when comparing with sham-saline group of animals (A). For the statistical analyses one-way ANOVA and Student's *t* test have been performed. Results have been considered significant when: one-way ANOVA and post hoc Dunnett test, * $p<0,05$; * $p<0,01$; ** $p<0,001$. Student's *t* test: $^{\#}p<0,05$.

Fig. 5

Real time PCR of NGF and its receptors, p75 and trK-A. The relative expression of NGF is increased in all the groups with respect to the sham group of animals (C) and also in 2VO-NGF group comparing with 2VO-saline (D). The opposite happens in the case of the high affinity NGF receptor trK-A mRNA, observing a decrease in all the groups with respect to sham group of animals (A). The mRNA level of the low affinity NGF receptor p75 is not significantly altered within the groups studied except in the NGF injected sham group of animals (B). Statistical analysis results have been considered significant when: one-way ANOVA and post hoc Dunnett test, * $p<0,01$; ** $p<0,001$. Student's *t* test: $^{\#}p<0,05$.

Fig. 7

Real time PCR of VEGF and its receptors, Flt-1 and Flk-1 in the retina. The relative expression of VEGF and its Flt-1 receptor is increased in the 2VO group with respect to the sham group of animals (D) while the relative expression of Flk-1 decreases in group 2VO comparing with sham-group (F). Statistical analysis results have been considered significant when: Student's *t* test: $^{**}p<0,01$.

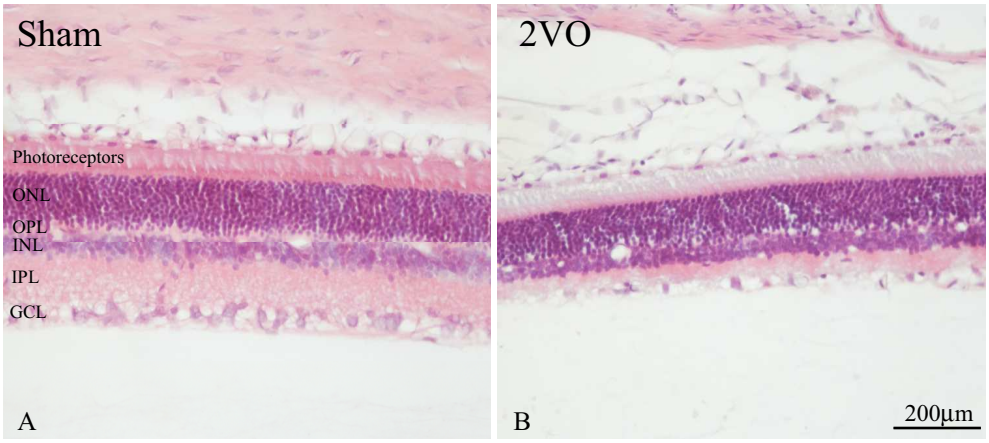

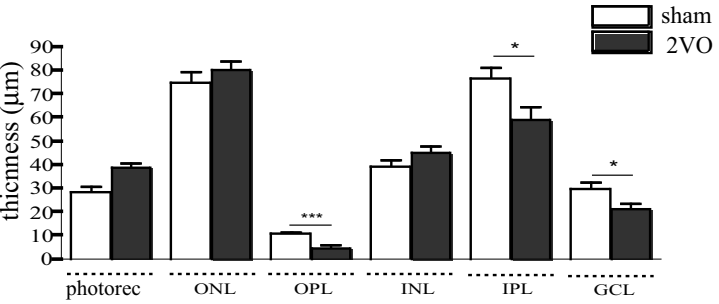

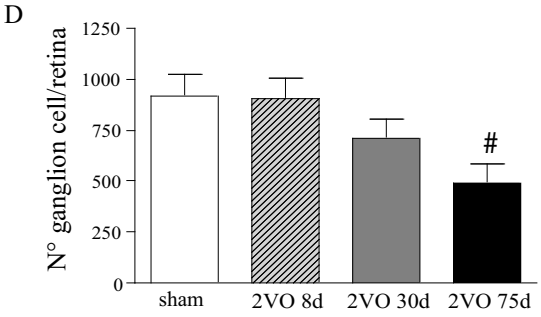

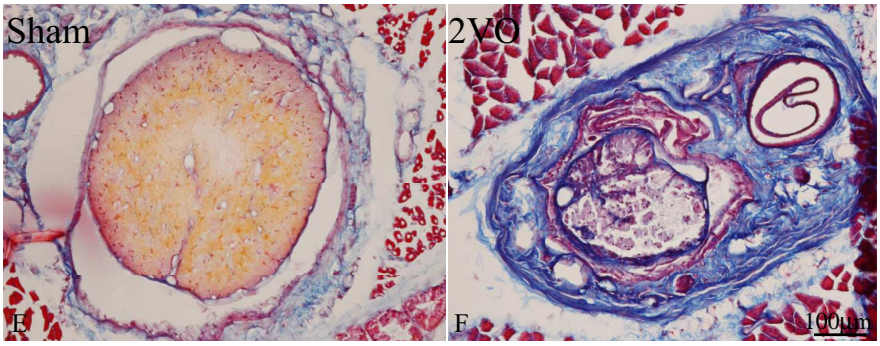

Diameter of optic nerve

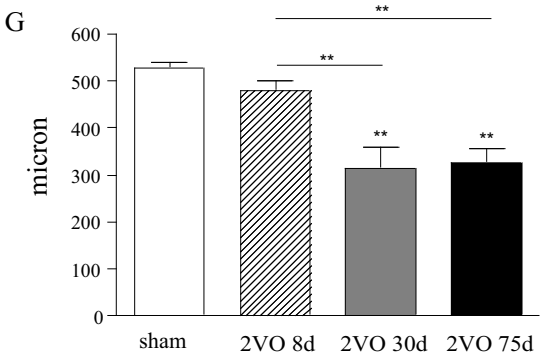

Fig.1

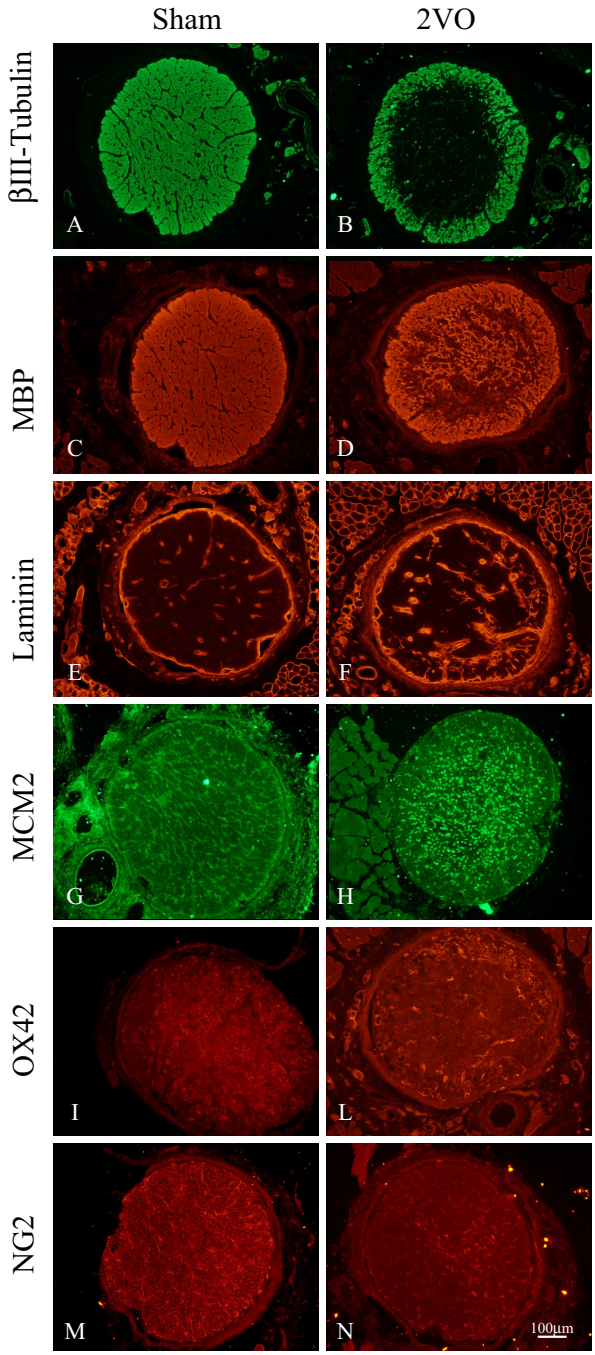
Sham
2VO
βIII-Tubulin
MBP
Laminin
MCM2
OX42
NG2
A
B
C
D
E
F
G
H
I
L
M
N
100μm

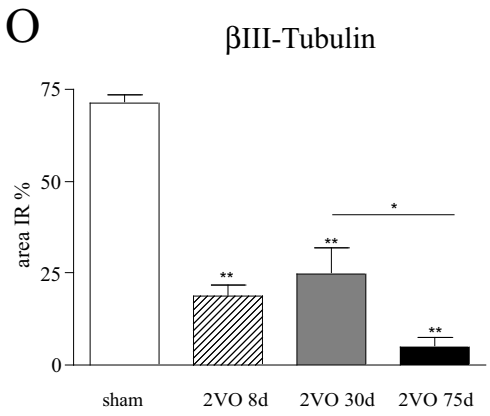
O
βIII-Tubulin
area IR %
75
50
25
0
sham
2VO 8d
2VO 30d
2VO 75d

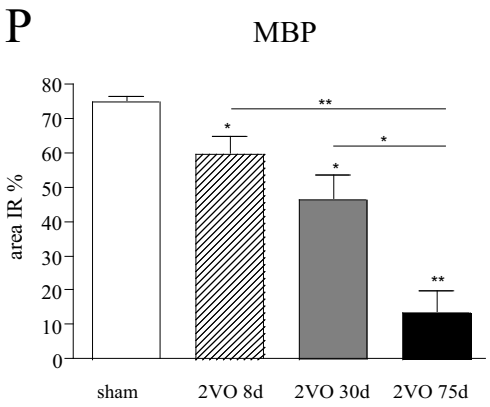
P
MBP
area IR %
80
70
60
50
40
30
20
10
0
sham
2VO 8d
2VO 30d
2VO 75d

Fig. 2

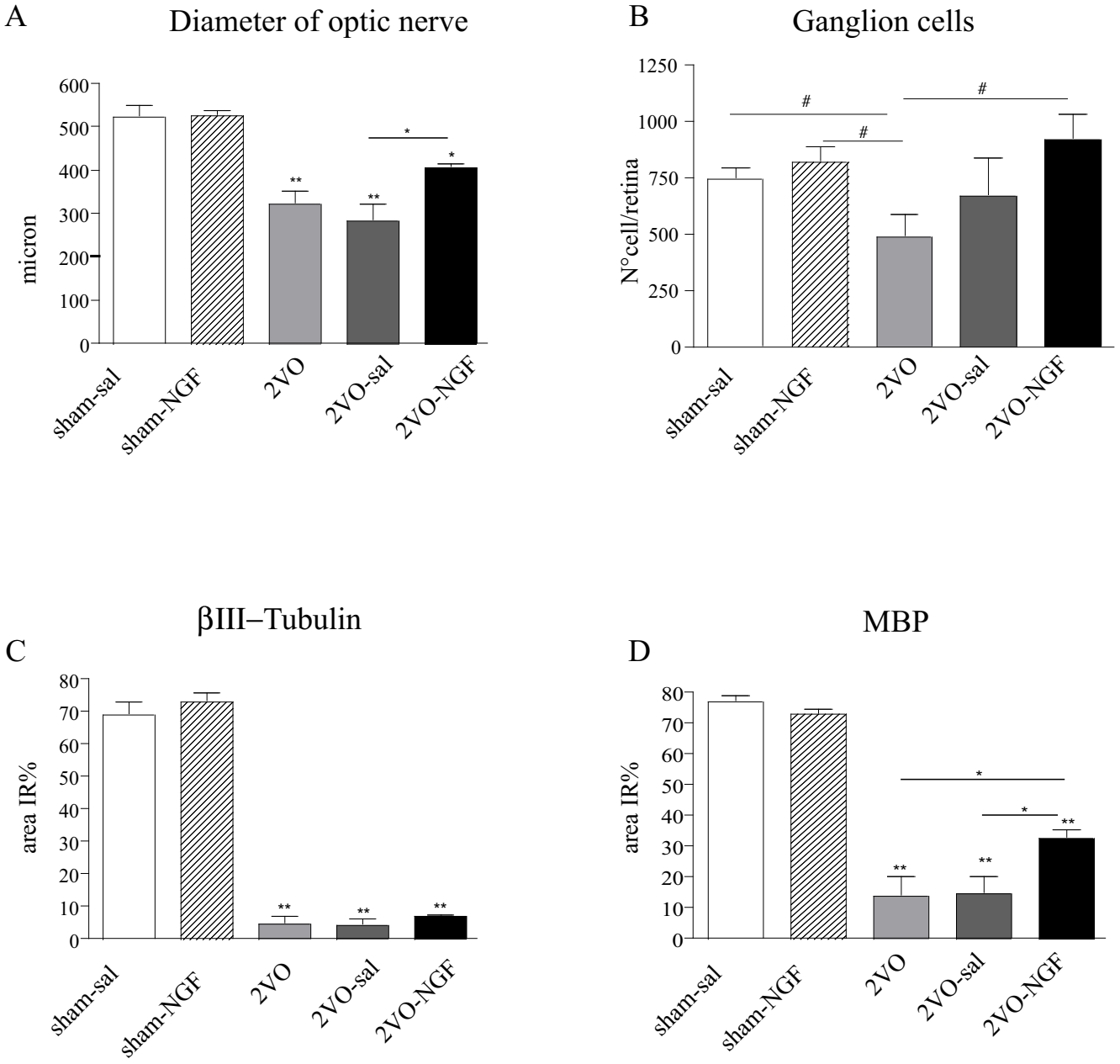
A
Diameter of optic nerve
micron
600
500
400
300
200
100
0
**
**
*
*
sham-sal
sham-NGF
2VO
2VO-sal
2VO-NGF
B
Ganglion cells
N°cell/retina
1250
1000
750
500
250
0
#
#
#
sham-sal
sham-NGF
2VO
2VO-sal
2VO-NGF
C
βIII–Tubulin
area IR%
80
70
60
50
40
30
20
10
0
**
**
**
sham-sal
sham-NGF
2VO
2VO-sal
2VO-NGF
D
MBP
area IR%
80
70
60
50
40
30
20
10
0
*
*
**
**
**
sham-sal
sham-NGF
2VO
2VO-sal
2VO-NGF

Fig.3

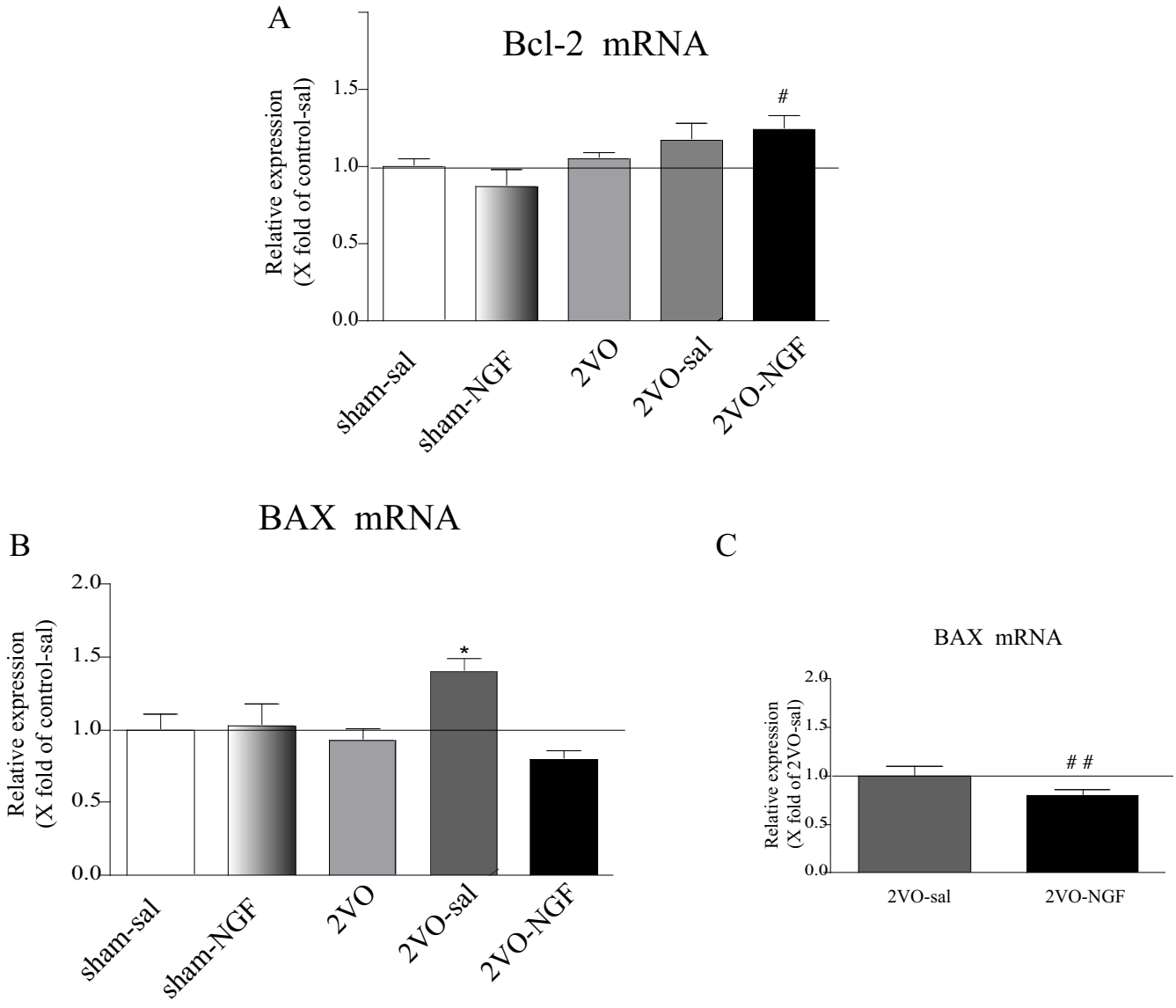
A
Bcl-2 mRNA
Relative expression
(X fold of control-sal)
1.5
1.0
0.5
0.0
#
sham-sal
sham-NGF
2VO
2VO-sal
2VO-NGF
B
BAX mRNA
Relative expression
(X fold of control-sal)
2.0
1.5
1.0
0.5
0.0
*
sham-sal
sham-NGF
2VO
2VO-sal
2VO-NGF
C
BAX mRNA
Relative expression
(X fold of 2VO-sal)
2.0
1.5
1.0
0.5
0.0
# #
2VO-sal
2VO-NGF

Fig. 4

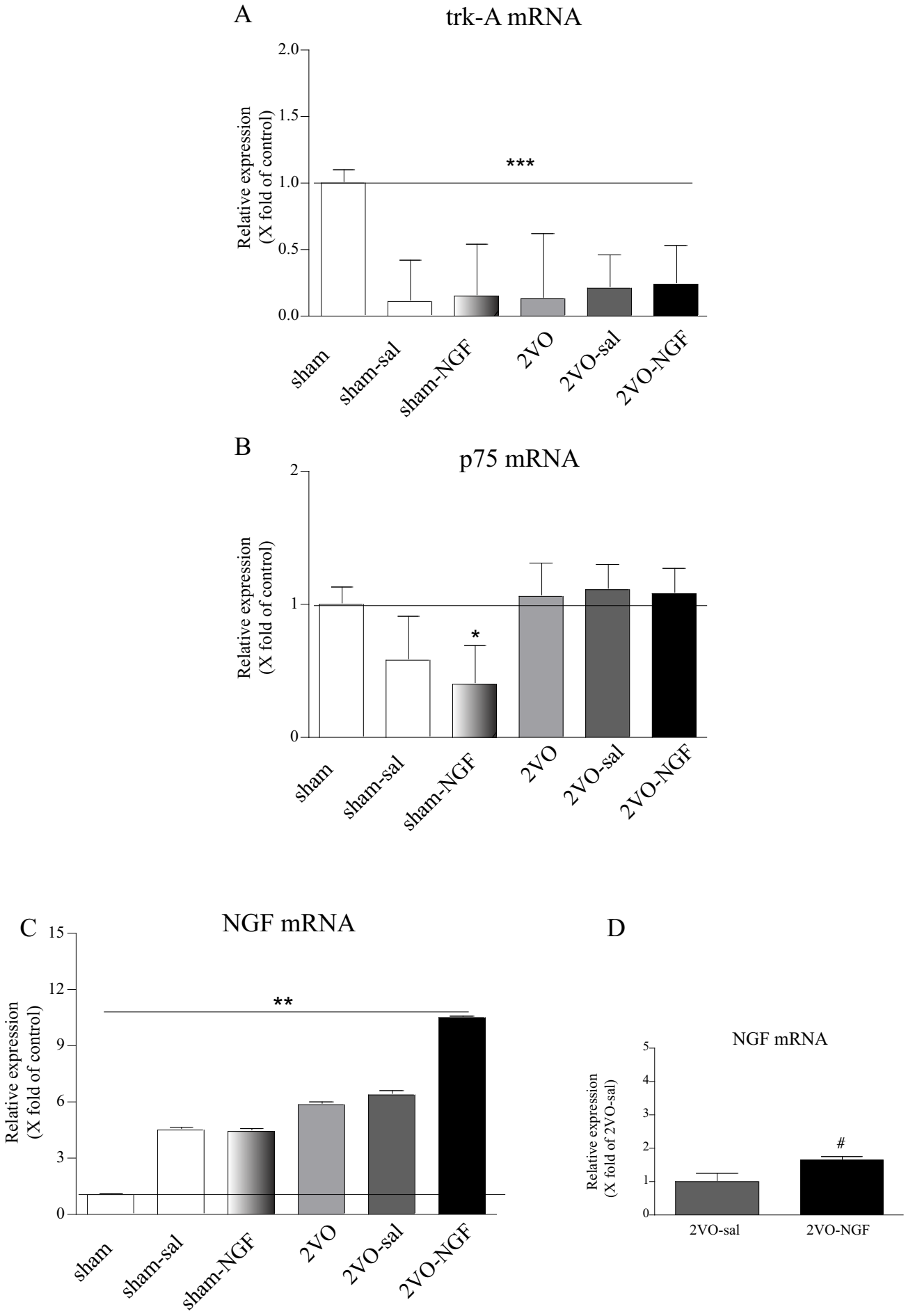
A
trk-A mRNA
Relative expression
(X fold of control)
2.0
1.5
1.0
0.5
0.0
***
sham
sham-sal
sham-NGF
2VO
2VO-sal
2VO-NGF
B
p75 mRNA
Relative expression
(X fold of control)
2
1
0
*
sham
sham-sal
sham-NGF
2VO
2VO-sal
2VO-NGF
C
NGF mRNA
Relative expression
(X fold of control)
15
12
9
6
3
0
**
sham
sham-sal
sham-NGF
2VO
2VO-sal
2VO-NGF
D
NGF mRNA
Relative expression
(X fold of 2VO-sal)
5
4
3
2
1
0
#
2VO-sal
2VO-NGF

Fig. 5

VEGF mRNA

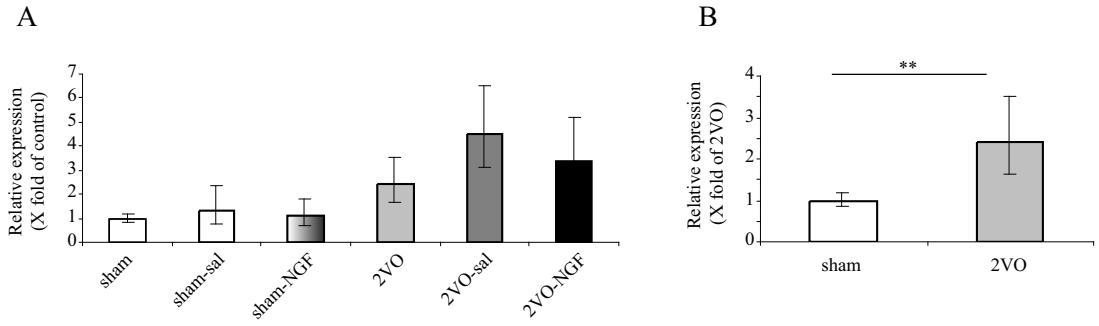

Flt-1 mRNA

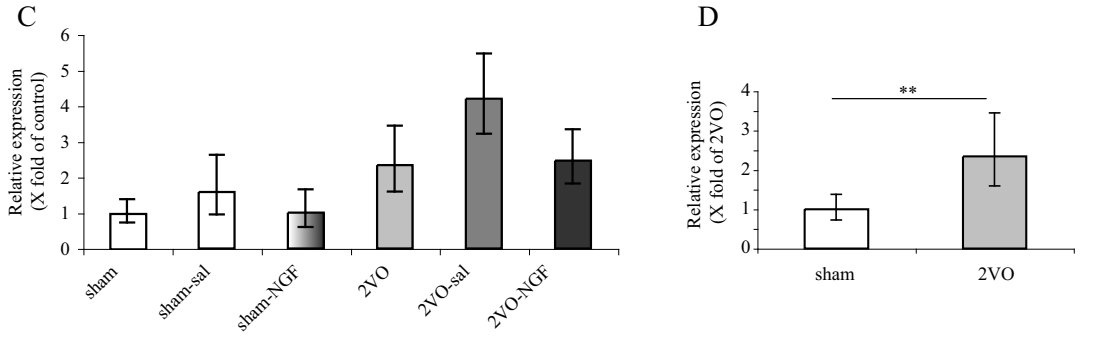

Flk-1 mRNA

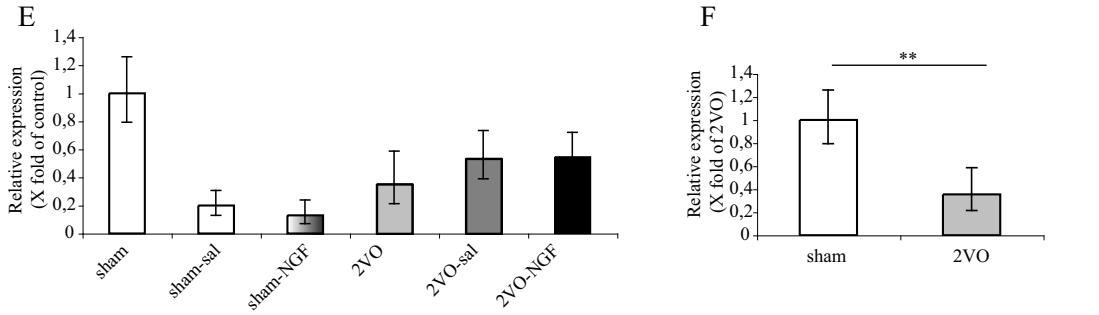

Fig. 6

BRAIN RESEARCH 1098 (2006) 186–195

available at www.sciencedirect.com

www.elsevier.com/locate/brainres

BRAIN RESEARCH

Research Report

A molecular study of hippocampus in dogs with convulsion during canine distemper virus encephalitis

D'Intino Giulia[a,1], *Vaccari Francesca*[b,1], *Sivilia Sandra*[a], *Scagliarini Alessandra*[a], *Gandini Gualtiero*[c], *Giardino Luciana*[a], *Calzà Laura*[a,*]

[a]*Department of Veterinary Morphophysiology and Animal Production, DIMORFIPA, University of Bologna, Via Tolara di Sopra 50, 40064 Ozzano Emilia, Bologna, Italy*
[b]*Department of Veterinary Public Health, Biotechnology Lab., University of Bologna, Italy*
[c]*Department of Veterinary Clinical Sciences, Internal Medicine Section; Alma Mater Studiorum-University of Bologna, Italy*

ARTICLE INFO

Article history:
Accepted 16 April 2006
Available online 9 June 2006

Keywords:
Epilepsy
Brain-derived neurotrophic factor
Nerve growth factor
Neuropeptide
Glutamate

ABSTRACT

In this study, we have investigated the expression of the nuclear transcription factor (c-Fos, NFkB), growth factors (nerve growth factor—NGF, brain-derived neurotrophic factor—BDNF), peptides (enkephalin, galanin) and glutamate transporter (AA 504–523 rat EAAC1) in 6 dogs sacrificed immediately after seizure attack during encephalomyelitis due to canine distemper virus (CDV) (as assessed by clinical examination, RT-PCR and viral RNA detection either in blood or brain tissue and CDV immunohistochemistry in brain slices). In all these CDV affected dogs, the observed neurological signs included untreatable seizures, leading to cluster seizure activity and status epilepticus. In the inter-ictal phase abnormal mentation, postural and gait deficits and sometimes involuntary movements such as myoclonus were recorded. The same investigation was carried out in 5 control dogs affected by different disorders, all characterized by the absence of seizures. Brains were dissected out immediately after euthanasia and fixed; sections collected from the dorsal hippocampus were processed for immunohistochemistry. By comparing hippocampus sections obtained from dog with and without seizure, the following regulations were observed. A strong up-regulation of glutamate transporter throughout the cell layers was found together with the onset of nuclear Fos and NFkB-IR in the pyramidal cell layer X. Among the investigated peptides, we observed a slight increase in enkephalinergic fibers and a strong up-regulation of mu-opioid receptors, whereas galanin-IR seemed to be weaker. Finally, both NGF and BDNF expression was strongly up-regulated. BDNF-IR was mainly localized in the apical dendrite in pyramidal neurons. To our knowledge, these data offer the first indication that molecular events described in experimental kindling also occur during spontaneous pathology in animal species sharing close similarities to human neuropathology.

* *Corresponding author*. Fax: +39 051 792956.
E-mail address: lcalza@vet.unibo.it (L. Calzà).
[1] These authors contributed equally to this paper.

0006-8993/$ – see front matter © 2006 Elsevier B.V. All rights reserved.
doi:10.1016/j.brainres.2006.04.051

1. Introduction

Studies on kindling and status epilepticus models of epilepsy have indicated that the brain reorganizes itself in response to excess neural activation (McCormick and Contreras, 2001; Morimoto et al., 2004). This reorganization, which extends from the molecular to the network level in a time window ranging from milliseconds to days, starts from the activation of glutamate receptors and includes second messengers, expression of immediate early genes and other transcription factors, neurotrophic factors, axon guidance molecules, neurogenesis, sprouting and synaptogenesis. All these changes are under active investigation in order to develop effective anti-convulsant and neuroprotective therapies (Rogawski and Loscher, 2004). However, it is still not known whether the molecular changes described in experimental animals reflect molecular events in human pathology. Although research in neuropathology and neuropharmacology has benefited substantially from data obtained in experimental animals, for example, rodents and non-human primates, a significant proportion of human neurological disorders cannot be adequately mimicked in laboratory animals. In particular, epilepsy, one of the most common neurological problems worldwide, is still hampered by the absence of any adequate experimental model covering all clinical syndromes (Chang and Lowenstein, 2003).

In recent years, an increasing interest in using the canine brain as a model for human neurological diseases has emerged, with dog being used both for experimentally induced and naturally occurring diseases (Cummings et al., 1996; Loscher, 1997; Cotman et al., 2002; Milgram et al., 2002; Dimakopoulos, 2003; Switonski et al., 2004). The advantages in using canines for brain studies stem from the close similarities between humans and dogs in the physiological and behavioral features of their life styles. In fact, canines share many of the same environmental conditions as humans and can perform a sophisticated repertoire of complex cognitive behaviors. Moreover, the brain of canines shows many pathological changes common to human, starting from age-altered beta-amyloid and presenilin processing (Head et al., 2000; Head and Torp, 2002), where neuropathology is significantly associated with cognitive performance and eventually with decline (Cummings et al., 1996; Cotman et al., 2002; Head et al., 2000). Moreover, epileptic dogs are among the few genetic animal models of epilepsy with spontaneously occurring seizures and is the only genetic animal model that allows animals with pharmacoresistant seizures to be distinguished from those with pharmacosensitive seizures (Loscher, 1997). Moreover, encephalitis due to canine distemper virus (CDV) that is a member of the genus *Morbillivirus* (family Paramyxoviridae) has been associated with multiple sclerosis (MS) because of extensive demyelination and the postulated viral origin of MS (Hodge, 1997).

In this perspective, a postmortem study of canine brain suffering from spontaneous neurological diseases offers an excellent "bridge" between experimental animals and human pathologies. We have investigated molecular changes in the hippocampus of dogs that have been euthanized because of intractable status epilepticus. The specific aim of the study was to investigate early molecular regulation, which was extensively analyzed in the hippocampus in experimental kindling during spontaneous pathology (Gall et al., 1990; Hughes et al., 1999; Morimoto et al., 2004). We have included in the study dogs affected by CDV encephalitis, which is the most common cause of secondary epilepsy in juvenile dogs (Koestner, 1989) euthanized during convulsion and age-matching controls (e.g., dogs affected by encephalitis with no trace of epilepsy in their clinical history). In particular, we investigated the expression of the nuclear transcription factor (c-Fos, NFkB), growth factors (nerve growth factor—NGF, brain-derived neurotrophic factor—BDNF), peptides (enkephalin, galanin) and glutamate transporter (AA 504–523 rat EAAC1).

2. Results

2.1. *Clinical findings*

Relevant clinical data are reported in Table 1.

2.1.1. *Group A*

The clinical history of group A dogs was characterized in all cases by acute onset and quick progression of the disease. All the dogs displayed seizure activity (in three cases documented with videos), which can be described as follows: initially the dogs showed complex partial seizures, mostly characterized by impairment of consciousness, chewing activity, salivation and twitching of the muscles of the head. As soon as the disease progressed, the seizures tended to become more frequent and severe and switched to clusters of generalized tonic–clonic seizures leading in some cases to status epilepticus. Neurological inter-ictal impairment was observed in all cases.

Table 1 – Relevant clinical data of animals included in the study

ID	Breed	Sex	Age (months)	Final diagnosis
Group A				
1	English setter	F	6	CDV with seizures, tetraparesis, myoclonus
2	Mixed	M	12	CDV with seizures, paresis, myoclonus
3	Mixed	M	3	CDV with seizures, paresis, myoclonus
4	Mixed	F	3	CDV with seizures, paresis, myoclonus
5	Yorkshire	F	2	CDV with seizures, paresis, myoclonus
6	Corso	F	15	CDV with seizures, paresis
Group B				
7	German shepherd	F	2	CDV without seizures
8	Mixed	F	54	Meningoencephalitis due to Aspergillus
9	Bulldog	M	3	Parvovirosis infection
10	Maremmano shepherd	M	36	Meningoencephalitis due to Prototheca
11	Mixed	F	14	Meningoencephalitis due to unknown agent

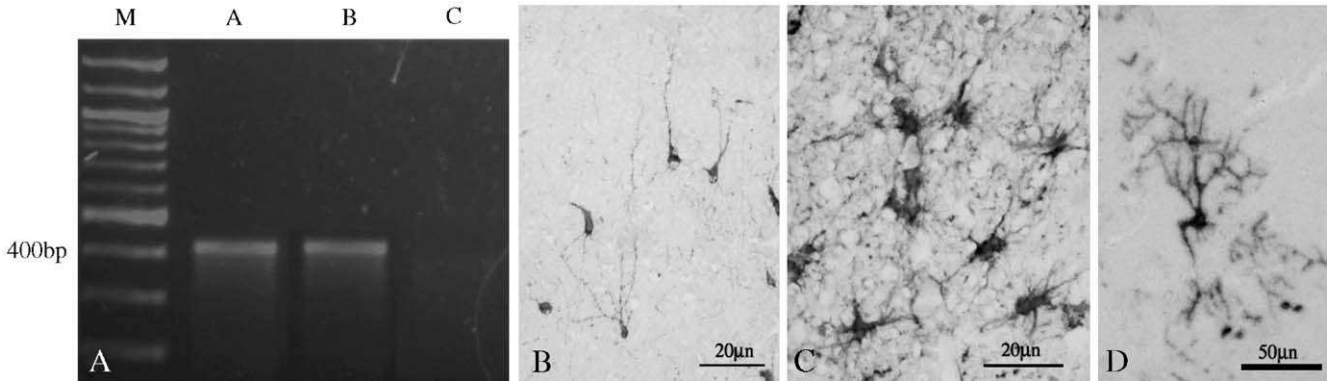

Fig. 1 – (A) Electrophoresis of the P gene PCR product. Specific 429-bp products were amplified from RNA of canine distemper virus. Lane M: 100-bp molecular weight marker; lane A: positive control; lane B: diagnostic sample (nr. 2); lane C: negative control. (B) Immunostaining of viral protein visualized by ABC (B, C) illustrates the different morphology of infected cells, ascribed to neurons (B). (C) In situ detection of CDV mRNA (D) in cerebellum.

Neurological examination (in a few dogs taken in the post-ictal phase) in all cases showed abnormal mentation resulting in depressed to stuporous mental status and mild to severe disorientation. Other findings included in most cases tetraparesis, proprioceptive impairment and involuntary movements such as myoclonus, affecting mainly the limbs and the head. Despite the common finding of an abnormal menace reaction, cranial nerve examination was normal in most cases. The neurological abnormalities led to a multifocal nervous system disorder being diagnosed, which mainly affected the forebrain structures. Clinicopathological abnormalities were confined to detection of lymphopenia in three cases. RT-PCR, brain immunohistochemistry and in situ hybridization results are reported in Fig. 1. All group A dogs were positive for the above-mentioned tests. Therapy with anti-convulsants was started in dogs 5 and 6. In detail, in the last 24h, dog 5 was treated with diazepam at the dosage of 1mg/kg IV QID (Valium®). Dog 6 had phenobarbital treatment for 5days at the dosage of 3mg/kg IM BID (Luminale®).

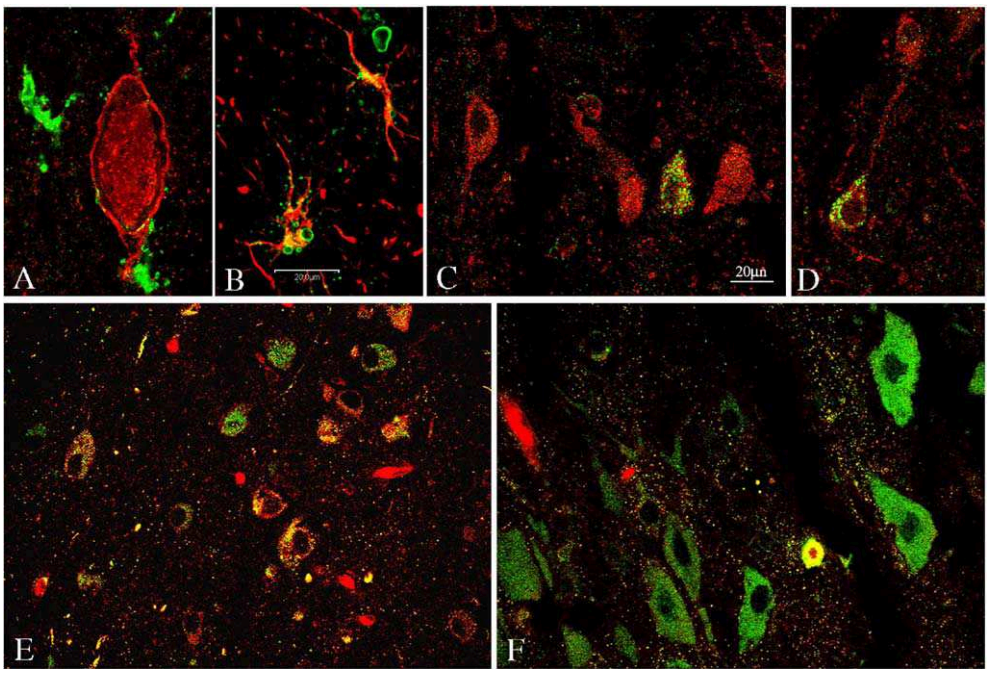

Fig. 2 – Confocal images illustrating the co-distribution of CDV protein (green) in NG2(red: A)- and GFAP (red: B)-positive cells, possibly indicating the presence of the virus in astrocytes and oligodendrocyte precursor cells, respectively. Images C to F illustrate co-distribution of brain-derived neurotrophic factor (green: E), opioid receptor mu subtype (green: C and D) and nerve growth factor (red: F) in glutamate transporter-positive (red: C–E; green: F) neurons in the hippocampal formation of CDV-infected canine with convulsion. Scale bar: 20µm.

2.2. CDV in the CNS

The distribution of the virus in different regions and cell type in the CNS was studied using in situ hybridization for the detection of the mRNA encoding for the nucleoprotein (N) of the virus, and immunohistochemistry for the CDV surface envelope antigen detection (Fig. 1). The results of both in situ hybridization and immunohistochemistry show a widespread distribution of the CDV in the white and grey matter, involving different cell types. In most of the brain areas, including hippocampus, a large number of infected cells extend from the white to the grey matter reaching the external layers (Fig. 1; ABC detection of the viral protein and in situ hybridization detection of the viral mRNA). High-power micrographs illustrate the different morphology of the infected cells, which may be ascribed to neuronal (B and D) or glial (C) morphology. By double immunocytochemical staining, it was possible to confirm that all cell types in the CNS can be infected by CDV. Examples of co-localization of the viral protein in astrocytes and NG2-positive oligodendrocyte precursor cells are reported in Fig. 2. Panels A and B show laser scan microscopy images of sections double stained for CDV (green) and GFAP (red: A) or NG2 (red: A). Merged images in Figs. 2F and I indicate that the virus is localized in astrocytes and NG2-positive oligodendrocyte precursor cells.

2.3. Molecular changes in the hippocampus

Molecular changes in dogs with seizures due to CDV encephalitis immediately before death compared to animals with encephalitis not showing seizures at any of the clinical stages have been studied in the CA1–CA3 fields of the hippocampus. The main results are illustrated in Figs. 3 and 5, and the semiquantitative analysis of observed changes is reported in Fig. 4. Seizure induces a strong up-regulation of immunoreactivity for the nuclear transcription factor c-*fos*, NFkB and EAAT3 (Fig. 3). Also peptide immunostaining is modified. Galanin immunostaining is quite highly localized in the pyramidal cell layer of the dorsal hippocampus in non-kindling dogs (Fig. 5), whereas in convulsive dogs immunostaining spreads, involving also other cell layers, and single neuron staining seem to decrease. A slight increase in enkephalin immunostaining, which appears as increased density of positive fibers, is instead observed in kindling animals compared to non-kindling (Fig. 5), and this corresponds to a strong up-regulation of MOR expression in the pyramidal layer (Fig. 3). Finally, growth factors are also

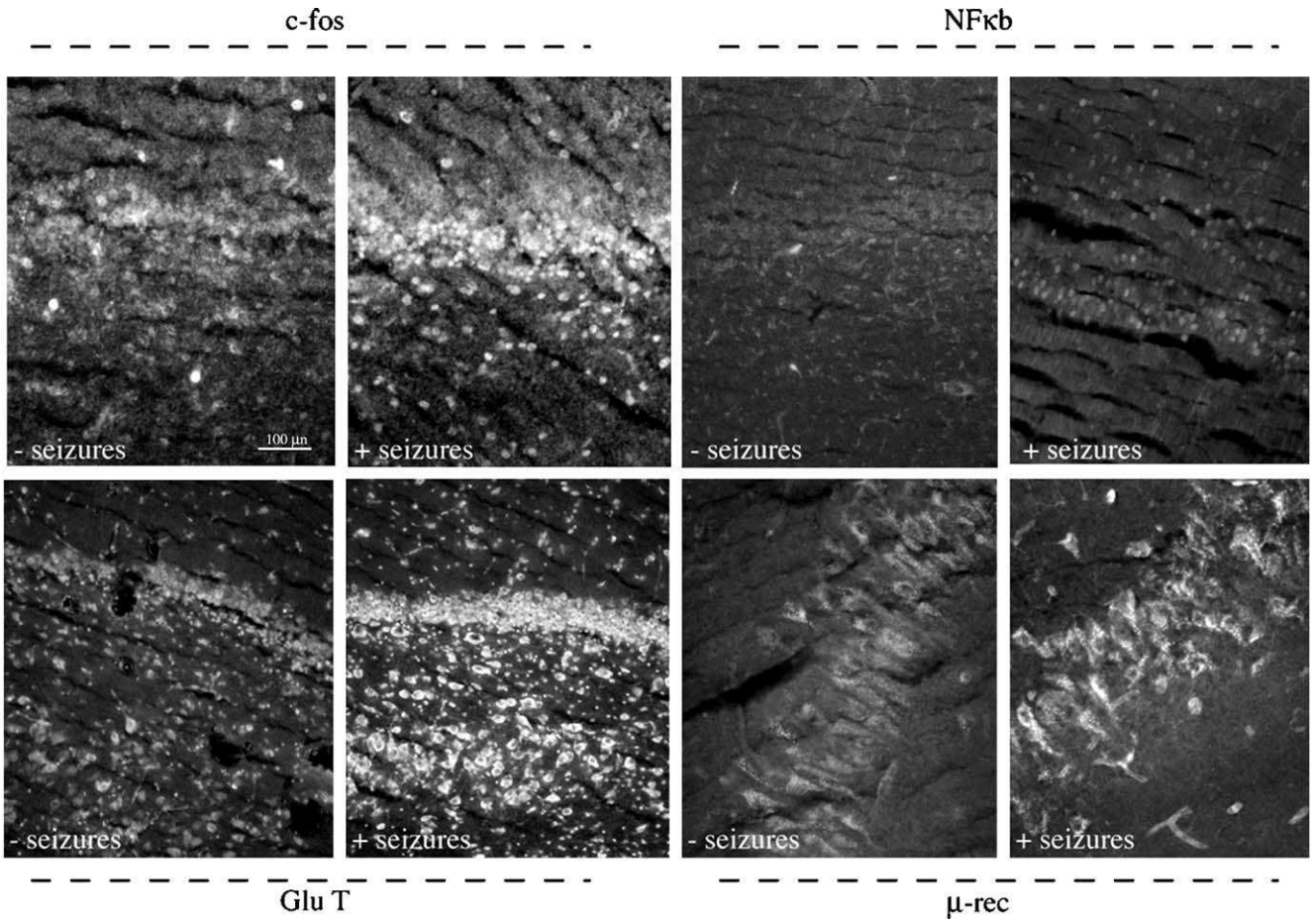

Fig. 3 – Micrographs illustrate immunoreactivity for the nuclear transcription factor c-*fos*, NFkB, glutamate transporter, opioid receptor mu subtype (M and N) in the hippocampal cortex of animals without and with seizures. Scale bar: 100 µm.

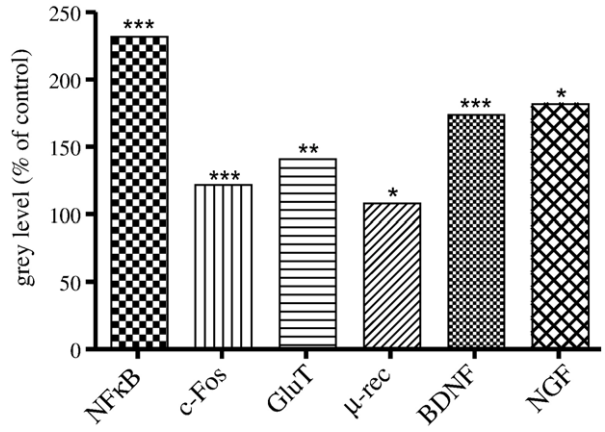

Fig. 4 – Semi-quantitative evaluation of immunostaining for peptides and transcription factors in the hippocampal cortex of seizuring dogs, as expressed as percentage changes respect to control, non-seizuring dogs. Statistical analysis: one-way ANOVA and Dunnett's post hoc test (*$P \leq 0.05$; **$P \leq 0.01$; ***$P \leq 0.001$). Abbreviations: BDNF, brain-derived neurotrophic factor; Glu-T, glutamate transporter.

up-regulated in animals with seizure. In particular, BDNF immunoreactivity, which is hardly detectable in non-kindling animals, accumulates in kindling animals and shows a subcellular localization in apical dendrites of the pyramidal neurons (Fig. 5). Double-labeling experiments (Fig. 2) indicate that expression of BDNF (green: E), opioid receptor mu subtype (green: C, D) and NGF (red: F) also occurs in EAAT3-positive (red: C–E; green: F) neurons. In particular, a punctate staining for MOR is observed in some of the EAAT3-positive neurons in the pyramidal layer.

3. Discussion

In the present paper, we describe molecular changes in the hippocampus of 6 dogs with intractable secondary epilepsy due to CDV encephalitis. The dogs were sacrificed immediately after seizures, thus allowing molecular analysis of the hippocampus during cerebral hyperactivity in comparison to dogs without seizure activity. The main results found in epileptic dogs were the following: up-regulation of c-*fos*, NFkB, NGF, BNDF, enkephalin and EAAT3 and down-regulation of galanin immunoreactivity in the pyramidal layer of the hippocampus. To our knowledge, these data offer the first indication that molecular events described in

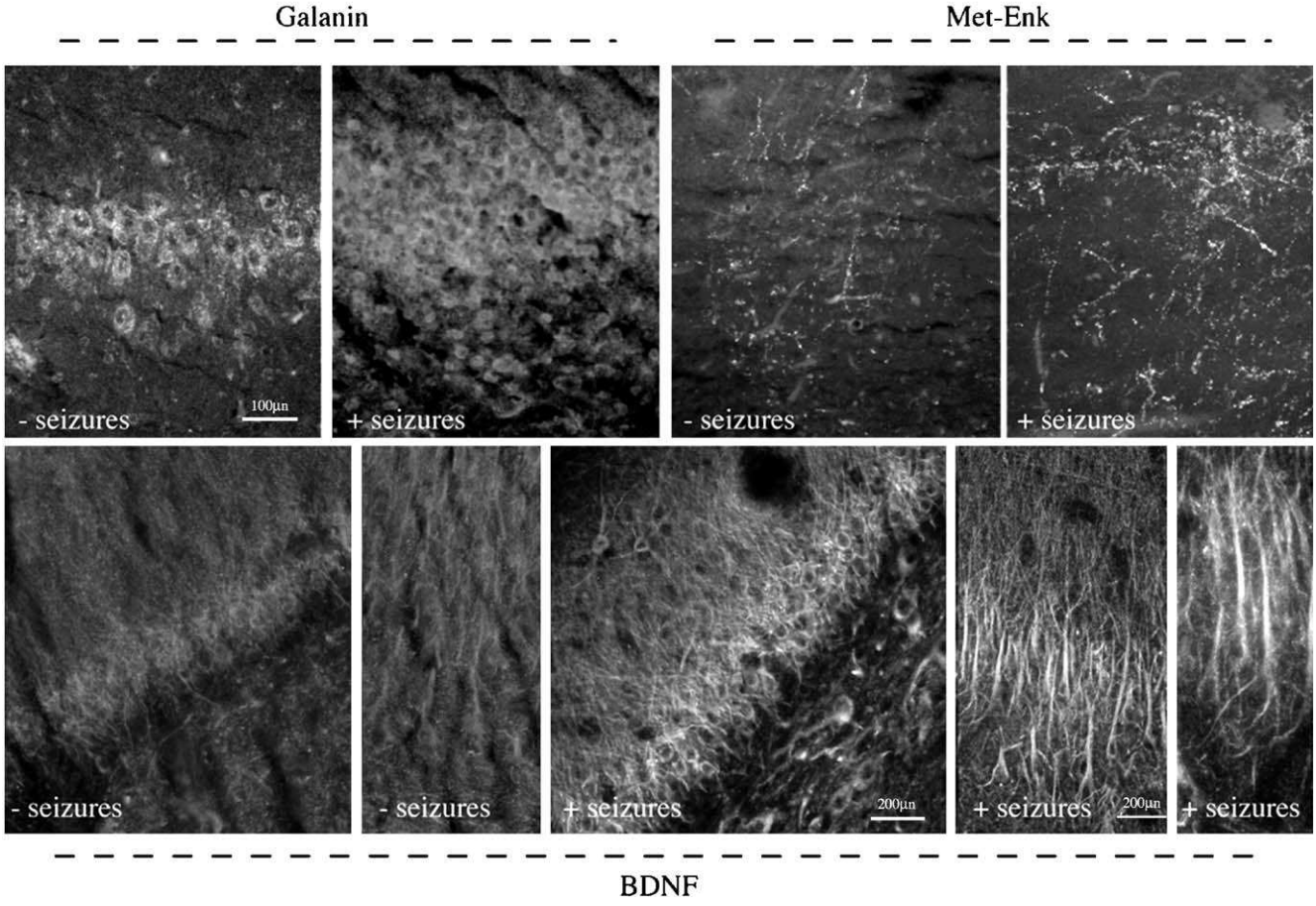

Fig. 5 – Micrographs illustrate immunoreactivity for the peptides galanin, Met-enkephalin and BDNF in the hippocampal cortex of animals without and with seizures. Scale bar: 100 μm.

experimental seizures also occur during spontaneous disease in an animal species sharing similarities with human neuropathology.

3.1. *CDV infection of the brain parenchyma*

CDV is a highly contagious pathogen that occurs worldwide which causes a fatal disease in Canidae. Acute encephalomyelitis is a common manifestation of distemper in dogs without adequate immune protection that, after a short progressive course of the disease, almost invariably leads to the death of the affected animals. The clinical signs of the disease may reflect a focal, multifocal or diffuse distribution of CNS lesions (Koutinas et al., 2002). In the cases reported here all the dogs belonging to group A showed nervous abnormalities consistent with the classical features of the acute multifocal/diffuse infection of the CNS. Most representative signs included complex partial and generalized tonic-clonic seizures, abnormal mental status. In more prolonged cases myoclonus became evident.

From a histopathological point of view, all group A dogs belong to the multifocal form, showing extensive viral distribution and in all main cell types, e.g., neurons, astrocytes, microglia, oligodendrocytes and oligodendrocyte precursor cells in the brain, as defined by morphological features.

We also confirmed the presence of the virus in astrocytes, which was suspected on a morphological basis and according to in vitro studies, but never proved by double-labeling experiments (Zurbriggen et al., 1993) and (Vandevelde and Zurbriggen, 1995), and proved its presence in NG2-positive cells. NG2-positive cells have been identified as oligodendrocyte precursor cells (Stallcup, 2002), and in fact a severe oligodendrocyte pathology supports extensive demyelination in canine distemper (Zurbriggen et al., 1998; Schobesberger et al., 1999; Schobesberger et al., 2002). However, NG2 can be also expressed by other cell types in glial scarring after injury, including tissue macrophage (Sandvig et al., 2004), and microglial cells are in fact activated in canine distemper lesions (Stein et al., 2004).

3.2. *Seizure-induced molecular regulation in the hippocampus*

Epilepsy is characterized by a spontaneous tendency for recurrent seizure produced by synchronous and sustained firing of a population of neurons in the brain (Goetz, 2003). The hippocampal formation is a brain structure that is highly susceptible to the development of recurrent seizure and a key region in experimental seizure and epilepsy, which also undergoes severe degeneration (McCormick and Contreras, 2001; Morimoto et al., 2004). In the dog, nuclear pyknosis followed by neuronal atrophy and loss is observed during kainic acid-induced status epilepticus (Hasegawa et al., 2003). A number of experimental epilepsy studies in laboratory animals have focused on the identification of the cascade of molecular events, acting as both epilepsy trigger, autopropagation and self-enhancement mechanism, cell death and/or protection during prolonged seizure (Morimoto et al., 2004), in order to develop effective anti-epileptic drugs (Rogawski and Loscher, 2004). Here we suggest that most of the molecular events, which have been described in the hippocampus during experimental seizure in rodents, also occur in spontaneous epilepsy in Canidae.

According to our data, we can trace the sequence of neurochemical changes acutely determined in the hippocampus by seizure in secondary, CDV-mediated epilepsy. An enhancement of transmission in excitatory systems, particularly the glutamatergic system, which produces an overexcitation of neurons, has been indicated as a possible mechanism for epileptic discharge (Morimoto et al., 2004). In epileptic dogs, we observed an up-regulation of glutamate-transporter expression in pyramidal neurons in the hippocampus, suggesting that this mechanism is active also in these animals. An increased expression of the neuronal glutamate transporter, which powerfully regulates extracellular glutamate via re-uptake mechanism, has been described in rodents and patients affected by temporal lobe epilepsy (Mathern et al., 1999; Crino et al., 2002). This has been considered a compensatory mechanism to excess extracellular glutamate, as also proved by exacerbation of epilepsy and brain injury in mice lacking glutamate transporter (Tanaka et al., 1997).

The excess of extracellular glutamate causes an overstimulation of both ionotropic and metabotropic glutamate receptors, which in turn have short- and long-term effects. The first wave of genetic response described in rodents involves increased transcription and translation of the family of immediate-early gene (IEG) transcription factors, whose prototypic members, Fos and Jun, are expressed in the nucleus of neurons (Dragunow et al., 1987) and (Hughes et al., 1999). Once they have been induced it is believed that these IEGs then go on to regulate a further, delayed, but usually more prolonged (perhaps permanent), expression of effector genes (the second wave of gene expression) by interacting with the AP-1 site in the regulatory regions of these genes (Hughes and Dragunow, 1995). The expression of these target genes which may encode structural proteins, enzymes, ion channels, neurotransmitters, neuropeptides and growth factors then results in long-lasting or permanent changes in morphology, structure and function of the nervous tissue (Gall et al., 1990; Gall, 1993; Hughes et al., 1999). In spontaneously epileptic dogs there is an up-regulation of Fos protein in the pyramidal layer. Moreover, NFkB also appears in all layers of the hippocampus. NFkB is widely known for its ubiquitous role in inflammation and immune responses, as well as in the control of cell division and apoptosis (Mattson and Camandola, 2001), and anti-epileptic drugs are able to decrease the inflammation-induced activation of NfkB (Vezzani and Granata, 2005). Seizure activity results in a rapid induction of nuclear factor-kappa B in adult rat limbic structures (Rong and Baudry, 1996), and its NMDA-dependent activation may contribute to kainate-induced hippocampal degeneration in hamster (Won et al., 1999). However, in spite of the fact that NfkB activation in glial cells during epilepsy is associated to inflammation and neuronal degeneration, its activation in neurons, as observed in our seizuring CDV-infected dogs, protects them against degeneration (Vezzani and Granata, 2005).

Neuronal overactivity, but also glutamate excitotoxicity, leads to a strong up-regulation of neurotrophin synthesis and release in the hippocampus (Gall, 1992; Hartmann et al.,

2001). Pyramidal layer neurons in epileptic dogs are in fact strongly immunostained for neurotrophins. In particular, BDNF seems to accumulate not only in the cell body, but mainly in apical dendrites in pyramidal neurons. A similar pattern of intracellular distribution has been described in experimental seizure. BDNF mRNA and protein, which are both strongly up-regulated (Gall, 1993; Calzà et al., 1996), accumulate in dendrites in all hippocampal subfields after pilocarpine and kainic acid seizures and in selected subfields after other epileptogenic stimuli (Tongiorgi et al., 2004). BDNF up-regulation during seizure seems to be involved in promoting excitability in the hippocampus, but also in maintaining dendrite integrity and favoring axonal sprouting in the hippocampus (Binder et al., 2001; Jankowsky and Patterson, 2001).

Several neuropeptides also participate in synaptic regulation of glutamatergic transmission in the hippocampus and their synthesis and distribution is altered during seizure. Opioids are thought to control the excitability of hippocampal principal neurons by inhibiting GABAergic interneurons, thus resulting in increased excitability and propagation of excitatory activity through the network of area CA1 (McQuiston and Saggau, 2003). ENK-IR is associated with both the perforant path and mossy fiber system and MOR-IR profiles are found in all layers of the hippocampus. In particular, MOR-IR, but not mRNA, is present in the pyramidal layer of rodents, where it does not co-localize with glutamate transporter 1 (Stumm et al., 2004). In non-epileptic dogs, distribution of ENK and MOR in the hippocampus corresponds to that described in rats. In epileptic dogs, we observed both a slight, but clear, increase in ENK-IR fiber in the hippocampus and a strong up-regulation of MOR expression in the pyramidal layer. Also this regulation corresponds to what is observed in rodents. ENK-IR actually dramatically increases within the mouse hippocampal mossy fiber axonal system during kainic-acid induce seizures (Gall, 1988), and treatments that induce seizure cause an increase in MOR-IR that may be associated with the sprouting of MOR-expressing nerve terminals (Alreja et al., 2000) or dendrites (Drake and Milner, 1999). In epileptic animals, we also found that a small percentage of EAAT3-IR cells in the pyramidal layer of the hippocampus also express a punctate MOR-IR, suggesting a pre-synaptic localization on afferent nerve terminals.

Finally, galanin-IR is also regulated in epileptic versus non-epileptic dogs, being absent in the hippocampus of non-epileptic dogs and expressed in the cell body within the pyramidal layer during seizure. Galanin is a 29–30 AA neuropeptide that antagonizes excitatory glutamatergic neurotransmission in the hippocampus (Mazarati et al., 2001). Seizure induces a complex regulation of hippocampal galanin in animal models of status epilepticus, depending on the time after seizure induction, characterized by disappearance of IR-fiber from the hilus and appearance of IR neurons (Mazarati et al., 1998). Pharmacological and molecular biological evidence suggests it has potent anticonvulsant effects (Mazarati et al., 2000). In fact, adeno-associated virus vector galanin expression and secretion (Haberman et al., 2003) and (Lin et al., 2003) such as ectopic overexpression of galanin (Kokaia et al., 2001) attenuate seizures and related neuronal death in the hippocampus.

In conclusion, we observed that molecular changes described in the hippocampus in experimental models of epilepsy in rodents during seizure also occur in spontaneously epileptic dogs, an animal species sharing many similarities with human neurological diseases including epilepsy, which thus provides new insight into the therapeutic effort based on this experimental evidence.

4. Experimental procedures

4.1. *Animals and tissue samples*

In accordance with the Italian and Regional (Emilia-Romagna local government) regulation referring to animal safety and welfare, eleven dogs of various breeds and ages admitted for physical and neurological examination at the teaching Hospital of the Faculty of Veterinary Medicine of the University of Bologna were included in the study.

All the dogs underwent a complete physical and neurological examination. Diagnostic work-up included a complete cell count (CBC), serum biochemical profile, detection of RNA through reverse transcriptase-polymerase chain reaction for CDV in blood and, in selected cases, cerebrospinal fluid (CSF).

Depending on the presence/absence of seizures activity, the dogs were divided in two groups: group A ($n = 6$) included dogs with seizure activity and group B ($n = 5$) included dogs without seizures. See Table 1 for relevant clinical data. Due to poor general conditions, all the group A dogs, except one which died spontaneously, were subsequently euthanized at the owner's request and, immediately thereafter, subjected to complete necropsy and CNS sampling. Euthanasia was performed when the dogs were in status epilepticus and consisted of premedication with 15 μg/kg IV Medetomidine (Domitor®) followed by general anesthesia by means of IV injection of thiopental sodium (Pentothal®) 10 mg/kg and injection 70 mg/kg of embutamide (Tanax®).

Brain tissue sampling was carried out starting from human brain banking expertise (Riederer et al., 1995). The brain was removed 1–3 h postmortem, and parts of the left brain (parietal lobe of the cerebral cortex, hippocampus, dorsal paraflocculus of the cerebellum, hypothalamus and basal forebrain) were dissected and fixed in either 10% neutral-buffered formalin, to be processed to paraffin wax blocks, or in 4% w/v paraformaldehyde, 14% v/v picric acid saturated solution in 0.2 M Sorensen phosphate buffer pH 6.9, for 24 h and retained in Sorensen's buffer 0.1 M, pH 7.5 containing 5% of sucrose for histopathological and immunohistochemical examinations.

4.2. *RNA extraction and RT PCR for CDV*

For the detection of the viral nucleic acid, RNA was extracted from all tissue samples and blood using a commercial kit, Rneasy mini kit (Qiagen) according to the manufacturer's instructions. Reverse transcriptase-polymerase chain reaction (RT-PCR) was performed using a one-step RT PCR System (AB gene, Surrey, UK). Oligonucleotides used as specific primers were as follows: forward 5′-ATG TTT ATG ATC ACA GCG GT-3′, reverse 5′-ATT GGG TTG CAC CAC TTG

TC-3′, which amplify a 429-bp fragment of the phosphoprotein (P) gene (Barret et al., 1993) with the following cycling conditions: reverse transcription at 47 °C for 30 min and inactivation at 94 °C for 2 min, followed by 40 cycle at 94 °C for 30 s, 58 °C for 30 s and 72 °C for 45 s, with a final extension at 72 °C for 5 min after the last cycle. The PCR products were analyzed on a 2% ethidium bromide-stained agarose gel using Fluors Multimage (Biorad).

4.3. *Probe and in situ hybridization for CDV*

Viral riboprobe, of approximately 150 bases, was prepared as previously described (Zurbriggen et al., 1993). In situ hybridization was performed as described (Zurbriggen et al., 1993). Deparaffinized sections (4 μm) were rehydrated, washed with PBS and treated for 20 min with 0.2 M HCl. The samples were then incubated with proteinase K (5 μg/ml) in 1 M Tris–HCl (pH 8) and 0.1 M $CaCl_2$ for 15 min at 37 °C. Samples were then fixed with 4% paraformaldehyde in PBS, followed by prehybridization performed at 50 °C for 2 h in 50% formamide, 5× SSC, 10× Denhardt's and 100 μg/ml yeast RNA. Prehybridized sections were then hybridized at 50 °C overnight in a humid chamber with 50% formamide, 10× dextran sulfate, 5× SSC, 100 μg/ml yeast RNA and 1 μg labeled RNA probe/100 μl. After hybridization, excess labeled RNA was removed by successive washes with SSC and treatment with Rnase (Boehringer Mannheim). The detection system consisted of an anti-digoxigenin antibody conjugated with alkaline phosphatase diluted 1:200, and the substrates nitroblue tetrazoliumchloride (NBT) and 5-bromo-4-chloro-3-indolyl phosphate (BCIP) (Boehringer Mannheim Biochemica, Germany).

4.4. *Immunohistochemistry*

For virus detection, tissues collected from all the dogs were fixed in 10% buffered formalin and embedded in paraffin wax. Serial paraffin sections (4 μm) were cut, dewaxed, and rehydrated through graded alcohols. Endogenous peroxidase was quenched with 0.1% H_2O_2 diluted in phosphate-buffered saline (PBS; pH 7.4) for 30 min at RT. Antigens masked by formalin fixation were recovered by boiling the samples in 6 M urea in a microwave oven for 3 min and non-specific binding components were blocked with 5% goat serum for 30 min at RT. The sections were subsequently incubated with CDV nucleoprotein-specific monoclonal antibody D110 (kindly provided by Prof. A. Zurbriggen, Institute of Animal Neurology, University of Berne, Switzerland) for 2 h at 37 °C. The second incubation was performed using goat anti-mouse IgG diluted 1:40 for 30 min at RT followed by addition of a peroxidase–anti-peroxidase (PAP) complex. The antigen–antibody reaction was visualized by treating the samples with chromogen diaminobenzidine and hydrogen peroxidase for 10 min. Finally, the sections were rinsed in Tris-buffered saline (TBS; pH 7.6) and mounted with mounting medium.

For double-labeling analysis of virus in identified cells in the central nervous system and for hippocampus analysis, tissue samples were frozen in solid CO_2, cut in a cryostat (14-μm-thick sections) and processed for indirect immunofluorescence or TSA intensification techniques. Briefly, the sections were first hydrated in phosphate-buffered saline (PBS; 0.1 M) for 20 min at RT followed by incubation at 4 °C overnight in humid atmosphere with the primary antisera diluted in PBS/Triton 0.3%. The following primary antisera were used: mouse anti-CDV (Biodesign International, ME); rabbit anti-glial fibrillary acidic protein (56 kDa GFAP, cross-reactivity in bovine and rat; Eurodiagnostica, Bologna, Italy); rabbit anti-NG2 (chondroitin sulfate proteoglycan, truncated form, >280 NG2 protein; Chemicon International, Inc., Temecula, CA); rabbit anti-c-*fos* (c-Fos p62 of human origin, identical to corresponding mouse sequence; Santa Cruz Biotechnology, Santa Cruz, CA); anti-NFkB (amino terminal domain p65 human; Santa Cruz Biotecnology, Santa Cruz, CA); rabbit anti-brain-derived neurotrophic factor (BDNF, recombitant human; Santa Cruz Biotecnology, Santa Cruz, CA); anti-nerve growth factor (NGF, amino-terminus, mouse origin; Santa Cruz Biotechnology, Santa Cruz, CA); goat anti-neuronal glutamate transporter (EAAT3, corresponding to the amino acid 504–523 from the carboxy-terminus of the cloned rat EAAC1; Chemicon International, Inc., Temecula, CA); rabbit anti-met-enkephalin (ENK, Peninsula Laboratories, Inc); rabbit anti-galanin (porcine; Peninsula Laboratories, Inc., San Carlos, CA); and guinea pig anti-opioid receptor mu subtype (MOR1, synthetic peptide corresponding to the AA 384–398 from the carboxy-terminus cloned rat μ opioid receptor 1; Chemicon International, Inc., Temecula, CA). The sections were then rinsed in PBS, incubated for 30 min at 37 °C with secondary antibodies labeled with green or red fluorochrome (Jackson) diluted 1:75 in PBS/Triton 0.3%, rinsed again in PBS and finally mounted in glycerol and PBS (3:1, v/v) containing 1,4-phenylendiamine, 0.1 g/l. Species cross-reactivity of the antisera was evaluated by alignment analysis of the respective proteins (ClustalW and Bioedit softwares), obtaining homologies ranging from 96% to 64%. Staining specificity was assessed by in vitro overnight pre-incubation of the antiserum with the respective antigen (100 μg of antigen/ml diluted antiserum). This treatment prevented staining. For double experiments, two primary antisera raised in different animal species on the first days, and two appropriate secondary antisera conjugated with red and green fluorochromes on the second day, were applied concomitantly. Sections were then rinsed in PBS and mounted (as above).

TSA Plus intensification technique (Perkin Elmer Life Science, Boston, MA) was also used for both CDV detection and hippocampus analysis. All the antibodies used were pre-incubated with bovine serum albumin (BSA, Sigma) 0.1% in PBS at least for 1 h and then diluted in PBS/Triton 0.3% to reach the final dilution. The samples were rinsed in TNT buffer (0.1 M Tris–HCl, pH 7.5; 0.15 M NaCl; 0.3% Triton X-100) for 20 min at RT and blocked by treatment with TNB buffer (0.1 M Tris–HCl, pH 7.5; 0.15 M NaCl; 0.5% blocking reagent) for 30 min at RT. After blocking, the sections were incubated with horse-radish peroxidase (HRP)-labeled anti-rabbit immunoglobulins (Dako, Denmark) diluted 1:200 in TNB buffer for 30 min at RT. The samples were next rinsed in TNT buffer, incubated in fluorophore tyramide diluted in amplification diluent for 10 min, washed in TNT buffer and mounted as indicated.

4.5. *Microscopy, image analysis and figure preparation*

Preparations were then examined using a Nikon Microphot FXA microscope. Color slides were then loaded via a Nikon SuperCool Scan 4000. Some images were obtained through a Nikon Eclipse 600 microscope equipped with a DXM1200 digital camera. Sections were also analyzed using the laser scanning microscope Olympus FluoView 500, equipped with Ar (488nm) and HeNe-G (543nm) laser and appropriate filters. Single plane and multiplane scanning were used to assess cellular co-distribution. Final figures were generated using Adobe Photoshop 6.0 and Adobe Illustrator 9.2 software. Immunostaining quantification was performed by computerized procedure of microdensitometry using the ImageProPlus software (MEDIA CYBERNETICS, Ma, USA). Briefly, immunostaining for each antigen was evaluated by measuring grey level in 10 different fields in 5 section of the positive area of the hippocampus. The background value, as measured as grey level in adjacent non-immunoreactive area, was subtracted to each value. Statistical analysis was performed by one-way ANOVA and Dunnett's post hoc test.

Acknowledgments

The technical assistance of Nadia De Sordi is gratefully acknowledged. This work was supported by Fondazione Carisbo, Bologna, Italy, and Pathophysiology Center for the Nervous System, Hesperia Hospital, Modena, Italy.

REFERENCES

Alreja, M., Shanabrough, M., Liu, W., Leranth, C., 2000. Opioids suppress IPSCs in neurons of the rat medial septum/diagonal band of Broca: involvement of mu-opioid receptors and septohippocampal GABAergic neurons. J. Neurosci. 20, 1179–1189.

Binder, D.K., Croll, S.D., Gall, C.M., Scharfman, H.E., 2001. BDNF and epilepsy: too much of a good thing? TRENDS Neurosci 24, 47–53.

Calzà, L., Giardino, L., Ceccatelli, S., Hokfelt, T., 1996. Neurotrophins and their receptors in the adult hypo- and hyperthyroid rat after kainic acid injection: an in situ hybridization study. Eur. J. Neurosci. 8, 1873–1881.

Chang, B.S., Lowenstein, D.H., 2003. Epilepsy. New Engl. J Med. 349, 1257–1266.

Cotman, C.W., Head, E., Muggenburg, B.A., Zicker, S., Milgram, N.W., 2002. Brain aging in the canine: a diet enriched in antioxidants reduces cognitive dysfunction. Neurobiol. Aging 23, 809–818.

Crino, P.B., Jin, H., Shumate, M.D., Robinson, M.B., Coulter, D.A., Brooks-Kayal, A.R., 2002. Increased expression of the neuronal glutamate transporter (EAAT3/EAAC1) in hippocampal and neocortical epilepsy. Epilepsia 43, 211–218.

Cummings, B.J., Head, E., Ruehl, W., Milgram, N.W., Cotman, C.W., 1996. The canine as an animal model of human aging and dementia. Neurobiol. Aging 17, 259–268.

Dimakopoulos, A.C., Mayer, R.J., 2003. Aspects of neurodegeneration in the canine brain. J. Nutr. 132, 1579S–1582S.

Dragunow, M., Peterson, M.R., Robertson, H.A., 1987. Presence of c-*fos*-like immunoreactivity in the adult rat brain. Eur. J. Pharmacol. 135, 113–114.

Drake, C.T., Milner, T.A., 1999. Mu opioid receptors are in somatodendritic and axonal compartments of GABAergic neurons in rat hippocampal formation. Brain Res. 849, 203–215.

Gall, C., 1988. Seizures induce dramatic and distinctly different changes in enkephalin, dynorphin, and CCK immunoreactivities in mouse hippocampal mossy fibers. J. Neurosci. 8, 1852–1862.

Gall, C., 1992. Regulation of brain neurotrophin expression by physiological activity. TiPS 13, 401–403.

Gall, C.M., 1993. Seizure-induced changes in neurotrophin expression: implications for epilepsy. Exp. Neurol. 124, 150–166.

Gall, C., Lauterborn, J., Isackson, P., White, J., 1990. Seizures, neuropeptide regulation, and mRNA expression in the hippocampus. Prog. Brain Res. 83, 371–390.

Goetz, 2003. Textobook of Clinical Neurology, Sauders

Haberman, R.P., Samulski, R.J., McCown, T.J., 2003. Attenuation of seizures and neuronal death by adeno-associated virus vector galanin expression and secretion. Nat. Med. 9, 1076–1080.

Hartmann, M., Heumann, R., Lessmann, V., 2001. Synaptic secretion of BDNF after high-frequency stimulation of glutamatergic synapses. EMBO J. 20, 5887–5897.

Hasegawa, D., Orima, H., Fujita, M., Nakamura, S., Takahashi, K., Ohkubo, S., Igarashi, H., Hashizume, K., 2003. Diffusion-weighted imaging in kainic acid-induced complex partial status epilepticus in dogs. Brain Res. 983, 115–127.

Head, E., Torp, R., 2002. Insights into Aβ and presenilin from a canine model of human brain aging. Neurobiol. Disease 9, 1–10.

Head, E., Thornton, P.L., Tong, L., Cotman, C.W., 2000. Initiation and propagation of molecular cascades in human brain aging: insight from the canine model to promote successful aging. Prog. Neuro-Psychopharmacol. Biol. Psychiat. 24, 777–786.

Hodge, M.J., Wolfson, C., 1997. Canine distemper virus and multiple sclerosis. Neurology. 49 (2 Suppl 2), S62–S69.

Hughes, P., Dragunow, M., 1995. Induction of immediate–early genes and the control of neurotransmitter-regulated gene expression within the nervous system. Pharmac. Rev. 47, 133–178.

Hughes, P.E., Alexi, T., Walton, M., Williams, C.E., Dragunow, M., Clark, R.G., Gluckman, P.D., 1999. Activity and injury-dependent expression of inducible transcription factors, growth factors and apoptosis-related genes within the central nervous system. Prog. Neurobiol. 57, 421–450.

Jankowsky, J.L., Patterson, P.H., 2001. The role of cytokines and growth factors in seizures and their sequelae. Prog. Neurobiol. 63, 125–149.

Koestner, A., 1989. Neuropathology of canine epilepsy. Probl Vet Med. 1, 516–534.

Kokaia, M., Holmerg, K., Nanobashvili, A., Xu, Z.Q., Kokaia, Z., Lendahl, U., Hilke, S., Theodorsson, E., Kahl, U., Bartfai, T., Lindvall, O., Hokfelt, T., 2001. Suppressed kindling epileptogenesis in mice with ectopic overexpression of galanin. Proc. Natl. Acad. Sci. USA 98, 14006–14011.

Koutinas, A.F., Polizopoulou, Z.S., Baumgaertner, W., Lekkas, S., Kontos, V., 2002. Relation of clinical signs to pathological changes in 19 cases of canine distemper encephalomyelitis. J. Comp. Pathol. 126, 47–56.

Lin, E.J., Richichi, C., Young, D., Baer, K., Vezzani, A., During, M.J., 2003. Recombinant AAV-mediated expression of galanin in rat hippocampus suppresses seizure development. Eur. J. Neurosci. 18, 2087–2092.

Loscher, W., 1997. Animal models of intractable epilepsy. Prog. Neurobiol. 53, 239–258.

Mathern, G.W., Mendoza, D., Lozada, A., Pretorius, J.K., Dehnes, Y., Danbolt, N.C., Nelson, N., Leite, J.P., Chimelli, L., Born, D.E.,

Sakamoto, A.C., Assirati, J.A., Fried, I., Peacock, W.J., Ojemann, G.A., Adelson, P.D., 1999. Hippocampal GABA and glutamate transporter immunoreactivity in patients with temporal lobe epilepsy. Neurol. 52, 453–472.

Mattson, M.P., Camandola, S., 2001. NF-kB in neuronal plasticity and neurodegenerative disorders. J. Clin. Invest. 107, 247–254.

Mazarati, A.M., Liu, H., Soomets, U., Sankar, R., Shin, D., Katsumori, H., Langel, U., Wasterlain, C.G., 1998. Galanin modulation of seizures and seizure modulation of hippocampal galanin in animal models of status epilepticus. J. Neurosci. 18, 10070–10077.

Mazarati, A.M., Hohmann, J.C., Bacon, A., Liu, H., Sankar, R., Steiner, R.A., Wynick, D., Wasterlain, C.G., 2000. Modulation of hippocampal excitability and seizures by galanin. J. Neurosci. 20, 6276–6281.

Mazarati, A.M., Langel, U., Bartfai, T., 2001. Galanin: an endogenous anticonvulsant? Neuroscientist 7, 506–517.

McCormick, D.A., Contreras, D., 2001. On the cellular and network bases of epileptic seizures. Annu. Rev. Physiol. 63, 815–846.

McQuiston, A.R., Saggau, P., 2003. Mu-opioid receptors facilitate the propagation of excitatory activity in rat hippocampal area CA1 by disinhibition of all anatomical layers. J. Neurophysiol. 90, 1936–1948.

Milgram, N.W., Head, E., Muggenburg, B., Holowachuk, D., Murphey, H., Estrada, J., Ikeda-Douglas, C.J., Zicker, S.C., Cotman, C.W., 2002. Landmark discrimination learning in the dog: effects of age, antioxidant fortified food, and cognitive strategy. Neurosci. Biobehav. Rev. 26, 679–695.

Morimoto, K., Fahnestock, M., Racine, R.J., 2004. Kindling and status epilepticus models of epilepsy: rewiring the brain. Prog. Neurobiol. 73, 1–60.

Riederer, P., Gsell, W., Calzà, L., Franzek, E., Jungkunz, G., Jellinger, K., Reynolds, G.P., Crow, T., Cruz-Sanchez, F.F., Beckmann, H., 1995. Consensus on minimal criteria of clinical and neuropathological diagnosis of schizophrenia and affective disorders for post mortem research. Report from the European Dementia and Schizophrenia Network (BIOMED I). J. Neural Transmission, General Sec. 102, 255–264.

Rogawski, M.A., Loscher, W., 2004. The neurobiology of antiepileptic drugs. Nat. Rev. 5, 553–564.

Rong, Y., Baudry, M., 1996. Seizure activity results in a rapid induction of nuclear factor-kappa B in adult but not juvenile rat limbic structures. J. Neurochem. 67, 662–668.

Sandvig, A., Berry, M., Barrett, L.B., Butt, A., Logan, A., 2004. Myelin-, reactive glia-, and scar-derived CNS axon growth inhibitors: expression, receptor signaling, and correlation with axon regeneration. Glia 46, 225–251.

Schobesberger, M., Zurbriggen, A., Summerfield, A., Vandevelde, M., Griot, C., 1999. Oligodendroglial degeneration in distemper: apoptosis or necrosis? Acta Neuropathol 97, 279–287.

Schobesberger, M., Zurbriggen, A., Doherr, M.G., 2002. Demyelination precedes oligodendrocyte loss in canine distemper virus-induced encephalitis. Acta Neuropathol. 103, 11–19.

Stallcup, W.B., 2002. The NG2 proteoglycan: past insights and future prospects, 2002. J Neurocytol. 31, 423–435.

Stein, V.M., Czub, M., Schreiner, N., Moore, P.F., Vandevelde, M., Zurbriggen, A., Tipold, A., 2004. Microglial cell activation in demyelinating canine distemper lesions. J. Neuroimmunol. 153, 122–131.

Stumm, R.K., Zhou, C., Schulz, S., Hollt, V., 2004. Neuronal types expressing μ- and δ-opioid receptor mRNA in the rat hippocampal formation. J. Comp. Neurol. 469, 107–118.

Switonski, M., Szczerbal, I., Nowacka, J., 2004. The dog genome map and its use in mammalian comparative genomics. J. Appl. Genet. 45, 195–214.

Tanaka, K., Watase, K., Manabe, T., Yamada, K., Watanabe, M., Takahashi, K., Iwama, H., Nishikawa, T., Ichihara, N., Kikuchi, T., Okuyama, S., Kawashima, N., Hori, S., Takimoto, M., Wada, K., 1997. Epilepsy and exacerbation of brain injury in mice lacking the glutamate transporter GLT-1. Science 276, 1699–16702.

Tongiorgi, E., Armellin, M., Giulianini, P.G., Bregola, G., Zucchini, S., Paradiso, B., Steward, O., Cattaneo, A., Simonato, M., 2004. Brain-derived neurotrophic factor mRNA and protein are targeted to discrete dendritic laminas by events that trigger epileptogenesis. J. Neurosci. 24, 6842–6852.

Vandevelde, M., Zurbriggen, A., 1995. The neurobiology of canine distemper virus infection. Vet. Microbiol. 44, 271–280.

Vezzani, A., Granata, T., 2005. Brain Inflammation in Epilepsy: Experimental and Clinical Evidence. Epilepsia 46 (Issue 11), 1724.

Won, S.J., Ko, H.W., Kim, E.Y., Park, E.C., Huh, K., Jung, N.P., Choi, I., Oh, Y.K., Shin, H.C., Gwag, B.J., 1999. Nuclear factor kappa B-mediated kainate neurotoxicity in the rat and hamster hippocampus. Neuroscience 94, 83–91.

Zurbriggen, A., Muller, C., Vandevelde, M., 1993. In situ hybridisation of virulent canine distemper virus in brain tissue, using digoxigenin-labeled probes. Am. J. Vet. Res. 54, 1457–1461.

Zurbriggen, A., Schmid, I., Graber, H.U., Vandevelde, M., 1998. Oligodendroglial pathology in canine distemper. Acta Neuropathol. 95, 71–77.

Hippocampus

In Vitro Assay for Neurogenesis and Gliogenesis in Adult Human Dentate Gyrus

Journal:	*Hippocampus*
Manuscript ID:	HIPO-07-039
Wiley - Manuscript type:	Research Article
Keywords:	Adult human stem cells, neuroprecursor cells, neurogenesis, dentate gyrus, temporal lobe epilepsy

In Vitro Assay for Neurogenesis and Gliogenesis in Adult Human Dentate Gyrus

Michela Paradisi*, Mercedes Fernández*, Sandra Sivilia*, GianLuca Marucci°, Marco Giulioni#, Eugenio Pozzati#, Mino Zucchelli#, Fabio Calbucci#, Tiziana Antonelli§, Luciana Giardino*, Laura Calzà*

*Animal Stem Cell Laboratory, DIMORFIPA, University of Bologna; °Section of Pathology, Dep. Oncology, Bellaria Hospital, University of Bologna;
§Section of Pharmacol., Dep. Experim. Clin. Med., University of Ferrara;
#Neuroscience Dep., Neurosurgery Section, Bellaria Hospital, Bologna

* *these authors equally contributed to the study*

running title*: *Neurogenesis in human hippocampus

number:

- ***text pages 16***
- ***figures 5***
- ***tables 2***

Grant Sponsor Regione Emilia-Romagna (Assessorato Attività Produttive, PRRIITT Projects, L.C.), IRET Foundation, Ozzano Emilia, Bologna, L.G., L.C., Fondazione CARISBO, Bologna, E.P.

Grant Number 3

.

Correspondence:

Laura Calzà, MD
ASC-Lab, DIMORFIPA, University of Bologna
Via Tolara di Sopra 50
40064 Ozzano Emilia (Bologna)
Italy
Phone +39 051 2097947
Fax +39 051 2097953
Email **laura.calza@unibo.it**

ABSTRACT

Adult neurogenesis is the process by which new neurons are created in the mature central nervous system (CNS). This phenomenon has been shown to occur in particular in two neurogenic areas of the brain i.e. the subventricular zone (SVZ) and the dentate gyrus (DG) of the hippocampal formation, in a wide variety of species including humans. We have studied the neurogenesis in the DG of adult patients subjected to antero-mesial temporal resection due to pharmacoresistant temporal lobe epilepsy (TLE) by using the in vitro neurosphere assay approach. Presurgical duration of epilepsy was from 20 to 33 years. Histological examination evidenced hippocampal sclerosis (HS) in all the cases studied, observing granule cells dispersion in the DG or an architectural type of cortical dysplasia in the patients used for these studies. Herein we demonstrate that neural cells with characteristics of stem/precursor cells can be derived from the DG of adult chronic epileptic pharmacoresistant patients. Neuro precursor cells (NPCs) in vitro proliferated in the presence of mitogens (EGF, bFGF), forming clusters or neurospheres that grew with the days in culture. The proliferation rate was higher when both mitogens were included in the medium of culture. When mitogens were removed from the medium, cells spontaneously differentiated giving rise to all three neuronal cell phenotypes, neurons (musashi-1-, doublecortin-, β-tubulin-immunoreactive cells), astrocytes (vimentin-, GFAP-immunoreactive cells) and oligodendrocytes (RIP-, CNPase-immunoreactive cells). From these results we can hypothesize that neurogenesis can persist in patients with chronic epilepsy which present HS and in some cases also febrile seizure (FS). *

** part of the data were presented at the 7th European Congress on Epileptology and published as abstract in Epilepsia, 47(S3):1-271, 2006, p263*

Keywords: **Adult human stem cells, neuroprecursor cells, neurogenesis, dentate gyrus, temporal lobe epilepsy**

Introduction.

It is well established that neurogenesis occurs in two main areas of the adult mammalian brain, i.e. the dentate gyrus (DG) of the hippocampus and the subventricular zone (SVZ) (Shivraj Sohur et al., 2006). Neurogenesis in adult involves cell proliferation, migration and differentiation. This process can lead to the integration of new neurons into existing circuits keeping a controlled number of neurons also thanks to a controlled apoptotic rate (Panchision and McKay, 2002). Proliferation and integration of new neurons into the adult tissue is highly dependent upon environment and systemic factors such as age, hormones, pharmacological treatments, systemic and neurological diseases like ischemia, neurodegenerative disorders, epilepsy and depression (Mackowiak et al., 2004).

Multipotent, self renewing neural precursor cells (NPCs) can be derived from the SVZ and the DG, cultured and expanded in vitro. Upon appropriate conditions, these NPCs differentiate into the three main cell types which compose the central nervous system (CNS), neurons, astrocytes and oligodendrocytes (Reynolds and Weiss, 1992; Johansson et al., 1999a; Rietze et al., 2001; Doetsch, 2003; Hack et al., 2004). Moreover, when appropriately stimulated, these cells can also generate non-neural lineage, thus showing stem cell-like properties (Greco and Recht, 2003; Mondal et al., 2004). According to this, cells isolated from the SVZ and from the DG are also named “neural stem cells” (NSCs). Thanks to these studies, mainly including mouse and rat-derived NPCs, an increasing number of molecular signals either genetically or epigenetically regulated have being proved to be involved in the fate of neural stem cells opening new perspectives also for cell therapy (Bazan et al., 2004; Emsley et al., 2005).

In spite of the extensive literature on murine neural stem cells, little is known about neurogenesis in the human brain and very few studies demonstrated the isolation of NPCs from the SVZ (Kirschenbaum et al., 1994; Eriksson et al., 1998; Nunes et al., 2003; Westerlund et al., 2003; Moe et al., 2005) or the DG of the hippocampus (Johansson et al., 1999b; Kukekov et al., 1999; Arsenijevic et al., 2001) in adult human brain.

In this study, we derived NPCs from the DG of patients affected of pharmacoresistant epilepsy which were subjected to mesial TLE, by using the well established neurosphere assay (Gage et al., 1995; Campos, 2004; Fernandez et al., 2006). By this approach we set the optimal conditions to make NPCs proliferate and studied spontaneous lineage of generated cells after differentiation by immunocytochemistry.

Material and Methods.

Patients.

Dentate gyrus neurogenesis was studied in four patients which clinical diagnosis was pharmacoresistant TLE. Presurgical duration of epilepsy was 33, 30, 20 and 25 years and the age at surgery was 39, 41, 32 and 27 years, respectively. Two of the patients were right sided and the other two were left sided. Two were males, the other two were females. All the patients studied presented hippocampal sclerosis (HS) and a remarkable history of febrile seizures (FS) was present in cases 1, 3 and 4. Clinical data of patients included in the study are reported in Table I. Informed written consent was obtained from each patient. After surgery, the tissue sample including the DG of the hippocampus was divided for histopathology and tissue culture for neurospheres generation.

Pathological material and methods.

After surgery, a fresh tissue sample including the DG of the hippocampus was used for culture, in order to obtain neurospheres. The remaining tissue was fixed in 10% buffered formalin and paraffin embedded for routine histological diagnosis. Blocks were serially cut and stained with hematoxylin, eosin and Kluver. For immunohistochemistry we used the ABC approach. An epitope retrieval method was employed as follows. Sections were first steamed in citrate buffer for 5 min, then cooled for another 5 min and finally immunostained with anti-GFAP (Dako, clone 6F2, dilution 1:1200) and anti NeuN (Chemicon, clone NeuN, dilution 1:500) antisera.

Hippocampal sclerosis was evaluated according to well established criteria (GM-1). The presence of cortical dysplasia was investigated and classified following the scheme proposed by Palmini et al. (2004) (GM-2).

Neurosphere Generation and Proliferation.

The protocol herein used is based on well established procedures for animal tissue samples (Fernández et al., 2004, 2006) with some modifications. The main steps of the procedure are illustrated in Fig 1. Tissue samples collected from the DG of the hippocampus were brought to the clean lab in ice-cold HBSS (Hanks Balanced Salt Solution -Invitrogen-), 100U-100 g/mL of penicillin-streptomycin (Sigma) solution and processed within one hour after surgery. Tissue was then incubated with a solution of trypsin (1,3 mg/mL - Sigma-) and hyaluronidase (0,7 mg/mL - Sigma-) in HBSS / 5,4 mg/mL D-glucose (Sigma) / 15 mM HEPES (Invitrogen), at 37° for 45 min, then treated with DNase (1000 U -Sigma-) in order to digest DNA. The obtained suspension was filtered through a nylon mesh filter (70 m -Falcon-) and washed with a solution consisting on 40

mg/mL BSA (Sigma), 20 mM HEPES, 1x EBSS (Earle's Balanced Salt Solution -Invitrogen-) and centrifuged at 1500 rpm for 5 min. The pellet was then washed with a 0,5x HBSS / 0,3 mg/mL sucrose (Merk) solution in order to remove myelin fragments. Cell pellet was resuspended in serum-free culture medium, DMEM:F12 GlutaMAX I (Invitrogen) supplemented with 8mM HEPES, 2% B27 (Invitrogen), 0,5% N2 (Invitrogen) and 100U-100 g/mL of penicillin-streptomycin. Obtained cells were counted and plated at a density of 2,4 x 10^4 cell/cm^2. Mitogens, EGF (epidermal growth factor) (20ng/mL) and bFGF (basic fibroblast growth factor) (10ng/mL), were added every 48 hours and half of the medium was changed once a week, observing the formation of cell aggregates within the first week. The number and the size of the forming neuroshperes were assessed along the days in culture by counting and photographing them at 3, 6, 16 and 22 DIVs (days in vitro) and using generated images for the analysis of their mean diameter with the Image-Pro Plus software (Media Cybernetics, MD, USA). Both parameters, number and size of formed neurospheres, have been considered in order to calculate the proliferation rate by the formula:

Proliferation Rate = mean diameter x n°neurospheres

Neurospheres were splitted after 22-28 days in culture and obtained cells were plated onto poly-L-lysine (50 g/mL -Sigma-) coated coverslips. The cells were cultured in the same medium without the addition of mitogens and maintained in these conditions for 12 days in order to let them to spontaneously differentiate.

Immunocytochemistry.

For the immunocytochemical procedure differentiated cells after 12 days in vitro were fixed with 4% paraformaldehyde in phosphate buffer (0,1 M) for 20 min at room temperature (RT), washed with PBS and incubated with blocking solution (PBS / 0,3% Triton / 2% BSA / 1% of the normal serum in which secondary antibodies used had been prepared) for 1 hour at RT, incubating then primary antibodies overnight at 4°C. The description of primary antibodies used in this study has been included in Table II. After washing with PBS, cells were incubated with secondary antibodies (Cy2- conjugated AffiniPure Donkey anti-Rabbit IgG (H+L), Cy2- conjugated AffiniPure Donkey anti-Mouse IgG (H+L), Cy2- conjugated AffiniPure Donkey anti-Goat IgG (H+L) -Jackson Immunoresearch West Grove PA, USA-) diluted in PBS / 0,3% Triton, for 30 min at 37°C. For nuclear staining, cells were washed with PBS and incubated with a solution of 1 g/mL Hoechst 33258 in PBS / 0,2% Triton for 20 min at RT, washed again with PBS and finally mounted in phenylendiamine solution (0.1% 1,4-phenylendiamine -Sigma-, 50% glycerine -Sigma-, carbonate/bicarbonate buffer pH 9,2). Neurospheres were observed and photographed by an

inverted Olympus IX70 microscope and phase contrast filter equipped with a digital photocamera Camedia C-5060. For the analysis of fluorescent stained cells we used the microscope Olympus Provis IX70 supplied with F-View II camera and Cell^ Imaging Software (Münster, Germany), equipped with the following filters: WG2 (ex 510-550nm, DM 570, emission 590nm), NU2 (ex 360-370nm, DM 400, emission 420nm), NIBA2 (ex 470-490, DM 505, emission 510-550nm).

Statistical Analyis.

Prism software (GraphPad Software, San Diego, CA, USA) was used for graphs preparation and statistical analyses which were carried out by using one-way ANOVA and Tukey's post hoc test to compare the different experimental groups. Results were considered significant when the probability of their occurrence from chance alone was less than 5%.

Results.

We studied the neurogenesis in the DG of four patients who underwent to tailored anterior-mesial temporal resection for pharmacoresistant TLE. The main features of clinical history are reported in Table I. Neurophysiological non-invasive pre-surgical studies (interictal electroencephalogram - EEG- and ictal video-EEG recording) were carried out in all cases. Magnetic Resonance Imaging (MRI) showed hippocampal sclerosis (Fig. 1A), associated with suspect of polar cortical dysplasia in all cases. According to the anatomo-electro-clinical data obtained by neurophysiological study and MRI, these patients were submitted to tailored antero-mesial temporal resection with amygdalo-hippocampectomy. The post-operative course was uneventful.

Histological examination evidenced hippocampal sclerosis in all the four cases (Honavar and Meldrum, 1997). Hippocampal sclerosis is characterized by neuronal loss in the CA1, CA3 and CA4 (endfolium) subfields of the hippocampus, as showed by NeuN-immunostaining (Fig. 2A), accompanied by fibrillary gliosis. In case 4 a significant granule cells dispersion in the DG was present (Fig. 2B). Furthermore in cases 1 and 3 microscopic study showed an architectural type cortical dysplasia in the temporal lobe specimen.

After tissue disaggregation and culture in the described condition, cell clusters or neurospheres started to be observed by the first week, progressively increasing their size with the days in culture. We first studied different mitogen culture conditions as i) no mitogens, ii) bFGF alone (10ng/ml) or iii) EGF (20 ng/ml)+bFGF (10ng/ml). We found that the presence of both mitogens (EGF+bFGF) in the culture medium favours the formation of neurospheres, as the diameter analysis and the proliferation rate have demonstrated. Fig. 3 shows pictures of

neurospheres at 22 DIV in the conditions above described, no mitogens (A), bFGF (B) and EGF+bFGF (C). At this time (22 DIV) the neurospheres grown in the presence of EGF and bFGF (20 and 10 ng/ml, respectively) are bigger in size comparing with no mitogens- or bFGF-neurospheres, showing also a higher proliferation rate (Fig. 4E). In the base of these results, cells were routinely cultured in the presence of both mitogens in order to help along proliferation. The proliferation rate of cells along the days in vitro, 3, 6, 16 and 22 DIV, has been calculated considering both, the mean diameter value and the number of neurospheres generated at these different time points. Fig. 4, panels A, B, C and D, shows neurospheres at 3, 6, 16 and 22 DIVs, respectively. In the graph (Fig. 4E) the proliferation rate of cells at these different times in culture have been represented. Even though cell aggregates could be observed after some days in culture, the most of the neurospheres were generated between the second and the third week of culture (Fig. 4E).

After neurosphere splitting, single cells were cultured onto glass coated substrates in order to favour their attachment to the surface and let them to spontaneously differentiate for 12 days. At this time cells presented a differentiated morphology, the most of them resembling to neuronal, astroglial and oligodendroglial phenotypes, what was then confirmed by immunocytochemistry. We used antibodies against antigens recognized as markers for undifferentiated precursors, neuroblasts, neurons, astrocytes and oligodendrocytes. Fig 5 shows immunoreactive cells for Musashi (proliferating multipotent neural precursors A), doublecortin (neuronal progenitors B) vimentin (immature astroglia C, G, H), beta-tubulin-Tuj1 (differentiating neurons E, F), GFAP (-glial fibrillary acidic protein-, mature astrocytes J-M), CNPase (-2',3'-cyclic nucleotide 3'-phosphohydrolase-, mature oligodendrocytes O,P) and “Rip” (immature oligodendrocytes Q). Most of the cells express Musashi-immunoreactivity, however doublecortin-IR cells showing branched elongations are also present at this early differentiation time. A high number of cells are beta-tubulin-Tuj1-immunoreactive (IR) (see E compared to D for nuclear staining of the same field), showing these immunoreactive cells bipolar morphology (F), whereas vimentin-IR cells possess thin elongations dividing into finer branching (G, H). Many multipolar cells also express GFAP-IR which morphology resembles to fibrous astrocytes (K-M). Finally, some cells express markers associated to oligodendrocyte lineage, such as “Rip” (Q) and CNPase (O, P). The morphology of these cells, i.e. short and richly branched processes, is also suggestive for oligodendrocytes.

Discussion.

In this paper we demonstrated that NPCs might be derived from human hippocampus after a long story of neurological diseases leading to a diffuse hippocampus sclerosis involving the neurogenic area of the DG. Cells from this damaged area slowly proliferate in vitro in the presence of mitogens, in most of the cases generating neurospheres, and are able to spontaneously differentiate into neurons, astrocytes and oligodendrocytes after mitogen withdrawal, thus exhibing all the main characteristics of NPCs, as have been described in rat and mouse species.

Some authors have performed in vivo studies in the DG of hippocampal tissue from patients affected of TLE, using for that a high number of samples (Crespel et al., 2005; Fahrner et al., 2006). However, to our knowledge, only few ex-vivo studies succeeded in isolating NPCs from adult human hippocampus using the neurosphere in vitro assay. NPCs cultured in suspension in serum-free medium forms aggregates, which are composed of stem cells, progenitor cells and also more differentiated cells (Bez et al., 2003). This mixed cell population system has been well characterized and have been proved to be a valuable method to expand neural precursors (Wang et al., 2006) and to identify stem cells also in view of clonal selection (Suslov et al., 2002). Our protocol to isolate proliferating cells from the human brain provided results consistent with the other published papers using the same techniques (Roy et al., 2000; Arsenijevic et al., 2001). From all analysed samples, i.e. pieces of the hippocampus DG, we obtained cells able to proliferate and to expand in the presence of mitogens (EGF and/or bFGF). In our conditions, neurospheres presented a higher proliferation rate (mean diameter x n° neurospheres) when cells were culture in the presence of both mitogens, so that we can argue that our cultures are EGF- and bFGF-responsive NPCs. However we observed that the growth/proliferation of cells in the cultures was not synchronized. As has been previously proposed the size of formed neurospheres might reflect the responsiveness to growth factors and other culture conditions of the stem/progenitor cells that compose cell aggregates (Suslov et al., 2002). Culture of neurospheres is a mixed population of stem/precursor cells differing lag times (time for a cell to reach the specific maximum growth rate) prior to the initiation of cluster formation. This could explain the fact that not all the cell clusters possess the same size at a specific day of the culture and that not all the cells present the same grade of maturation after the same period in culture under spontaneously differentiating conditions. When allowed to differentiate after mitogens withdrawal, we obtained all cell types forming the mature CNS, i.e. neurons, astrocytes and oligodendrocytes. We used very stringent conditions for proliferation and differentiation of NPCs, such as serum-deprived medium and a short differentiation time, e.g. 12 days after mitogen withdrawal. These conditions favour the study of

intrinsic differentiation capability of these cells. Moreover, it should be also considered that tissue is derived from patients with a very long disease history and severe sclerosis.

For immunocytochemical characterization of cells derived from neurospheres after mitogens withdrawal, we used a wide panel of antisera (see Table II). The RNA-binding protein Musashi-l (Msi-1), in mammals is commonly considered a specific marker for stem/progenitor cells of neural origin, associated with maintenance and/or asymmetric cell division of neural progenitor cells (Kaneko et al., 2000; Maslov et al., 2004). In mammals, Msi-1 and Msi-2 have been identified in mice, but only Msi-1 is expressed in humans, predominantly in proliferating multipotent neural precursor cells that may give rise to neurons and/or glia (Sakakibara et al., 1996). The expression of m-Msi-1 is largely down-regulated with the successive progression of neurogenesis. Most of cells derived from our neurospheres express Msi-1 at day 12 after mitogen withdrawal, what constitutes evidence of differentiation at this early time studied. However, also neuroblasts, as defined by doublecortin expression, were found in our culture and differentiation conditions. Doublecortin is exclusively expressed in neuronal progenitor cells, which are committed to become granule cells (Brown et al., 2003). A discrete number of cells also express β-tubulin-Tuj1-immunoreactivity, what confirms the capability of our cells to evolve toward differentiated neurons (Katsetos et al., 2003). Astroglial cells were also found at different maturation stages as indicated by the presence of both vimentin- and GFAP-positive cells. Expression of intermediate filament proteins in astrocytes shows a sequential change: vimentin is initially expressed and later replaced by GFAP, both proteins being simultaneously expressed during the transition period (Pixley and De Vellis, 1984; Sancho-Tello et al. 1995). Finally, oligodendrocyte lineage is confirmed by the presence of early markers such as Rip, which is expressed by immature oligodendrocyte (Friedman et al., 1989; Song et al., 2002), and CNPase, an enzyme associated to myelin sheath formation (Reynolds and Wilkin, 1988; Reynolds et al., 1989), which denotes a later stage for oligodendrocyte maturation (Reynolds and Hardy, 1997; Levine et al., 2001). Conversely to what other authors have described (Crespel et al., 2005) we have instead obtained mature differentiated neural cells as confirmed by the presence of β-tubulin-, GFAP- and CNPase- immunoreactive cells after 12 days in culture from adult chronic pharmacoresistant epileptic patients. Morphological features of all derived cells are consistent with the immunostaining. Doublecortin-positive cells have triangle-shaped cell body, with long, finely branched neuritis which form elegant nets. β-tubulin-positive cells are bipolar cells with very long processes also showing varicosities. Morphology of GFAP-positive cells corresponds to protoplasmatic and fibrous astrocytes, whereas both immature (Rip-positive) and mature (CNPase-positive) cells are small, with numerous, short elongations.

We derived neurospheres from the DG of TLE patients, in which the histo-pathological analysis revealed a severe sclerosis. Most of the animal model based on acute epilepsy showed increased precursor proliferation and neurogenesis in the DG (Parent et al., 2006), whereas studies considering animal models for chronic TLE report a severe decline in dentate neurogenesis (Hattiangady et al., 2004). Studies performed on tissue sections derived from mesial TLE indicate an increase in the number of neural precursors, thus proliferation, in chronic epilepsy (Crespel et al., 2005). However, this progenitor proliferation is not followed by enhanced neurogenesis (Fahrner et al., 2006) as occurs in most epilepsy animal models (Parent et al., 2006). According to this, neurosphere assay seems to be a more sensitive approach to explore residual proliferation and differentiation capabilities in human tissue and could help us to study the mechanisms that control proliferation and differentiation in healthy and pathological adult brain.

The in vitro neurosphere derivation that we have herein used might provide a useful tool to study neurogenic potential, also to explore if the hypothesis that aberrant neurogenesis during development could be part of the pathophysiology of the mesial TLE. Further studies including a larger number of samples, possibly derived from different ages of the disease, are necessary to better characterize the stimulating factors that can induce cellular lineage and to investigate the role that a persistent post-natal neurogenesis may have in the development of an epileptic network and cortical dysplasia.

ACKNOLEDGEMENTS

Supported by Regione Emilia-Romagna (Assessorato Attività Produttive, PRRIITT Projects L.C.), IRET Foundation, Ozzano Emilia **,** Bologna, L.G., L.C., Fondazione CARISBO, Bologna, E.P.

REFERENCES

1. Arsenijevic Y, Villemure J-G, Brunet J-F, Bloch JJ, Déglon N, Kostic C, Zurn A, Aebischer P. 2001. Isolation of multipotent neural precursor residing in the cortex of the adult human brain. Exp Neurol 170:48-62.
2. Bazan E, Alonso FJ, Redondo C, Lopez-Toledano MA, Alfaro JM, Reimers D, Herranz AS, Paino CL, Serrano AB, Cobacho N, Caso E, Lobo MV. 2004. In vitro and in vivo characterization of neural stem cells. Histol Histopathol 19:1261-1275.
3. Bez A, Corsini E, Curti D, Biggiogera M, Colombo A, Nicosia RF, Pagano SF, Parati EA. 2003. Neurosphere and neurosphere-forming cells: morphological and ultrastructural characterization. Brain Res 993:18-29.
4. Brown JP, Couillard-Despres S, Cooper-Kuhn CM, Winkler J, Aigner L, Kuhn HG. 2003. Transient expression of doublecortin during adult neurogenesis. J Comp Neurol 467:1-10.
5. Campos LS. 2004. Neurospheres: insights into neural stem cell biology. J Neurosci Res 78:761-769.
6. Crespel A, Rigau V, Coubes P, Rousset MC, de Bock F, Okano H, Baldy-Moulinier M, Bockaert J, Lerner-Natoli M. 2005. Increased number of neural progenitors in human temporal lobe epilepsy. Neurobiol Disease 19:436-450.
7. Doetsch F. 2003. the glial identity of neural stem cells. Nat Neurosci 6:1127-1134.
8. Emsley JG, Mitchell BD, Kempermann G, Macklis JD. 2005. Adult neurogenesis and repair of the adult CNS with neural progenitors, precursors and stem cells. Prog Neurobiol 75:321-341.
9. Eriksson PS, Perfilieva E, Bjork-Eriksson T, Alborn AM, Nordborg C, Peterson DA, Gage FH. 1998. Neurogenesis in the adult human hippocampus. Nat Med 4:1313-1317.
10. Fahrner A, Kann G, Flubacher A, Heinrich C, Freiman TM, Zentner J, Frotscher M and Haas CA. 2006. Granulle cell dispersion is not accompanied by enhanced neurogenesis in temporal lobe epilepsy patients. Exp neurol in press.
11. Fernández M, Pirondi S, Manservigi M, Giardino L, Calzà L. 2004. Thyroid hormone participates in the regulation of neural stem cells and oligodendrocyte precursor cells in the central nervous system of adult rat. Eur J Neurosci 20: 2059-2070
12. Fernández M, Paradisi M, Giardino L and Calzà L. 2006. To know neural stem proprieties from diseased brains: a critical step for brain repair: In: Grier EV, editor. Neural Stem Cells Research. New York: Nova Sciences Publishers Inc. p 77-97.

13. Friedman B, Hockfield S, Black JA, Woodruff KA, Waxman SG. 1989. In situ demonstration of mature oligodendrocytes and their processes: an immunocytochemical study with a new monoclonal antibody, rip. Glia 2:380-90.
14. Gage FH, Ray J and Fisher LJ. 1995. Isolation, characterization, and use of stem cells from the CNS. Annu Rev Neurosci 18:159-192.
15. Giulioni M, Pozzati E, Zucchelli M, Bubboli G, Tinuper P, Marucci G, Paradisi M, Fernandez M, Giardino L, Calzà L, Tassinari CA, Calbucci F. Dentate gyrus neurogenesis in human temporal lobe epilepsy, 7th European Congress Epileptology, Helsinki July 2-6,2006. Epilepsy, in press.
16. Greco B, Recht L. 2003. Somatic plasticity of neural stem cells: fact or fancy? J Cell Biochem 88: 51-56.
17. Hack MA, Sugimori M, Lundberg C, Nakaafuku M, Gotz M. 2004. Regionalization and fate specification in neurospheres: the role of Olig2 and Pax6. Mol Cell Neurosci 25:664-678.
18. Hattiangady B, Rao MS, Shetty AK. 2004. Chronic temporal lobe epilepsy is associated with severely declined dentate neurogenesis in the adult hippocampus. Neurobiol Dis 17:473-490.
19. Honavar M, Meldrum BS. 1997. In: Graham DI, Lantos PL eds. Epilepsy in: Greenfield's Neuropathology. Sixth Edition, London, pg. 931-971.
20. Johansson CB, Momma S, Clarke DL, Risling M, Lendahl U, Frisén J. 1999a. Identification of a neural stem cell in the adult mammalian central nervous system. Cell 96:25-34.
21. Johansson CB, Svensson M, Wallstedt L, Janson AM, Frisén J. 1999b. Neural stem cells in the adult human brain. Exp Cell Res 253:733-736.
22. Kaneko Y, Sakakibara S, Imai T, Suzuki A, Nakamura Y, Sawamoto K, Ogawa Y, Toyama Y, Miyata T, Okano H, Musashi L. 2000. An evolutionally conserved marker for CNS progenitor cells including neural stem cells. Dev Neurosci 22: 139-153.
23. Katsetos CD, Herman MM, Mork SJ. 2003. Class III beta-tubulin in human development and cancer. Cell Motil Cytoskeleton 55: 77-96.
24. Kirschenbaum B, Nedergaard M, Preuss A, Barami K, Fraser RA, Goldman SA. 1994. In vitro neuronal production and differentiation by precursor cells derived from the adult human forebrain. Cereb Cortex 4:576-589.
25. Kukekov VG, Laywell ED, Suslov O, Davies K, Scheffler B, Thomas LB, O'Brien TF, Kusakabe M, Steindler DA. 1999. Multipotent stem/progenitor cells with similar properties arise from two neurogenic regions of adult human brain. Exp Neurol 156:333-344.
26. Levine JM, Reynolds R, Fawcett JW. 2001. The oligodendrocyte precursor cell in health and disease. Trends in Neurosci 24:39-47.

27. Mackowiak M, Chocyk A, Markowicz-Kula K, Wedzony K. 2004. Neurogenesis in the adult brain. Pol J Pharmacol 56:673-687.
28. Maslov AY, Barone TA, Plunkett RJ, Pruitt SC. 2004. Neural stem cell detection, characterization, and age-related changes in the subventricular zone of mice. J Neurosci 24:1726-1733.
29. Moe MC, Varghese M, Danilov AI, Westerlund U, Ramm-Pettersen J, Brundin L, Svensson M, Berg-Johnsen J, Langmoen IA. 2005. Multipotent progenitor cells from the adult human brain: neurophysiological differentiation to mature neurons. Brain 128:2189-2199.
30. Mondal D, Pradhan L, LaRussa VF. 2004. Signal transduction pathways involved in the lineage-differentiation of NSCs: can the knowledge gained from blood be used in the brain? Cancer Invest 22:925-943.
31. Nunes MC, Roy NS, Keyoung HM, Goodman RR, McKhann G, Jiang L, Kang J, Nedergaard M, Goldman SA. 2003. Identification and isolation of multipotential neural progenitor cells from the subcortical white matter of the adult human brain. Nat Med 9:439-447.
32. Palmini A, Najm I, Avanzino G, Babb T, Guerrini R, Foldvary-Schaefer N, Jackson G, Lüders HO, Prayson R, Spreafico R, Vinters HV. 2004. Terminology and classification of the cortical dysplasias. Neurology 62 (Suppl 3):S2-S8.
33. Panchision DM, McKay RD. 2002. The control of neural stem cells by morphogenic signals. Curr Opin Genet Dev 12:478-487.
34. Parent JM, Elliot RC, Pleasure SJ, Barbaro NM, Lowenstein DH. 2006. Aberrant seizure-induced neurogenesis in experimental temporal lobe epilepsy. Ann Neurol 58:600-606.
35. Pixley SK, De Vellis J. 1984. Transition between radial glia and mature astrocytes studied with a monoclonal antibody to vimentin. Brain Res 5:201-209.
36. Reynolds R, Hardy R. 1997. Oligodendroglial progenitors labeled with the O4 antibody persist in the adult rat cerebral cortex in vivo. J Neurosci Research 47:455-470.
37. Reynolds R, Wilkin GP. 1988. Development of macroglial cells in rat cerebellum. II. An in situ immunohistochemical study of oligodendroglial lineage from precursor to mature myelinatin cell. Development 102:409-425.
38. Reynolds BA, Weiss S. 1992. Generation of neurons and astrocytes from isolated cells of the adult mammalian nervous system. Science 255:1707-1710.
39. Reynolds R, Carey EM, Herschkowitz N. 1989. Immunohistochemical localization of myelin basic protein and 2',3'-cyclic nucleotide 3'-phosphohydrolase in flattened membrane expansions produced by cultured oligodendrocytes. Neuroscience 28:181-188.

40. Rietze RL, Valcanis H, Brooker GF, Thomas T, Voss AK, Bartlett PF. 2001. Purification of a pluripotent neural stem cell from the adult mouse brain. Nature 412:736-739.
41. Roy NS, Wang S, Jiang L, Kang J, Benraiss A, Harrison-Restelli C, Fraser RAR, Couldwell WT, Kawaguchi A, Okano H, Nedergaard M, Goldman SA. 2000. In vitro neurogenesis by progenitor cells isolated from the adult human hippocampus. Nature 6:271-277.
42. Sakakibara S, Imai T, Hamaguchi K, Okabe M, Aruga J, Nakajima K, Yasutomi D, Nagata T, Kurihara Y, Uesugi S, Miyata T, Ogawa M, Mikoshiba K, Okano H. 1996. Mouse-Musashi-1, a neural RNA-binding protein highly enriched in the mammalian CNS stem cell. Dev Biol 176:230-242.
43. Sancho-Tello M, Vallès S, Montoliu C, Renau-Piqueras J, Guerri C. 1995. Developmental pattern of GFAP and vimentin expression in rat brain and radial glial cultures. Glia 15:157-166.
44. Shivraj Sohur U, Emsley JG, Mitchell BD, Macklis JD. 2006. Adult neurogenesis and cellular brain repair with neural progenitors, precursors and stem cells. Philos Trans R Soc Lond B Biol Sci 361:1477-1497.
45. Song H, Stevens CF, Cage FH. 2002. Astroglia induce neurogenesis from adult neural stem cells. Nature 417: 29-32.
46. Suslov ON, Kukekov VG, Ignatova TN, Steindler DA. 2002. Neural stem cell heterogeneity demonstrated by molecular phenotyping of clonal neurospheres. Proc Natl Acad Sci USA 99:14506-14511.
47. Wang TY, Sen A, Behie LA, Kallos MS. 2006. Dynamic behavior of cells within neurospheres in expanding populations of neural precursors. Brain Res 1107:82-96.
48. Westerlund U, Moe MC, Varghese M, Berg-Johnsen J, Ohlsson M, Langmoen IA, Svensson M. 2003. Stem cells from the adult human brain develop into functional neurons in culture. Exp Cell Res 289:378-383.

FIGURES

Fig. 1.

From brain MRI to single cell studies. A. MRI (magnetic resonance imaging) FLAIR (fluid attenuated inversion recovery). Coronal MRI FLAIR image suggestive of left hyppocampal sclerosis in the base of hyppocampal volume loss and increased signal of the hippocampal formation associated with mild increase in the temporal horn of the lateral ventricle. B. Histology of a representative coronal section of a normal hippocampus. C. Scheme of the different steps followed in the procedure of tissue culture: tissue dissociation (mechanic and enzymatic), cell expansion (proliferation) and differentiation, followed by immunocytochemical characterization.

Fig. 2.

Histological examination of hippocampal tissue. Panel A: Hippocampal sclerosis is characterized by neuronal loss in the CA1, CA3 and CA4 (endfolium) subfields of the hippocampus. Panel B shows an image of significant granule cells dispersion in the dentate gyrus, as observed in case 4.

Fig. 3.

Cell culture conditions. Cells cultured using different mitogens conditions exhibit different proliferation rate, as measured by multiplying the mean diameter and number of generated neurospheres. Images on the top are representative of neurospheres at 22 DIV without mitogens (A), in the presence of bFGF (10ng/ml) (B) and in the presence of both EGF+bFGF (20 and 10 ng/ml, respectively) (C). In the graph (D) the mean diameter value has been shown, indicating the number of generated neurospheres and the proliferation rate of each cell group. Data are expressed as mean ± SEM. Statistical analysis has been performed by using the one way ANOVA and Tukey's post-test. * $p<0.05$, ** $p<0.01$, when comparing with the no mitogen group of cells. ^{aaa} $p<0.001$, when comparing bFGF with EGF+bFGF group.

Fig. 4.

Cell proliferation and neurosphere generation over in vitro time. The number and the size of the generated neurospheres were monitored along the days in culture. In the upper part of the figure representative images of neurospheres after 3 (A), 6 (B), 16 (C) and 22 (D) days in vitro (DIVs) have been included. The proliferation rate after the indicated time have been represented in the

graph (E). The mean diameter values as well as the number of generated neurospheres have been included at the bottom of the graph.

Fig. 5.

Phenotype characterization of differentiated cells. Spontaneously differentiated cells after 12 DIVs and mitogen withdrawal, processed by immunocytochemistry. Panels A (musashi), B (doublecortin) and E, F (beta-tubulin) show neural cells; panels C, G, H (vimentin) and J, K, L, M (GFAP) show astroglial cells; panels O, Q (Rip) and P (CNPase) show oligodendroglial cells. Panels D, I and N show cell density of images E, J and O, respectively, as evidenced by Hoechst 33258 nuclear staining, at low-magnification. Scale bar in O (100µm) refers to panels C, D, E, I, J, N; scale bar in Q (100µm) refers to panels A, B, F, G, H, K, L, M, P.

TABLE I. Clinical and pathological features of enrolled patients. Main clinical and pathological features of patients included in the study as reported

Case N°	Sex	Age at surgery	Epilepsy duration	Side	Pathology	febrile seizures
1	Male	39	33	Right	Hippocampal sclerosis, architectural type cortical dysplasia	yes
2	Male	41	30	Left	Hippocampal sclerosis,	no
3	Female	32	20	Left	Hippocampal sclerosis, architectural type cortical dysplasia	yes
4	Female	27	25	Right	Hippocampal sclerosis, granule cells dispersion in the dentate gyrus	yes

Table II. Antibodies description. Antisera used in the study for the lineage characterization of the cells derived from human hippocampal NPCs (neuroprecursor cells).

ID	antigens	cross reactivity	hosts	suppliers	dilution
CNPase	purified human 2',3'-cyclic nucleotide 3'-phosphodiesterase	human, bovine, rat, canine, sheep, mouse, rabbit	mouse	CHEMICON International, Inc. Temecula, CA	1 : 1000
MAP2	bovine brain microtubule protein	human, cow, rat, mouse, chicken	rabbit	CHEMICON1	1 : 350
Vimentin	human vimentin	human, rat, goat, rabbit, bovine	mouse	NEN products Boston	1 : 20
βIII-tubulin	microtubules derived from rat brain	mammalian, chicken mouse		R&D system Minneapolis, MN	1 : 1000
GFAP	purified glial filament	human, porcine, chicken, rat	mouse	CHEMICON	1 : 200
MCM2	human mini-chromosome maintenance protein, type 2, amino terminal	mouse, rat, human	goat	Santa Cruz Biotechnology, Inc., Santa Cruz, CA	1 : 150
Doublecortin	human, C-terminus	mouse, rat, human	goat	Santa Cruz	1 : 100
NeuN	purified cell nuclei from mouse brain	human, rat, mouse, ferret, chick, salamander	mouse	CHEMICON	1 : 250
Nestin	rat-401	rat	mouse	BD Pharmingen San Diego, CA	1 : 500
RIP	rat olfactory bulb	rat, hamster	mouse	CHEMICON	1 : 2500
NG-2	cell line expressing a NG2 truncated form	rat, probably human	mouse	CHEMICON	1 : 75
Musashi	syntetic peptide AA 5-21 of Musashi	human, rodent	rabbit	CHEMICON	1 : 100

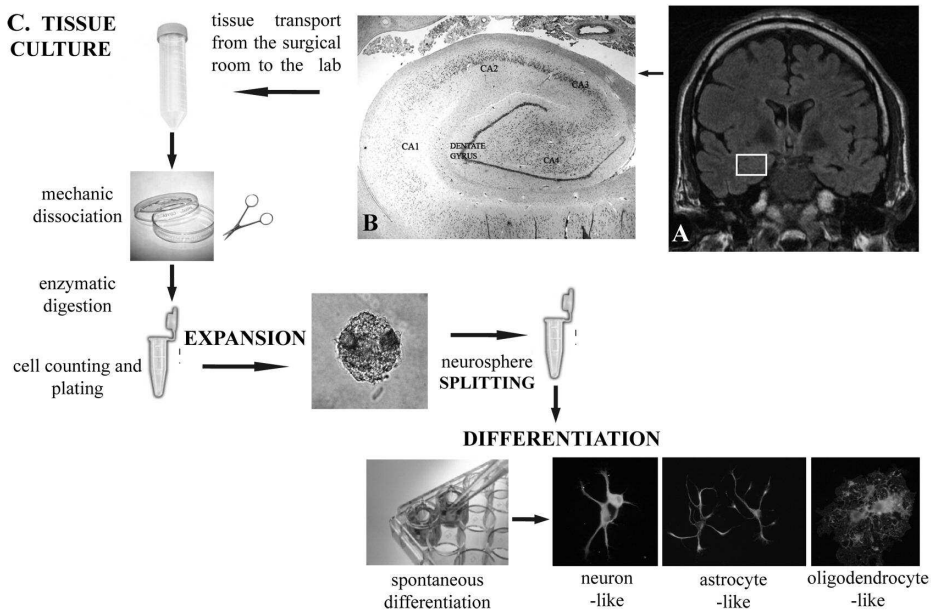

Fig. 1. From brain MRI to single cell studies. A. MRI (magnetic resonance imaging) FLAIR (fluid attenuated inversion recovery). Coronal MRI FLAIR image suggestive of left hyppocampal sclerosis in the base of hyppocampal volume loss and increased signal of the hippocampal formation associated with mild increase in the temporal horn of the lateral ventricle. B. Histology of a representative coronal section of a normal hippocampus. C. Scheme of the different steps followed in the procedure of tissue culture: tissue dissociation (mechanic and enzymatic), cell expansion (proliferation) and differentiation, followed by immunocytochemical characterization.

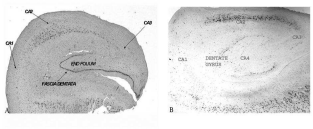

Histological examination of hippocampal tissue. Panel A: Hippocampal sclerosis is characterized by neuronal loss in the CA1, CA3 and CA4 (endfolium) subfields of the hippocampus. Panel B shows an image of significant granule cells dispersion in the dentate gyrus, as observed in case 4.

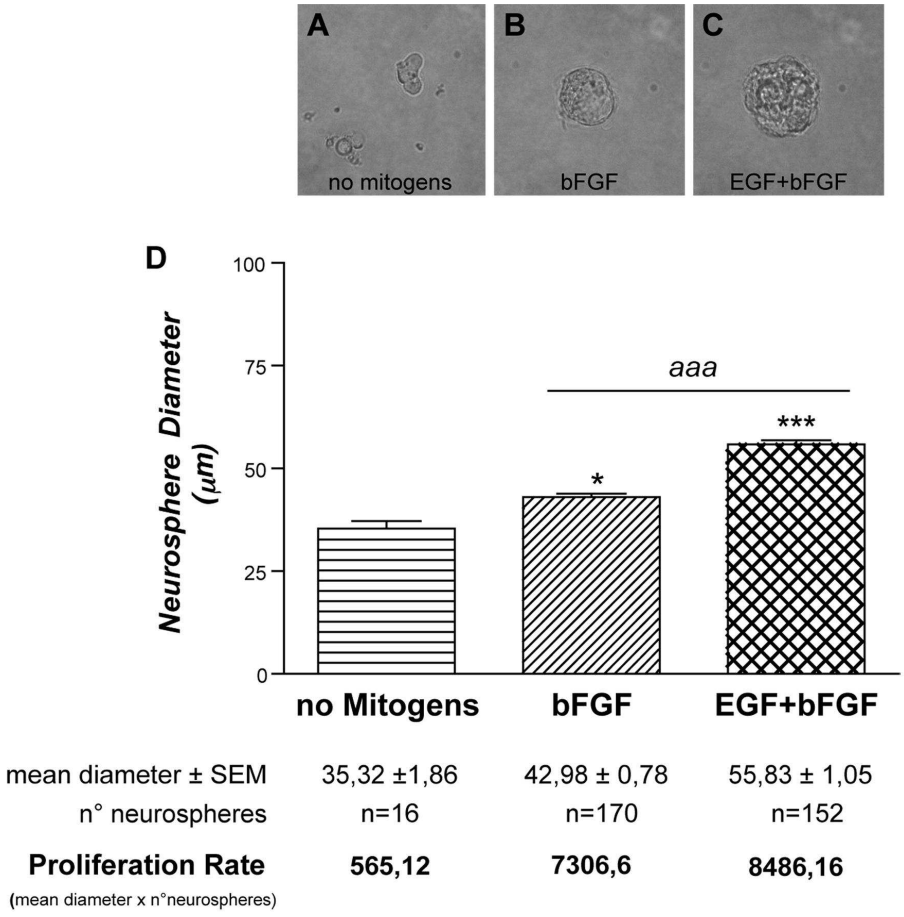

mean diameter ± SEM	35,32 ±1,86	42,98 ± 0,78	55,83 ± 1,05
n° neurospheres	n=16	n=170	n=152
Proliferation Rate (mean diameter x n°neurospheres)	**565,12**	**7306,6**	**8486,16**

Fig. 3. Cell culture conditions. Cells cultured using different mitogens conditions exhibit different proliferation rate, as measured by multiplying the mean diameter and number of generated neurospheres. Images on the top are representative of neurospheres at 22 DIV without mitogens (A), in the presence of bFGF (10ng/ml) (B) and in the presence of both EGF+bFGF (20 and 10 ng/ml, respectively) (C). In the graph (D) the mean diameter value has been shown, indicating the number of generated neurospheres and the proliferation rate of each cell group. Data are expressed as mean ± SEM. Statistical analysis has been performed by using the one way ANOVA and Tukey's post-test. * $p<0.05$, ** $p<0.01$, when comparing with the no mitogen group of cells. aaa $p<0.001$, when comparing bFGF with EGF+bFGF group.

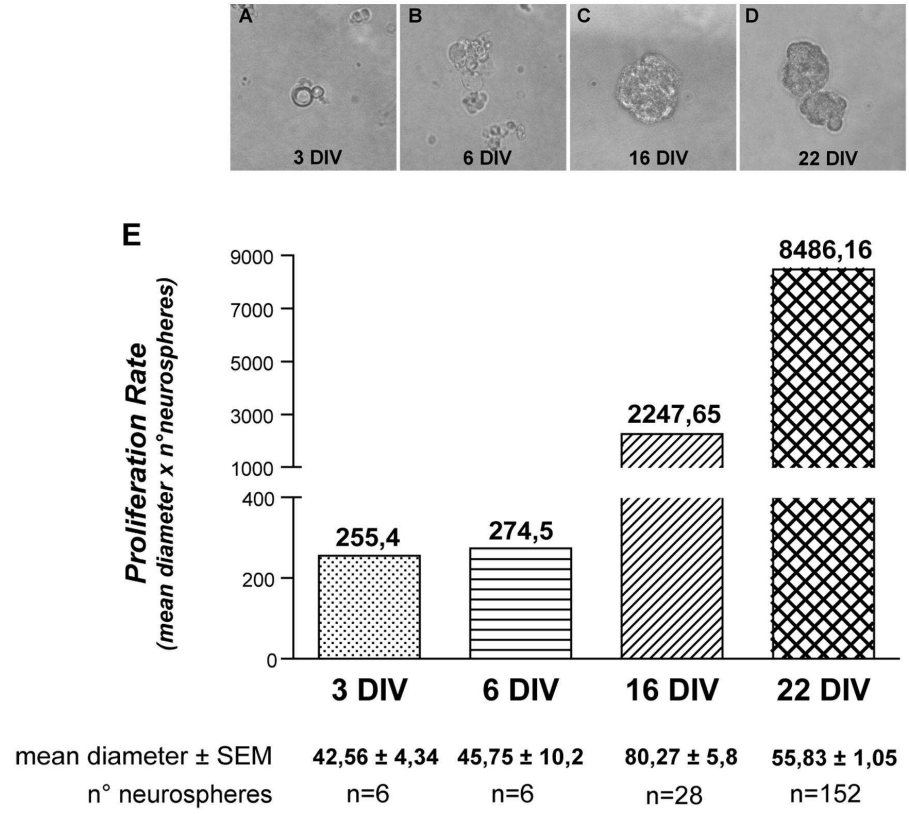

Fig. 4. Cell proliferation and neurosphere generation over in vitro time. The number and the size of the generated neurospheres were monitored along the days in culture. In the upper part of the figure representative images of neurospheres after 3 (A), 6 (B), 16 (C) and 22 (D) days in vitro (DIVs) have been included. The proliferation rate after the indicated time have been represented in the graph (E). The mean diameter values as well as the number of generated neurospheres have been included at the bottom of the graph.

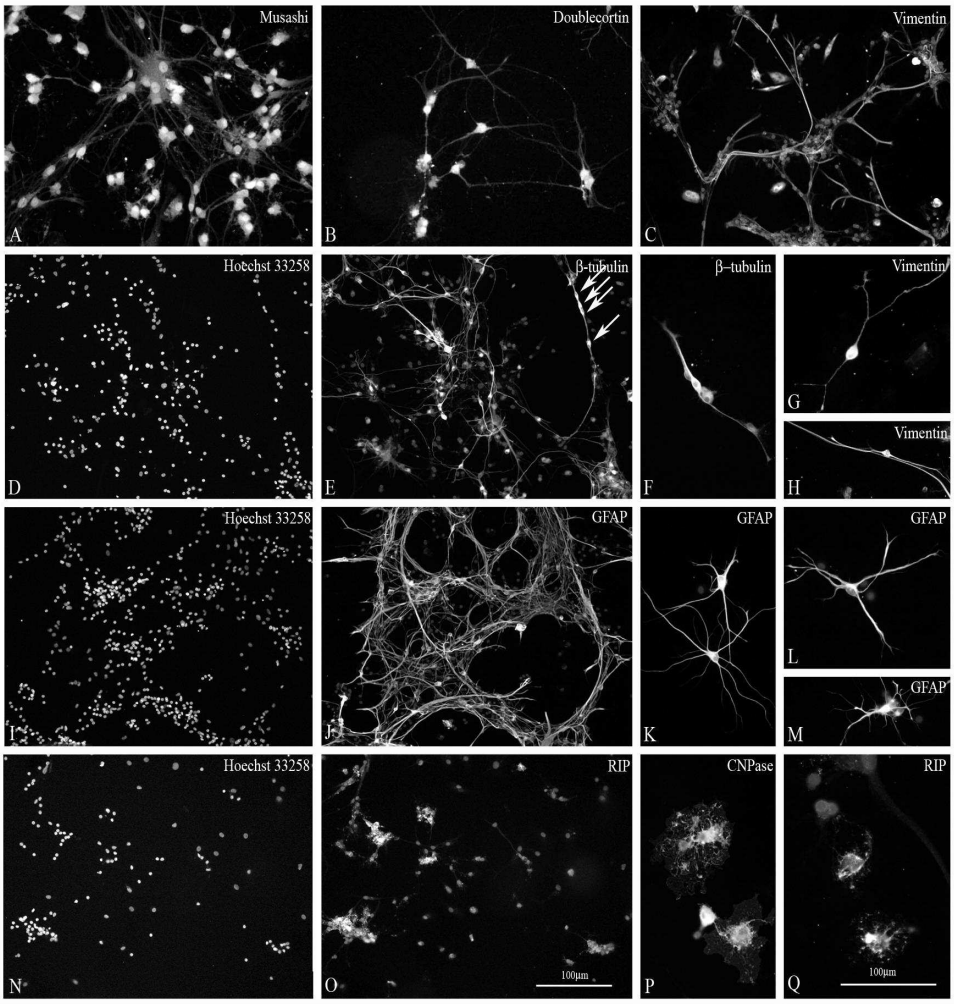

Fig. 5. Phenotype characterization of differentiated cells. Spontaneously differentiated cells after 12 DIVs and mitogen withdrawal, processed by immunocytochemistry. Panels A (musashi), B (doublecortin) and E, F (beta-tubulin) show neural cells; panels C, G, H (vimentin) and J, K, L, M (GFAP) show astroglial cells; panels O, Q (Rip) and P (CNPase) show oligodendroglial cells. Panels D, I and N show cell density of images E, J and O, respectively, as evidenced by Hoechst 33258 nuclear staining, at low-magnification. Scale bar in O (100μm) refers to panels C, D, E, I, J, N; scale bar in Q (100μm) refers to panels A, B, F, G, H, K, L, M, P.

Age-dependent impairment of hippocampal neurogenesis in chronic cerebral hypoperfusion.

Sivilia S., Giuliani A., Del Vecchio G., Giardino L., Calzà L.

Animal Stem Cell Laboratory, DIMORFIPA, University of Bologna,
Via Tolara di Sopra 50, 40064 Ozzano Emilia (Bologna), Italy

Key words: 2VO, rat, neurogenesis, doublecortin

Short running title**:** Hippocampal neurogenesis in chronic brain hypoperfusion

Correspondence:
Laura Calzà, MD
DIMORFIPA
University of Bologna
Via Tolara di Sopra 50
40064 Ozzano Emilia (Bologna), Italy
phone +39-051-792950
fax +39-051-792956
Email laura.calza@unibo.it

ABSTRACT

Aims. Acute ischaemic brain damage, both strokes and local ischaemia, are powerful stimulators of neurogenesis in the dental gyrus of the hippocampus in adult rat and mice. Since no data are available in chronic cerebral hypoperfusion, we investigated neurogenesis in rats after bilateral chronic occlusion of the carotid arteries (2VO).

Methods. 2VO was performed in 3- and 12-months old rats. Proliferation was investigated by BrdU-uptake and MCM2 nuclear immunoreactivity, neurogenesis by counting doublecortin-IR cells in the subgranular area of the dentate gyrus of the hippocampus.

Results. We found increased proliferation and neurogenesis in the subgranular area of the dentate gyrus of the hippocampus in adult (3-month old) rat 8 days after 2VO. This capability is lost in middle-aged (12-month old) rats.

Conclusions. Our data suggest that 2VO ligation can be a useful model for studying neurogenesis in experimental conditions mimicking long-lasting human pathologies also in the exploration of the uncertain relation between chronic brain hypoperfusion and age-related changes of cognitive function.

INTRODUCTION

Neurogenesis in the adult brain occurs in specific areas throughout life, e.g. in the subventricular zone at telencephalic level and the dentate gyrus of the hippocampus [1-3]. These areas contain precursor cells that can undergo mitotic division, as assessed by their capability to incorporate in vivo molecules intercalating into newly synthesized DNA in the S-phase cells such as bromodeoxi-uridine (BrdU), and to differentiate into neurons [4,5]. Moreover, when cultured in vitro according to the "neurosphere" system, precursor cells derived from both the SVZ and the hippocampus are able to differentiate into the three main types forming nervous tissue, e.g. neurons, astrocytes and oligodendrocytes, thus being defined as "neural stem cells" (NSCs) [6].

Extensive neurogenesis has been described in the dentate gyrus of the hippocampus of the adult brain not only in rodents, but also in primates [7] and humans [8]. It has been estimated that 9000 new cells are formed every day in the rat hippocampus [9]; some of these immature cells turn into fully differentiated granule cells [10] capable of sending axonal projections, containing synaptic vesicle proteins, to field CA3 [11]. Newly formed cells display passive membrane properties, action potentials and functional synaptic inputs similar to those found in mature dentate granule cells [12]. Thus, the hippocampal neurogenesis has a formidable potential impact not only on physiology, but also on brain pathologies involving learning and memory.

Neurogenesis in the hippocampus is highly regulated by different stimuli. Aging [13], experience [14,15], hormones and growth factors [16-18], drugs [19], may deeply modify in situ neurogenesis, altering proliferation rate, survival vs apoptosis and differentiation of newly generated cells, as well as integration into existing circuits. Moreover, hippocampal neurogenesis is severely altered in different neurodegenerative disease models, thus addressing many questions in view of their involvement in repair attempts and post-lesion functional recovery [20,21]. A series of reports using rodent stroke models have documented that acute ischemic brain injury stimulates adult neurogenesis in the hippocampal DG and that focal ischemic injury directs neuroblast migration to sites of damage in rodents [22-24] and also in non-human primates an increase in the number of new DG neurons is found after focal ischemia [25,26].

The potential of neurogenesis after chronic brain hypoperfusion is less clear, as it occurs in arterio/venous malformations and carotid stenosis/occlusion. The latter condition is common to middle-aged subjects, is a risk factor for stroke and is also arguably a possible risk factor for vascular dementia and to accelerate Alzheimer disease progression [27-29]. In this study, we investigated proliferation and neuronal differentiation of neural stem cells in the dentate gyrus of the hippocampus of rats having bilateral carotid occlusion (2VO model), a well-established model for brain chronic hypoperfusion [30-32]. Since chronic reduction of brain perfusion is a condition observed in humans starting from middle age, we included two age-groups in our study, e.g. 3-month and 12-month old rats, in order to evaluate the impact of aging on neurogenesis in this model.

MATERIALS AND METHODS

Animals and surgery

Male Sprague-Dawley albino rats (Charles River Italia, Calco, Varese) were used for this study. The animals were housed in polypropylene cages, 4 animals to a cage, under standard light/dark conditions (light on 7:00, off 19:00) with food pellets and water ad libitum. Chronic experimental cerebral hypoperfusion was induced by permanent bilateral occlusion of the common carotid arteries (2VO) [33,34], with sham-operated animals serving as controls (SHAM). Prior to surgery, the animals were anesthetized with ketamine hydrochloride (100 mg/kg IP). The common carotid arteries were exposed via a midline ventral cervical incision, carefully separated from their sheaths and vagal nerves, and permanently doubly ligated with 5-0 silk suture approximately 8 to 10 mm below the origin of the external carotid artery. The incision was then sutured. The same procedure was performed on the SHAM group but without actual ligation. Two age-groups (3 and 12-month old animals at the time of surgery) were included in the study, so that the final composition of the experimental groups was the following: 3-month old, sham operated, N=6; 3-month old, 2VO, N=12; 12-month old, sham operated, N=3; 12-month old, 2VO, N=3. Two different survival times (8, 75 days) after surgery were investigated in 3-month old animals, whereas 12-month old animals were sacrificed 8 days after surgery.

All animal protocols described herein were carried out according to the European Community Council Directives of 24 November 1986 (86/609/EEC) and approved by our intramural

committee and Italian Health Ministry (123/2004-B), in compliance with the guidelines published in the *National Institute of Health Guide for the Care and Use of Laboratory Animals*.

BrdU administration

Timing and dosage of BrdU administration was chosen to identify the lineage of newly generated cells, according to Kempermann et al.; Kuhn et al.; Christie and Cameron, [3,35,36]. Briefly, BrdU was administered intraperitoneally twice daily (75 mg/kg, Sigma, St. Louis, MO) for 3 days, and the rats perfused 9 days after the last BrdU injection. This protocol was applied in a long (75 days) 2VO survival time. Animals were then sacrificed as described for immunohistochemistry experiments. Sections were first incubated in 0.1 M PBS at room temperature for 30 min followed by incubation at 37°C for 30 min with HCl 2N. After rinsing in PBS for 20 min, the sections were incubated at 37°C for 4 min with pepsyne 0.025%. Sections were then processed for BrdU visualization by indirect immunofluorescence using rat anti-BrdU diluted in PBS/Triton 0.3%. For double experiments with BrdU, the immunohistochemical procedure was applied after BrdU visualization.

Immunohistochemistry

All animals were deeply anesthetized with Ketamine (Ketalar, Parke Davis, Italy) 10 mg/kg body weight, i.p. (+ diazepam. 2 mg/kg i.m.) and perfused through the ascending aorta with Tyrode-Ca^{2+} free, pH 6.9 (100 ml; 50 ml at 37°C, 50 ml ice-cold, for adult male rat, 50ml; 25 ml at 37 °C 25 ml ice-cold, for young male rats), followed by 4% paraformaldehyde in Sorensen phosphate buffer 0.1 M pH 7.0. During perfusion, animals were bathed in ice-cold water. The brains were then removed and immersed for 90 min in the same ice-cold fixative, before being rinsed for at least 48 h in 5% sucrose in 0.1M phosphate buffer. Brains were frozen in CO_2 and 14 mm thick coronal sections were then obtained from the dorsal hippocampus (bregma –3.30 mm level according to Paxinos&Watson, 1998) using a cryostat (Kriostat 1750, Leitz) and collected on gelatine coated slides. For immunofluorescence experiments, sections were first incubated in 0.1 M phosphate buffered saline (PBS) at room temperature for 10-30 min, followed by incubation at 4°C for 24h in a humid atmosphere with the primary antibodies diluted in PBS containing 0.3% Triton X-100, v/v (see Table I for the list of antisera used in this study). After rinsing in PBS for 20 min (2 x10 min), the sections

were incubated at 37°C for 30 min in a humid atmosphere with the secondary antisera conjugated with different fluorochromes: Cy™2- conjugated AffiniPure Donkey anti-Rabbit IgG (H+L) Jackson Immunoresearch West Grove PA, Cy™2- conjugated AffiniPure Donkey anti-Mouse IgG (H+L) Jackson Immunoresearch West Grove PA, Cy™2- conjugated AffiniPure Donkey anti-Goat IgG (H+L) Jackson Immunoresearch West Grove PA and Rhodamine Red™–X-conjugated AffiniPure Donkey anti-Rat IgG (H+L) Jackson Immunoresearch West Grove PA diluted in PBS triton 0.3%. Sections were then rinsed in PBS (as above) and mounted in glycerol containing 1,4-phenylendiamine 0.1 g/l.

Histopathology

Sections were incubated with nuclear dye Hoechst 33258 (Fluka) 1mg/ml in PBS/Triton 0.2% for 20 min at room temperature. Sections were then mounted in glycerol containing 1,4-phenylendiamine, 0.1 g/l. In the case of double staining with immunofluorescence, this protocol was applied after immunostaining.

Since a cholinergic denervation of the hippocampus has been described after 2VO ligation [45], esterase activity was investigated according to the histochemical technique of Hedreen et al. [37]. Briefly, sections were incubated in 01 M acetate buffer pH 6.0, followed by enzyme detection solution (0.1M sodium acetate buffer pH 6.0; 0.1M sodium citrate; 0.03M cupric sulfate pentahydrate; 0.1 mM potassium ferricyanide; acetylthiocholine iodide), 30 min at 37°C. After washing in acetate buffer, sections were briefly incubated in 1% ammonium sulfide followed by 0.1M sodium nitrate, 0.1% silver nitrate, 0.1M sodium nitrate. Finally, the sections were washed and mounted.

Microscopy, image analysis and figure preparation

Images from tissues were taken by Olympus AX70-PROVIS microscope equipped with motorized z-stage control and F-VIEW II CCD Camera. Images were obtained and processed using Cell^P software (Soft Imaging System, GmbH, MUNSTER Germany). Cell counting was bilaterally performed blind by two independent observers. For statistical analysis on six sections/animal were analyzed and sampled at level –3.14 mm from bregma according to the Paxinos and Watson stereotaxic atlas of the rat brain (Paxinos and Watson, 1998). Each experimental group was composed as follows: 3-month old sham operated rats N=6; 3-month old 2VO ligated (sacrificed 8 days after surgery) N=4; 3-month old 2VO ligated (sacrificed 75

days after surgery) N=8; 12-month old sham operated N=3 and 12-month old 2VO ligated (sacrificed 8 days after surgery) N=3;. Final figures were generated using Adobe Photoshop 6.0 and Adobe Illustrator 9.2 software.

RESULTS

Histopathology of the hippocampus of 2VO vs sham operated rat, as observed 75 days after ligation is shown in Fig 1. Images were obtained from one typical experiment. As already described [38,39], no substantial alterations of the hippocampal neural cytoarchitecture immunostaining were observed either 8 or 75 days after ligation in 3 month-old rats, in terms of cell density (A,B), esterase staining (C,D) and dendrite tree as depicted by MAP-2 immunostaining (E,G). A slight reactive gliosis, as defined by GFAP-immunostaining, was observed 8 days after 2VO ligation. Conversely, immunostaining for the neuronal protein MAP2 performed in CA1/2 field in old (Fig. 1F,H) animals 8 days after ligation indicate a substantial reduction in neuronal density and a corresponding increase in GFAP-immunostaining indicating astroglial reaction in 12 month-old rats.

To study the effect of brain hypoperfusion on cell proliferation and neurogenesis in the dentate gyrus of the hippocampus, we identified proliferating cells, as labelled by cell cycle-associated antigen MCM2 (minichromosome maintenance proteins, components of the prereplicative complex) (Fig. 2A) and neuroblasts, as identified by the microtubule binding protein doublecortin- (DCX) IR (Fig. 2B) [40]. Proliferation and neurogenesis were studied at 8 days, i.e. the post-lesion time at which the highest increase in proliferation is found after transient ischemia [41] and 75 days after ligation. Groups of MCM2-IR and BrdU-incorporating cells forming clusters localized at the inner border of the granule cell layer (subgranular zone) were observed in both sham-operated and 2VO animals in the 3-month old group. The small cell bodies of DCX-IR cells also resided in the subgranular zone, and fine processes extended into the granule cells layer. Double labelling experiments allowed us to establish that the proliferating cells, as labelled by BrdU, generated neuroblasts, as identified by DCX-IR, and then mature neurons, as identified by the neuron specific neuronal marker NeuN (see also x-y-plane projection of the IRs, which indicates the coexistence of nuclear labelling for BrdU and NeuN; Fig. 2D), whereas no newly generated GFAP- or S100-positive astrocytes were found (Fig. 2C). A discrete number of newly generated OPCs, as labeled by

NG2-antibody were observed in the hilus of legated animals, not in, but deeper respect to the sugranular zone.

In order to establish if chronic brain hypoperfusion alters hippocampal neurogenesis, we then counted the number of MCM2- and DCX-IR profiles in the dentate gyrus of sham-operated vs 2VO animals. We found a three-folds increase in the number of MCM2-IR cells and a slightly lower increase in DCX-IR cells in the dentate gyrus of 3-month old animals perfused 8 days after surgery. Proliferation capability was reduced 75 days after ligation, when also the number of DCX-IR cells did not differ from the control, sham-operated group (Fig. 3). Only single MCM2 and DCX-IR cells were detected in all analyzed sections obtained from the dentate gyrus of 12-months old animals undergoing either sham or 2VO surgery.

As it has been reported that hypoxia-ischemia induces DNA synthesis without cell proliferation in adult rodent brain [42], we analyzed the nuclear morphology of proliferating cells in 3-month old, 2VO ligated animals. Double-staining with Hoechst 33258 nuclear dye revealed no nuclear condensation or fragmentation of MCM2 and BrdU-IR cells (Fig. 2F,I).

DISCUSSION

The potential of adult neurogenesis for endogenous brain protection and, possibly, repair is under active investigation. Whereas neurogenesis has been extensively studied in animal models for focal or global ischemic brain insults mimicking stroke or cardiac arrest leading to near-total interruption of cerebral blood flow, no data are available for chronic brain hypoperfusion models leading to a progressive decrease of brain perfusion. In this study we demonstrated that an extensive proliferation of precursor cells leading to increased neurogenesis in the dentate gyrus of the hippocampus, as defined by the number of DCX-positive cells, occurs shortly (8 days) after surgery in a model of chronic brain hypoperfusion, when performed in young animals. Proliferation capability of neural precursors decreases to control level 75 days after ligation, when neurogenesis is back to control values. Precursor proliferation and neurogenesis are severely reduced in 12-month old animals, and are not stimulated by hypoperfusion due to 2VO ligation.

The bilateral occlusion of the common carotid arteries in rat (two-vessel occlusion, 2VO) is a well established model for chronic brain hypoperfusion without cerebral infarction, leading to retina and optic nerve degeneration [34, 39], white matter alteration [43], brain

capillary pathology [44] and, finally cognitive impairment due to cholinergic defects [45]. It has been suggested that this model can be helpful in exploring the uncertain relation between chronic brain hypoperfusion and cognitive function, with regard to both age-related decline and vascular dementia [27]. As in most vascular models, individual anatomical differences in the cerebrovascular anatomy at the circle of Willis of rodents can influence experimental variability [46-48]. However, consistent with previously published studies [33], the hippocampus, at least at the investigated times, did not show any significant alterations in hippocampal neural cytoarchitecture in 3-month old animals, whereas 12-month old rats showed extensive lesions of the hippocampus, with cell loss and astrogliosis 8 days after 2VO ligation, consistent with the age-dependent increase in severity of acute ischemia [36,49,50]. Accordingly, we suggest that 2VO ligation induces an acute reduction in blood flow, which is partially compensated over time in young but not middle-aged rats.

Here we show that 3-month old animals retain the capability of extensive proliferation and neurogenesis immediately after permanent carotid artery bilateral ligation. Using the cell cycle associated antigen MCM2 for counting proliferating cells, which is expressed in the G1 phase [3,42, 51], we demonstrated an increase in DNA synthesis in the neurogenic areas of the dentate gyrus. Since no images of nuclear alteration were found, and since double-labelling experiments using BrdU and neuronal markers and different experimental timing were used, we also proved that proliferation is followed by neurogenesis, as indicated by the increased number of DCX-IR profiles and NeuN-BrdU co-localization. This is particularly important since hypoxia and ischemia are among the factors that trigger abortive DNA synthesis without cell proliferation in the rat brain [42]. Double-labelling experiments with GFAP excluded newly generated astrocytes in the subgranular zone of dentate gyrus, but we cannot exclude that also microglia and oligoprecursor cells (OPCs) re-enter the cell cycle, thus accounting for part of the MCM2 and BrdU-positive cells. However, the correspondence of the percentage increase in MCM2- and DCX-IR profiles supports a substantial neural lineage of newly generated cells.

The rate of increase in proliferation that we found in 2VO ligated, 3-month old animals is similar to that observed in rats with transient ischemic lesions [41], suggesting that acute events after legation promote neural precursor cell proliferation. The increase in proliferation is actually lower, and not different from sham-operated animals when investigated 75 days after ligation. The molecular mechanisms underlying increased

neurogenesis due to blood flow reduction or arrest are still unknown. However, it has been suggested that the mechanisms involved in global and local ischemic insults could be different and involve excitatory neurotransmitters like glutamate, but also growth factors [23]. Conversely, neurogenesis was not stimulated 75 days after ligation, when gliosis was observed in the hippocampal formation. Reactive astrocytes could be one of the limiting factor for neurogenesis. Cell proliferation and neurogenesis in the dental gyrus increased in a mouse model deficient in glial fibrillary acid protein [52], suggesting that reactive astrocyte can effect subgranular stem cell niches, thus altering neurogenesis potential. However, our experiments allowed no evaluation of how many newly generated neurons were included in hippocampal circuits, and we can't exclude that neuronal loss and impaired neurogenesis may favor gliosis.

The capability to increase neural precursor proliferation and neurogenesis after 2VO chronic ligation is completely lost in 12-month old animals, at an age that is usually referred to as "middle age" in this rat strain [53]. Actually, in 12-month old control rats only a few scattered MCM2-IR, or BrdU-uptake, or DCX-IR cells were observed in the dentate gyrus of the hippocampus. Spontaneous, such as environmental- and drug- induced regulation of proliferation and neurogenesis in the hippocampus is age-dependent [24]. Herein we show that also pathological events able to strongly increase proliferation and neurogenesis fail in old animals, confirming the lower plastic and, possibly, repair capability of old brains. Other reports using BrdU uptake as sole marker to identify newborn cells indicated that also in 12-month old animals there is an increase in the number of newborn cells after acute ischemic insult [41]. However, as elegantly demonstrated by Kuan et al. [42], labelling of cell-cycle re-entry through DNA synthesis, as done by BrdU uptake, can be misleading, since hypoxia-ischemia induces DNA synthesis without cell proliferation.

In conclusion, our data suggest that 2VO ligation can be a useful model for studying neurogenesis in experimental conditions mimicking long-lasting human pathologies, also in view of substantial differences emerging across different models [24]. More extensive studies showing the final fate of newly generated cells in particular in terms of integration in existing circuits are necessary in order to speculate on the implications of these results for brain protection and repair in chronic brain hypoperfusion.

REFERENCES

1. Abrous DN, Koehl M, Le Moal M. Adult neurogenesis: from precursors to network and physiology. *Physiol Rev* 2005; **85**:523-69
2. Hagg T. Molecular regulation of adult CNS neurogenesis: an integrated view. *Trends Neuroscenci* 2005; **28**:589-95
3. Christie BR, Cameron HA. Neurogenesis in the adult hippocampus. *Hippocampus* 2006; **16**:199-207
4. Altman J, Das GD. Autoradiographic and histological evidence of postnatal hippocampal neurogenesis in rat. *J Comp Neurol* 1965; **124**:319-35
5. Gould E, Gross CG. Neurogenesis in adult mammals: some progress and problems. *J Neurosci* 2002; **22**:619-23
6. Reynolds BA, Weiss S. Generation of neurons and astrocytes from isolated cells of the adult mammalian central nervous system. *Science* 1992; **255:**1707-10
7. Kornack DR, Rakic P. Continuation of neurogenesis in the hippocampus of the adult macaque monkey. *Proc Natl Acad Sci U S A* 1999; **96**:5768-73
8. Eriksson PS, Perfilieva E, Bjork-Eriksson T, Alborn AM, Nordborg C, Peterson DA, Gage FH Neurogenesis in the adult human hippocampus. *Nat Med* 1998; **4**:1313-7
9. Cameron HA, McKay RD Adult neurogenesis produces a large pool of new granule cells in the dentate gyrus. *J Comp Neurol* 2001; **435**:406-17
10. Kempermann G, Gast D, Kronenberg G, Yamaguchi M, Gage FH. Early determination and long-term persistence of adult-generated new neurons in the hippocampus of mice. *Development* 2003; **130**:391-9
11. Markakis EA, Gage FH. Adult-generated neurons in the dentate gyrus send axonal projections to field CA3 and are surrounded by synaptic vesicles. *J Comp Neurol* 1999; **406**:449-60
12. Van Praag H, Schinder AF, Christie BR, Toni N, Palmer TD, Gage FH. Functional neurogenesis in the adult hippocampus. *Nature* 2002; **415**:1030-4
13. Kuhn HG, Dickinson-Anson H, Gage FH. Neurogenesis in the dentate gyrus of the adult rat: age-related decrease of neuronal progenitor proliferation. *J Neurosci* 1996;

16:2027-33

14. Kempermann G, Kuhn HG, Gage FH. Experience-induced neurogenesis in the senescent dentate gyrus. *J Neurosci* 1998; **18**: 206-12
15. Van Praag H, Kempermann G, Gage FH. Running increases cell proliferation and neurogenesis in the adult mouse dentate gyrus. *Nat Neurosci* 1999; **2**:266-70
16. Cameron HA, McKay RD. Restoring production of hippocampal neurons in old age. *Nat Neurosci* 1999; **2**:894-7
17. Aberg MA, Aberg ND, Hedbacker H, Oscarsson J, Eriksson PS. Peripheral infusion of IGF-I selectively induces neurogenesis in the adult rat hippocampus. *J Neurosci* 2000; **20**:2896-903
18. Fernandez M, Pirondi S, Manservigi M, Giardino L, Calzà L. Thyroid hormone participates in the regulation of neural stem cells and oligodendrocyte precursor cells in the central nervous system of adult rat. *Eur J Neurosci* 2004; **20**:2059-70
19. Brezun JM, Daszuta A. Depletion in serotonin decreases neurogenesis in the dentate gyrus and the subventricular zone of adult rats. *Neuroscience* 1999; **89**:999-1002
20. Taupin P Adult neurogenesis in mammals. *Curr Opin Mol Ther* 2006; **8**:345-51
21. Taupin P Stroke-induced neurogenesis: physiopathology and mechanisms. *Curr Neurovasc Res Review* 2006; **3**:67-72
22. Sharp FR, Liu J, Bernabeu R. Neurogenesis following brain ischemia. *Brain Res Dev Brain Res*. *Review* 2002; **134**:23-30
23. Kokaia Z, Lindvall O. Neurogenesis after ischaemic brain insults. *Curr Opin Neurobiol Review* 2003; **13**:127-32
24. Lichtenwalner RJ, Parent JM. Adult neurogenesis and the ischemic forebrain. *J Cereb Blood Flow Metab Review* 2006; **26**:1-20
25. Koketsu D, Furuichi Y, Maeda M, Matsuoka N, Miyamoto Y, Hisatsune T. Increased number of new neurons in the olfactory bulb and hippocampus of adult non-human primates after focal ischemia. *Exp Neurol* 2006; **199**:92-102
26. Tonchev AB, Yamashima T. Differential neurogenic potential of progenitor cells in dentate gyrus and CA1 sector of the postischemic adult monkey hippocampus. *Exp Neurol* 2006; **198**:101-13

27. Sarti C, Pantoni L, Bartolini L, Inzitari D. Cognitive impairment and chronic cerebral hypoperfusion: What can be learned from experimental models. *J Neurol Sci* 2002; **203-204**: 263-66
28. de la Torre JC Is Alzheimer's disease a neurodegenerative or a vascular disorder? Data, dogma, and dialectics. *Lancet Neurol Review* 2004; **3**:184-90
29. Roman GC. Vascular dementia prevention: a risk factor analysis. *Cerebrovasc Dis Review* 2005; **2**:91-100
30. Ni J, Ohta H, Matsumoto K, Watanabe H. Progressive cognitive impairment following chronic cerebral hypoperfusion induced by permanent occlusion of bilateral carotid arteries in rats. *Brain Res* 1994; **653**:231-6
31. Ni JW, Matsumoto K, Li HB, Murakami Y, Watanabe H. Neuronal damage and decrease of central acetylcholine level following permanent occlusion of bilateral common carotid arteries in rat. *Brain Res* 1995; **673**:290-6
32. De Jong GI, Farkas E, Stienstra CM, Plass JR, Keijser JN, de la Torre JC, Luiten PG. Cerebral hypoperfusion yields capillary damage in the hippocampal CA1 area that correlates with spatial memory impairment. *Neuroscience* 1999; **91**:203-10
33. Ohta H, Nishikawa H, Kimura H, Anayama H, Miyamoto M. Chronic cerebral hypoperfusion by permanent internal carotid ligation produces learning impairment without brain damage in rats. *Neuroscience* 1997; **79**:1039-50
34. Steven WD, Fortin T, Pappas BA. Retinal and optic nerve degeneration after chronic carotid ligation: time course and role of light exposure. *Stroke* 2002; **33**:1107-12
35. Kempermann G, Kuhn HG, Gage FH. More hippocampal neurons in adult mice living in an enriched environment. *Nature* 1997; **386**:493-5
36. Kuhn HG, Dickinson-Anson H, Gage FH. Neurogenesis in the dentate gyrus of the adult rat: age-related decrease of neuronal progenitor proliferation. *J Neurosci* 1996; **16**:2027-33
37. Hedreen JC, Bacon SJ, Price DL. A modified histochemical technique to visualize acetylcholinesterase-containing axons. *J Histochem Cytochem* 1985; **33**:134-40
38. Pappas BA, de la Torre JC, Davidson CM, Keyes MT, Fortin KT. Chronic reduction of cerebral blood flow in the adult rat: late-emerging CA1 cell loss and memory

dysfunction *Brain Research* 1995; **708**:50-58

39. Davidson CM, Pappas BA, Stevens WD, Fortin T, Bennett SAL. Chronic cerebral hypoperfusion: loss of pupillary reflex, visual impairment and retinal neurodegeneration. *Brain Research* 2000. **859**:96-103
40. Brown J, Cooper-Kuhn CM, Kempermann G, Van Praag H, Winkler J, Gage FH, Kuhn HG. Enriched environment and physical activity stimulate hippocampal but not olfactory bulb neurogenesis. *Eur J Neurosci* 2003; **17**:2042-6
41. Yagita Y, Kitagawa K, Ohtsuki T, Takasawa Ki, Miyata T, Okano H, Hori M, Matsumoto M. Neurogenesis by progenitor cells in the ischemic adult rat hippocampus. Stroke 2001; **32**:1890-6
42. Kuan CY, Schloemer AJ, Lu A, Burns KA, Weng WL, Williams MT, Strauss KI, Vorhees CV, Flavell RA, Davis RJ, Sharp FR, Rakic P. Hypoxia-ischemia induces DNA synthesis without cell proliferation in dying neurons in adult rodent brain. *J Neurosci* 2004; **24**:10763-72
43. Farkas E, Donka G, de Vos RA, Mihaly A, Bari F, Luiten PG. Experimental cerebral hypoperfusion induces white matter injury and microglial activation in the rat brain. *Acta Neuropathol (Berl)* 2004; **108**:57-64
44. De Jong GI, Farkas E, Stienstra CM, Plass JR, Keijser JN, de la Torre JC, Luiten PG. Cerebral hypoperfusion yields capillary damage in the hippocampal CA1 area that correlates with spatial memory impairment. *Neuroscience* 1999; **91**:203-10
45. de la Torre JC, Aliev G. Inhibition of vascular nitric oxide after rat chronic brain hypoperfusion: spatial memory and immunocytochemical changes. *J Cereb Blood Flow Metab*. 2005; **25**:663-72
46. Kitagawa K, Matsumoto M, Yang G, Mabuchi T, Yagita Y, Hori M, Yanagihara T. Cerebral ischemia after bilateral carotid artery occlusion and intraluminal suture occlusion in mice: evaluation of the patency of the posterior communicating artery. *J Cereb Blood Flow Metab* 1998; **18**:570-9
47. Laidley DT, Colbourne F, Corbett D. Increased behavioral and histological variability arising from changes in cerebrovascular anatomy of the Mongolian gerbil. *Curr Neurovasc Res* 2005; **2**:401-7

48. Seal JB, Buchn BN, Marks JD. New variability in cerebrovascular anatomy determines severity of hippocampal injury following forebrain ischemia in the Mongolian gerbil. *Brain Res* 2006; **1073-1074**:451-9
49. Yao H, Sadoshima S, Ooboshi H, Sato Y, Uchimura H, Fujishima M. Age-related vulnerability to cerebral ischemia in spontaneously hypertensive rats. *Stroke* 1991; **22**:1414-8
50. Jin K, Minami M, Xie L, Sun Y, Mao XO, Wang Y, Simon RP, Greenberg DA. Ischemia-induced neurogenesis is preserved but reduced in the aged rodent brain. *Aging Cell* 2004; **3**:373-7
51. Calza L, Giardino L, Pozza M, Bettelli C, Micera A, Aloe L. Proliferation and phenotype regulation in the subventricular zone during experimental allergic encephalomyelitis: in vivo evidence of a role for nerve growth factor. *Proc Natl Acad Sci U S A* 1998; **95**:3209-14
52. Larsson A, Wilhelmsson U, Pekna M, Pekny M. Increased cell proliferation and neurogenesis in the mice hippocampal dentate gyrus of old $GFAP^{-/-}Vim^{-/-}$ mice. *Neurochemical Research* 2004; **29**:2069-2073
53. Driscoll I, Howard SR, Stone JC, Monfils MH, Tomanek B, Brooks WM, Sutherland RJ. The aging hippocampus: a multi-level analysis in the rat. *Neuroscience* 2006; **139**:1173-85

TABLE 1.

Primary antisera and working conditions used in the study.

ID	Antigens	Hosts	Suppliers	dilution
Map-2	microtubule associated protein	Rabbit	Santa Cruz Biotechnology,Inc.	1 :300
GFAP	glial fibrillary acidic protein	Mouse	SIGMA	1 : 600
Mcm-2	mini-chromosome maintenance	Goat	Santa Cruz Biotechnology,Inc.	1 : 150
DCX	Doublecortin	Goat	Santa Cruz Biotechnology,Inc.	1 : 150
NeuN	neuronal nuclei	Mouse	CHEMICON	1 : 250
BrdU	Bromodeoxyuridine	Rat	ImmunologicalsDirect	1:100
S100	S-100	rabbit	Incstar	1:50
NG2	NG2 chondroitin sulfate proteoglycan	mouse	Chemicon	1:100

FIGURES

Fig.1

Histological (A, B: Hematoxylin-Eosin, HE), histochemical (C, D: esterase activity) and immunohistochemical (E-H) staining of the hippocampus of sham operated and 2VO ligated animals of the different age-groups. A,B: HE of hippocampus in 3-month old sham operated (A) and 2VO animals (B) 75 days after surgery. No reduction of cell density is observed in 2VO animals. C,D: esterase activity in the hippocampus of sham operated (C) and 2VO animals (D) 75 days after surgery. A slight reduction in esterase-positive fibers is observed in 2VO animals. E-H: immunostaining for MAP2 (green) and GFAP (red) in the CA1 hippocampal field of 3-month old sham operated (E) and 2VO (G) animals and 12-month old sham operated (F) and 2VO (H) animals, 8 days after surgery. Nuclear staining with Hoechst 33258 (blue) is used to visualize cell density distribution. MAP2-immunostaining clearly decreases in 12-month old but not in 3-month old ligated animals in the radial and lacunous-molecular layers. A gliosis, as described by GFAP-imunostaining, is observed in 2VO ligated animals, being stronger in old than in adult animals. Bars: A,B 200mm; C,D 100mm; E-H 100mm. *Abbreviations: o*: stratum oriens; *p*: stratum pyramidale; *r*: stratum radiatum; *lm*: stratum lacunosum-moleculare; *m*: stratum molecular; *g*: granule cells; *h*: hilus fasciae dentatae.

Fig. 2

Proliferating cells (A. MCM2-positive nuclei) and neurogenesis (B. DCX-immunoreactive cells) in the dentate gyrus of the hippocampus. Clusters of proliferating cells, as identified by antigens expressed during cell cycle (MCM2) or by BrdU uptake (C) are found in the subgranular layer of the dentate gyrus of the hippocampus of both sham-operated and 2VO ligated animals. Lineage of newly-generated cells is defined by immunolabelling of BrdU up-taking cells (C, D): BrdU-positive nuclei co-localize with DCX, which is a marker for neural precursors, and are co-distributed with NeuN, which is a marker for mature neural nuclei, as also indicated by the image with the right coordinates (X, Y and Z) of BrdU and NueN

immunostaining (yellow staining in D). Conversely, no GFAP+BrdU-positive cells were found. E-L: morphology of dividing nuclei. Hoechst 33258 (blue) nuclei dye showed that dividing nuclei, as identified either by MCM2-immunostaining (I, L) and BrdU-uptake (F,G), have normal morphology (no condensation, no pignosis). Bars: 100mm (A, B); 20mm (C-L).

Fig. 3

Quantitative evaluation of the number of MCM2- (A) and DCX-positive cells (B) in one side of the dentate gyrus of control (sham-operated) and legated (2VO) animals, 8 and 75 days after 2VO legation, as obtained by counting 6 section/animal, bilaterally. Data are presented as mean±SEM. 2VO ligation causes an increase in the number of proliferating cells, which turn into neurons in 3-month old (Y) but not in 12-month old (O) animals. Statistical analysis: one-way ANOVA and post hoc Tukey test, **P < 0.01; Student-*t*-test ^{c}P<0.001.

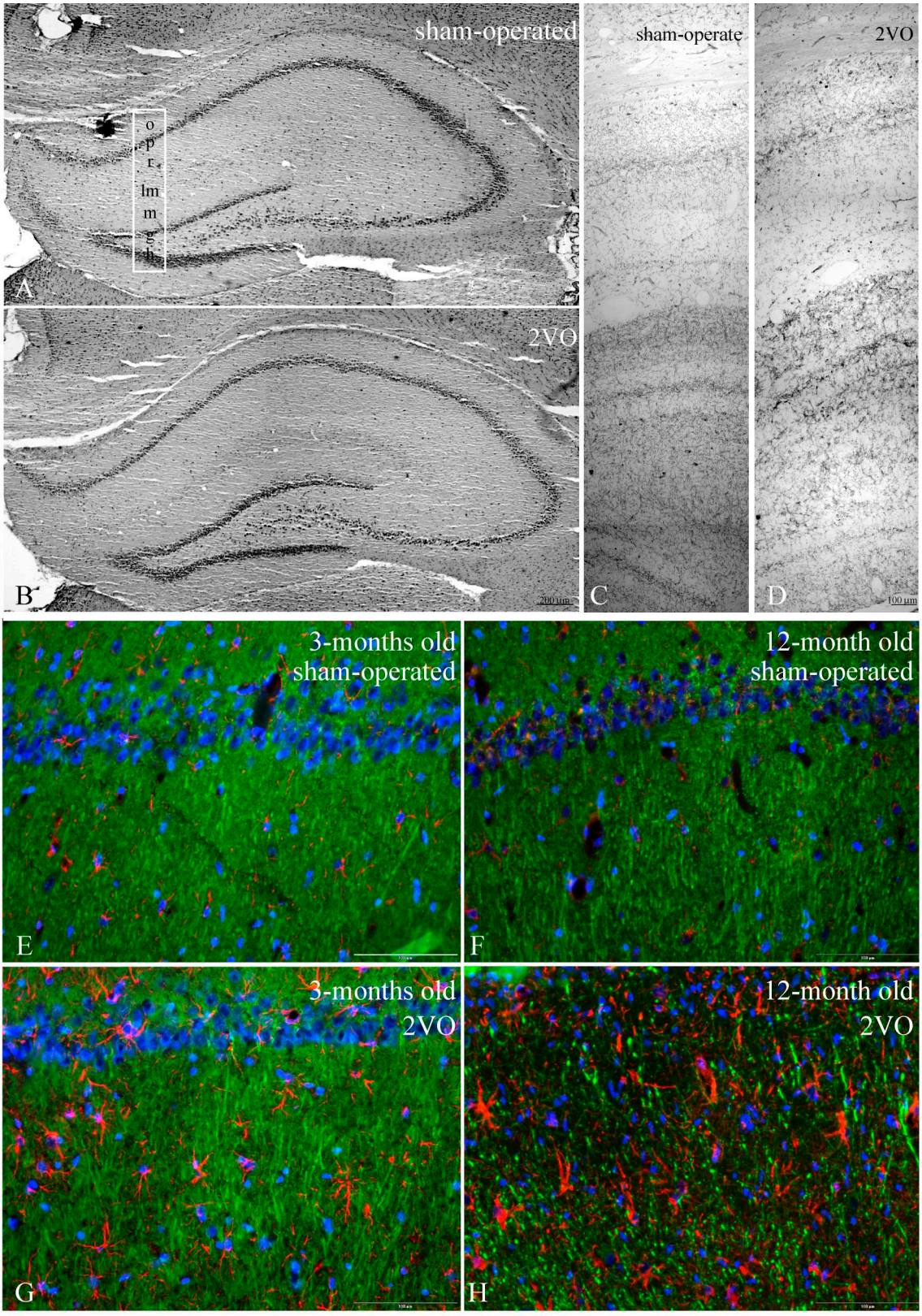
sham-operated
o
p
r
lm
m
g
h
A
2VO
B
200 µm
sham-operate
C
2VO
D
100 µm
3-months old
sham-operated
E
12-month old
sham-operated
F
3-months old
2VO
G
12-month old
2VO
H

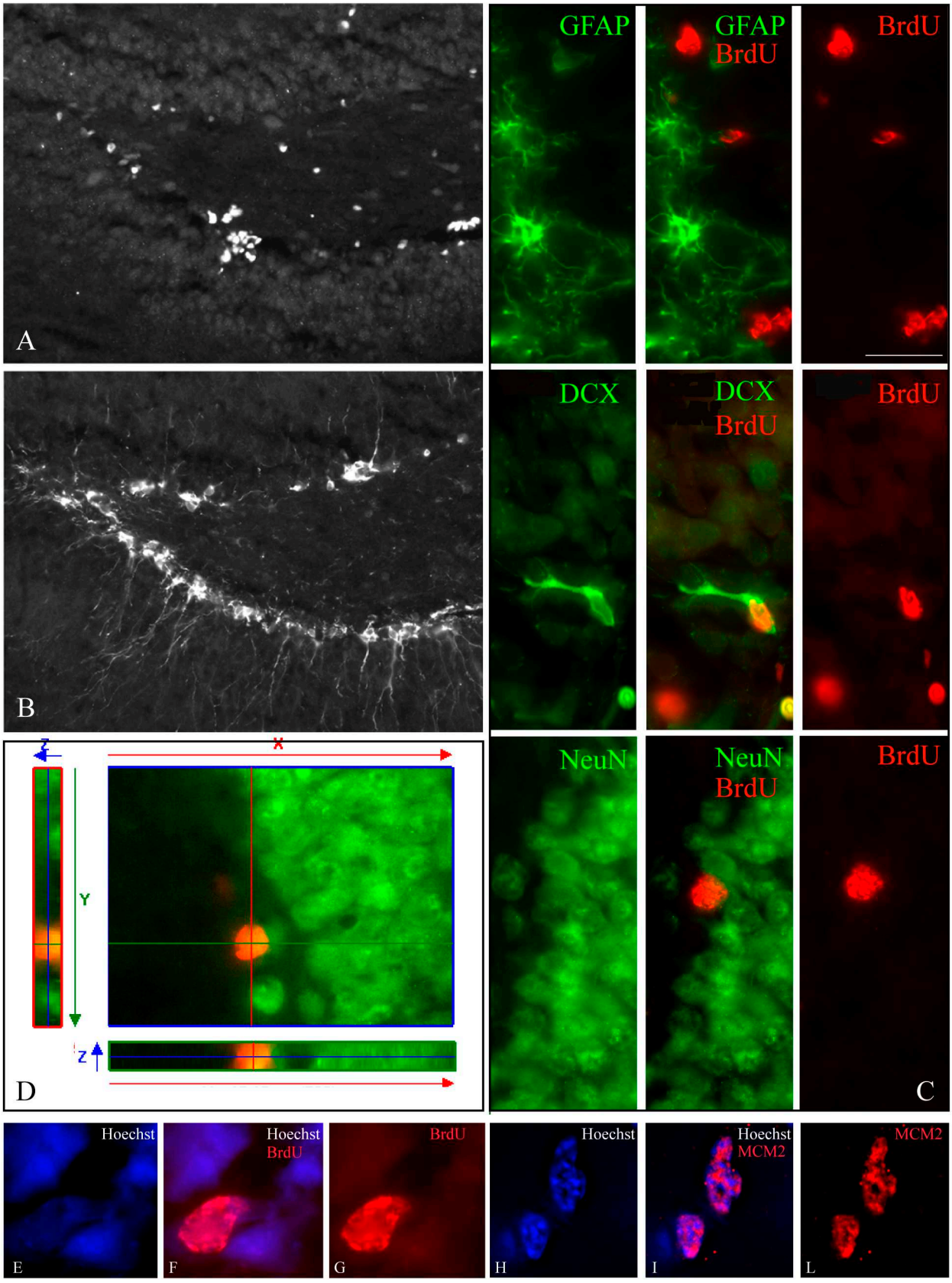
A
B
D
Z
X
Y
Z
GFAP
GFAP
BrdU
BrdU
DCX
DCX
BrdU
BrdU
NeuN
NeuN
BrdU
BrdU
C
Hoechst
E
Hoechst
BrdU
F
BrdU
G
Hoechst
H
Hoechst
MCM2
I
MCM2
L

A

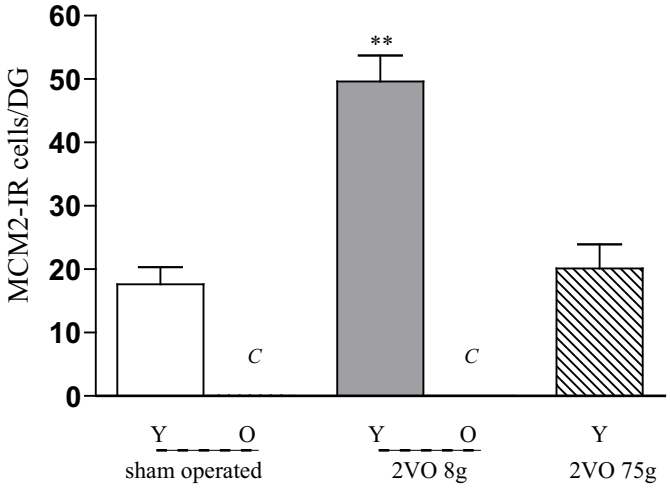
MCM2-IR cells/DG
60
50
40
30
20
10
0
**
C
C
Y
O
Y
O
Y
sham operated
2VO 8g
2VO 75g

B

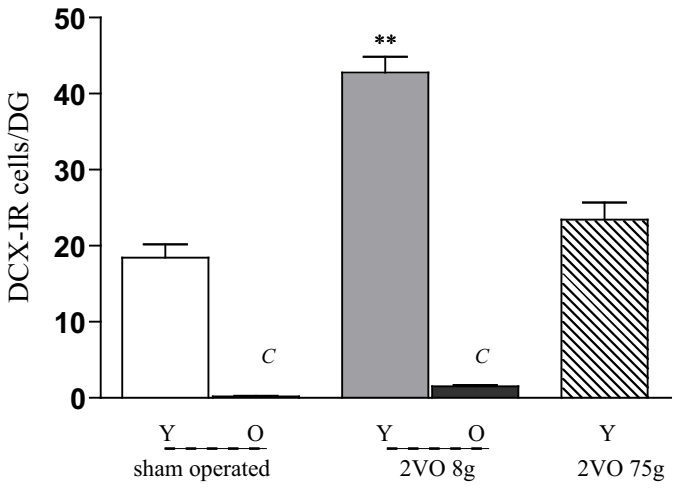
DCX-IR cells/DG
50
40
30
20
10
0
**
C
C
Y
O
Y
O
Y
sham operated
2VO 8g
2VO 75g